Technical Report

Finite Elements Q_1-Lagrange for the Linear Elasticity Problem

J. Figueiredo (*) - J. M. Viaño (**)

(*) Officina Mathematica. Universidade do Minho. Portugal.
em. jmfiguei@mct.uminho.pt

(**) Departamento de Matemática Aplicada. Universidade de Santiago de Compostela. Spain.
em. maviano@usc.es

December 2005

Contents

1. The continuous problem

1.1. Classical formulation

Let Ω be an open bounded connected set of $\mathbb{R}^2$ with piecewise C^1 boundary Γ. Let Γ_1 be a part of Γ having strictly positive measure and $\Gamma_2 = \Gamma - \Gamma_1$. We denote by $x = (x_1, x_2)$ a generic point of $\overline{\Omega} = \Omega \cup \Gamma$. For $x \in \Gamma_2$, we denote by $\nu(x) = (\nu_1(x), \nu_2(x))$ the outward unit vector normal to Γ_2 at the point x. If $v = (v_1, v_2)$ is a function defined on Ω taking values in $\mathbb{R}^2$, we consider

$$\varepsilon_{ij}(v) = \frac{1}{2}\left(\frac{\partial v_i}{\partial x_j} + \frac{\partial v_j}{\partial x_i}\right), \qquad 1 \le i, j \le 2, \tag{1.1}$$

and

$$\sigma_{ij}(v) = \lambda\left(\sum_{k=1}^{2} \varepsilon_{kk}(v)\right)\delta_{ij} + 2\mu\varepsilon_{ij}(v), \qquad 1 \le i, j \le 2, \tag{1.2}$$

where δ_{ij} denotes the Kronecker's symbol and λ and μ are constants such that

$$\lambda \ge 0, \quad \mu > 0.$$

Let us consider the following problem: given functions

$$f = (f_1, f_2) : \Omega \to \mathbb{R}^2 \qquad \text{and} \qquad g = (g_1, g_2) : \Gamma_2 \to \mathbb{R}^2,$$

find a function $u = (u_1, u_2)$ solution of

$$-\sum_{j=1}^{2} \frac{\partial}{\partial x_j}\sigma_{ij}(u) = f_i \quad \text{in} \quad \Omega, \quad 1 \le i \le 2, \tag{1.3a}$$

$$u_i = 0 \quad \text{on} \quad \Gamma_1, \quad 1 \le i \le 2, \tag{1.3b}$$

$$\sum_{j=1}^{2} \sigma_{ij}(u)\,\nu_j = g_i \quad \text{on} \quad \Gamma_2, \quad 1 \le i \le 2. \tag{1.3c}$$

The problem (1.3) describes the displacement field u with respect to the natural state of an elastic homogeneous isotropic solid subject to a density force f in Ω and a density force g on Γ_2 - see e.g. Raviart and Thomas (1998). The displacements u are imposed null over Γ_1. The coefficients λ and μ are the so-called Lamé's constants for the material occupying Ω and relate the coefficients σ_{ij} of the stress tensor to the coefficients ε_{ij} of the linearized strain tensor as given by (1.2).

1.2. Variational formulation

We use the standard notation for the classical spaces $L^2(\Omega)$ and $H^1(\Omega)$ (Sobolev space of order 1), see e.g. Adams (1975).

We denote by $(\cdot,\cdot)_0$ the inner product on $L^2(\Omega)$ and $\left[L^2(\Omega)\right]^2$, that is

$$\begin{aligned}(\xi, \zeta)_0 &= \int_\Omega \xi\zeta\, dx, \quad \xi, \zeta \in L^2(\Omega)\\ (u, v)_0 &= \sum_{i=1}^{2} (u_i, v_i)_0, \quad u, v \in \left[L^2(\Omega)\right]^2,\end{aligned}$$

where $u = (u_1, u_2)$ and $v = (v_1, v_2)$. The norms induced by these inner products will be denoted by $\|\cdot\|_0$:

$$\|\xi\|_0 = (\xi, \xi)_0^{1/2}, \quad \xi \in L^2(\Omega),$$

$$\|v\|_0 = (v, v)_0^{1/2} = \left(\sum_{i=1}^{2} \|v_i\|_0^2 \right)^{\frac{1}{2}}, \quad v \in \left[L^2(\Omega) \right]^2.$$

We further denote by $(\cdot, \cdot)_1$ the inner product on $H^1(\Omega)$ and $\left[H^1(\Omega) \right]^2$, that is

$$\begin{aligned} (\xi, \zeta)_1 &= (\xi, \zeta)_0 + \sum_{i=1}^{2} \left(\frac{\partial \xi}{\partial x_i}, \frac{\partial \zeta}{\partial x_i} \right)_0, \\ (u, v)_1 &= \sum_{i=1}^{2} (u_i, v_i)_1, \end{aligned}$$

and by $\|\cdot\|_1$ the corresponding induced norms:

$$\begin{aligned} \|\xi\|_1 &= (\xi, \xi)_1^{1/2}, \\ \|v\|_1 &= (v, v)_1^{1/2} = \left(\sum_{i=1}^{2} \|v_i\|_1^2 \right)^{\frac{1}{2}}. \end{aligned}$$

The following results are not trivial - see e.g. Duvaut and Lions (1972), Adams (1975):

Theorem 1. *(*Korn's inequality*) Let Ω be an open bounded connected set of $\mathbb{R}^2$ with piecewise C^1 boundary Γ and Γ_1 a part of Γ such that* $\text{meas}(\Gamma_1) \neq 0$. *Then, there exists a constant $C > 0$ such that*

$$\sum_{i,j=1}^{2} \|\varepsilon_{ij}(v)\|_{0,\Omega}^2 \geq C(\Omega, \Gamma_1) \, \|v\|_{1,\Omega}^2, \quad \forall v \in \left[H^1(\Omega) \right]^2,$$

such that $v = 0$ on Γ_1.

Theorem 2. *(*Trace theorem*) Let Ω be an open bounded connected set of $\mathbb{R}^2$ with piecewise C^1 boundary Γ. Then*

(i) there exists a unique bounded linear operator γ

$$\gamma : H^1(\Omega) \to L^2(\Gamma),$$

with the property that if $\xi \in C^1(\overline{\Omega})$, then $\gamma(\xi) = \xi|_\Gamma$ in the conventional sense;

(ii) the range of γ is dense in $L^2(\Gamma)$.

We also recall the Green's formula:

$$\int_\Omega \frac{\partial \xi}{\partial x_i} \, \zeta \, dx = -\int_\Omega \frac{\partial \zeta}{\partial x_i} \, \xi \, dx + \int_\Gamma \xi \zeta \, \nu_i \, d\gamma, \quad \forall \xi, \zeta \in H^1(\Omega), \quad i = 1, 2,$$

where $d\gamma$ denotes the one-dimensional measure of Γ.

We assume that $f = (f_1, f_2) \in \left[L^2(\Omega) \right]^2$ and $g = (g_1, g_2) \in \left[L^2(\Gamma_2) \right]^2$, and consider the space of admissible displacements

$$V = \left\{ v = (v_1, v_2) \in \left[H^1(\Omega) \right]^2 : (v_1, v_2) = (0, 0) \text{ on } \Gamma_1 \right\}. \tag{1.4}$$

Then, if u is a solution of problem (1.3) smooth enough to belong to V, we have

$$
\begin{aligned}
&u \in V: \\
&-\int_{\Omega} \sum_{i,j=1}^{2} \frac{\partial}{\partial x_j} \sigma_{ij}(u)\, v_i \, dx = \int_{\Omega} \sum_{i=1}^{2} f_i v_i \, dx, \quad \forall v = (v_1, v_2) \in V.
\end{aligned}
$$

Invoking Green's formula, we obtain

$$
\begin{aligned}
&u \in V: \\
&\int_{\Omega} \sum_{i,j=1}^{2} \sigma_{ij}(u)\, \varepsilon_{ij}(v)\ dx - \int_{\Gamma_2} \sum_{i,j=1}^{2} \sigma_{ij}(u)\, \nu_j v_i \, d\gamma = \int_{\Omega} \sum_{i=1}^{2} f_i v_i \, dx, \\
&\forall v = (v_1, v_2) \in V.
\end{aligned}
$$

Taking into account the condition (1.3c) involving the forces acting on Γ_2 , then u is a solution of the variational problem

$$
\begin{aligned}
&\text{Find } u \in V \text{ such that:} \\
&\int_{\Omega} \sum_{i,j=1}^{2} \sigma_{ij}(u)\, \varepsilon_{ij}(v)\ dx = \int_{\Omega} \sum_{i=1}^{2} f_i v_i \, dx + \int_{\Gamma_2} \sum_{i=1}^{2} g_i v_i \, d\gamma, \\
&\forall v = (v_1, v_2) \in V.
\end{aligned}
$$

Using the relation between the components of the stress tensor σ and those of the strain tensor ε (cf. (1.2)), then an equivalent form for the problem is

$$
\begin{aligned}
&\text{Find } u \in V \text{ such that:} \\
&\int_{\Omega} \sum_{i,j=1}^{2} \left\{ \lambda \left(\sum_{k=1}^{2} \varepsilon_{kk}(u) \right) \delta_{ij} + 2\mu \varepsilon_{ij}(u) \right\} \varepsilon_{ij}(v)\ dx = \int_{\Omega} \sum_{i=1}^{2} f_i v_i \, dx + \int_{\Gamma_2} \sum_{i=1}^{2} g_i v_i \, d\gamma, \\
&\forall v = (v_1, v_2) \in V,
\end{aligned}
$$

or

$$
\begin{aligned}
&\text{Find } u \in V \text{ such that:} \\
&\int_{\Omega} \lambda \operatorname{div} u \operatorname{div} v \, dx + \int_{\Omega} 2\mu \sum_{i,j=1}^{2} \varepsilon_{ij}(u)\, \varepsilon_{ij}(v)\ dx = \int_{\Omega} \sum_{i=1}^{2} f_i v_i \, dx + \int_{\Gamma_2} \sum_{i=1}^{2} g_i v_i \, d\gamma, \\
&\forall v = (v_1, v_2) \in V.
\end{aligned}
$$

Defining the bilinear form $a : V \times V \to \mathbb{R}$:

$$
a(u, v) = \int_{\Omega} \sum_{i,j=1}^{2} \sigma_{ij}(u)\, \varepsilon_{ij}(v)\ dx = \int_{\Omega} \lambda \operatorname{div} u \operatorname{div} v \, dx + \int_{\Omega} 2\mu \sum_{i,j=1}^{2} \varepsilon_{ij}(u)\, \varepsilon_{ij}(v)\ dx \tag{1.5}
$$

and the linear form $l : V \to \mathbb{R}$:

$$
l(v) = \int_{\Omega} \sum_{i=1}^{2} f_i v_i \, dx + \int_{\Gamma_2} \sum_{i=1}^{2} g_i v_i \, d\gamma, \tag{1.6}
$$

the variational continuous problem is written as

$$
\text{Find } u \in V \text{ such that: } a(u, v) = l(v), \ \forall v \in V. \tag{1.7}
$$

In order to prove the existence and uniqueness of solution of problem (1.7) we recall the Lax-Milgram's lemma:

Theorem 3. *(*Lax-Milgram lemma*): Let V be a real Hilbert space with norm $\|\cdot\|$, $a : V \times V \to \mathbb{R}$ a bilinear form and $l : V \to \mathbb{R}$ a linear form verifying:*

(i) a is continuous on V: $|a(u,v)| \leq M \, \|u\| \, \|v\|, \quad \forall u, v \in V, \quad M > 0$;

(ii) a is V-elliptic: $a(v,v) \geq \alpha \, \|v\|^2, \quad \forall v \in V, \quad \alpha > 0$;

(iii) l is continuous on V: $|l(v)| \leq C \, \|u\|, \quad \forall v \in V, \quad C > 0$.

Then there exists and unique element u satisfying:

$$u \in V, \quad a(u,v) = l(v), \quad \forall v \in V.$$

Since the space V defined by (1.4) is an Hilbert space (subspace of the Hilbert space $\left[H^1(\Omega)\right]^2$), in order to prove the existence and uniqueness of solution of problem (1.7) we only need to prove that the hypotheses of the Lax-Milgram's lemma hold.

We first show that the linear form defined by (1.6) is continuous on V. Let $v \in V$ be an arbitrary element of V. Then

$$\begin{aligned}
|l(v)| &= \left| \int_\Omega \sum_{i=1}^{2} f_i v_i \, dx + \int_{\Gamma_2} \sum_{i=1}^{2} g_i v_i \, d\gamma \right| \\
&\leq \left| \int_\Omega \sum_{i=1}^{2} f_i v_i \, dx \right| + \left| \int_{\Gamma_2} \sum_{i=1}^{2} g_i v_i \, d\gamma \right| \\
&= |(f,v)_{0,\Omega}| + |(g,v)_{0,\Gamma_2}| \\
&\leq \|f\|_{0,\Omega} \, \|v\|_{0,\Omega} + \|g\|_{0,\Gamma_2} \, \|v\|_{0,\Gamma_2} \\
&\leq \|f\|_{0,\Omega} \, \|v\|_{1,\Omega} + C \, \|g\|_{0,\Gamma_2} \, \|v\|_{1,\Omega}, \quad C > 0, \\
&\leq \|v\|_{1,\Omega} \left(\|f\|_{0,\Omega} + C \, \|g\|_{0,\Gamma_2} \right),
\end{aligned}$$

where we have used the Cauchy-Schwarz inequality and the continuity of the trace operator.

To show that the bilinear form a is continuous on V, we use the Cauchy-Schwarz inequality and write:

$$\begin{aligned}
|a(u,v)| &= \left| \int_\Omega \lambda \operatorname{div} u \operatorname{div} v \, dx + 2\mu \int_\Omega \sum_{i,j=1}^{2} \varepsilon_{ij}(u) \, \varepsilon_{ij}(v) \, dx \right| \\
&\leq \lambda \left| \int_\Omega \operatorname{div} u \operatorname{div} v \, dx \right| + 2\mu \left| \int_\Omega \sum_{i,j=1}^{2} \varepsilon_{ij}(u) \, \varepsilon_{ij}(v) \, dx \right| \\
&\leq \lambda \, |(\operatorname{div} u, \operatorname{div} v)_{0,\Omega}| + 2\mu \sum_{i,j=1}^{2} |(\varepsilon_{ij}(u), \varepsilon_{ij}(v))_{0,\Omega}| \\
&\leq \lambda \, \|\operatorname{div} u\|_{0,\Omega} \, \|\operatorname{div} v\|_{0,\Omega} + 2\mu \sum_{i,j=1}^{2} \|\varepsilon_{ij}(u)\|_{0,\Omega} \, \|\varepsilon_{ij}(v)\|_{0,\Omega}.
\end{aligned}$$

Given that all the norms in the above expression are $L^2(\Omega)$-norms of various combinations of first derivatives of u and v it follows that there is a constant $M > 0$ such that

$$|a(u,v)| \leq M \, \|u\|_{1,\Omega} \, \|v\|_{1,\Omega}$$

as required.

To prove the V-ellipticity of the bilinear form a we consider

$$\begin{aligned} a(v,v) &= \int_\Omega \lambda \left(\operatorname{div} v\right)^2 \, dx + 2\mu \int_\Omega \sum_{i,j=1}^{2} \left[\varepsilon_{ij}(v)\right]^2 \, dx \\ &\geq 2\mu \sum_{i,j=1}^{2} \|\varepsilon_{ij}(v)\|_{0,\Omega}^2 \,. \end{aligned}$$

Invoking the Korn's inequality, we obtain

$$a(v,v) \geq \alpha \, \|v\|_V^2$$

as required.

2. The approximate problem

2.1. Q_1-quadrilaterals

Let us consider the reference finite element $(\widehat{T}, \widehat{Q}_1, \widehat{\Sigma})$, where $\widehat{T}$ is the reference square $\widehat{T} = [0,1] \times [0,1]$ and $\widehat{\Sigma} = \{\widehat{a}_i,\ i = 1,2,3,4\}$ is the set of vertices of $\widehat{T}$ as shown in Figure 2.1. $\widehat{Q}_1$ denotes a space of polynomials defined on $\widehat{T}$ with variables $\widehat{x}_1, \widehat{x}_2$ of degree less than or equal to 1 in each variable:

$$\widehat{Q}_1 = \langle 1, \widehat{x}_1, \widehat{x}_2, \widehat{x}_1\widehat{x}_2 \rangle .$$

Given 4 points $a_1, a_2, a_3, a_4 \in \mathbb{R}^2$ we denote by T the convex hull of a_1, a_2, a_3, a_4. Assuming that T is not degenerated and denoting the set of vertices of T by $\Sigma_T = \{a_i^T,\ i = 1,2,3,4\}$, it can be shown that there is a unique invertible map $F_T : \widehat{T} \to \mathbb{R}^2$ such that

$$F_T = \begin{pmatrix} (F_T)_1 \\ (F_T)_2 \end{pmatrix} \in \left(\widehat{Q}_1\right)^2,$$

with the property

$$T = F_T(\widehat{T}) \quad \text{and} \quad a_i^T = F_T(\widehat{a}_i), \quad i = 1, ..., 4$$

(see Figure 2.2). Under these conditions we can define the "Q_1-finite element" (T, P_T, Σ_T) induced by the map F_T, where

$$P_T = \left\{ p : T \to \mathbb{R} : \widehat{p} = p \circ F_T \in \widehat{Q}_1 \right\}. \tag{2.1}$$

Since $\dim \widehat{Q}_1 = 4$, taking $\{\widehat{p}_1, \widehat{p}_2, \widehat{p}_3, \widehat{p}_4\}$ as a base of $\widehat{Q}_1$ having the property

$$\widehat{p}_i\left(\widehat{a}_j\right) = \delta_{ij}, \quad 1 \le i, j \le 4,$$

(see § 2.6), leads to

$$F_T\left(\widehat{x}\right) = \sum_{i=1}^{4} \left(a_i^T\right)\ \widehat{p}_i(\widehat{x}) \in \left(\widehat{Q}_1\right)^2.$$

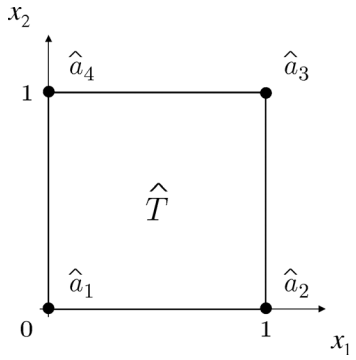

Figure 2.1: The reference element $\widehat{T}$

Furthermore, considering the definition of the space P_T (2.1) and taking $x = F_T\left(\widehat{x}\right)$, we get

$$\widehat{p}_i\left(\widehat{x}\right) = \left(p_i^T \circ F_T\right)\left(\widehat{x}\right) = p_i^T\left(x\right), \quad 1 \le i \le 4, \tag{2.2}$$

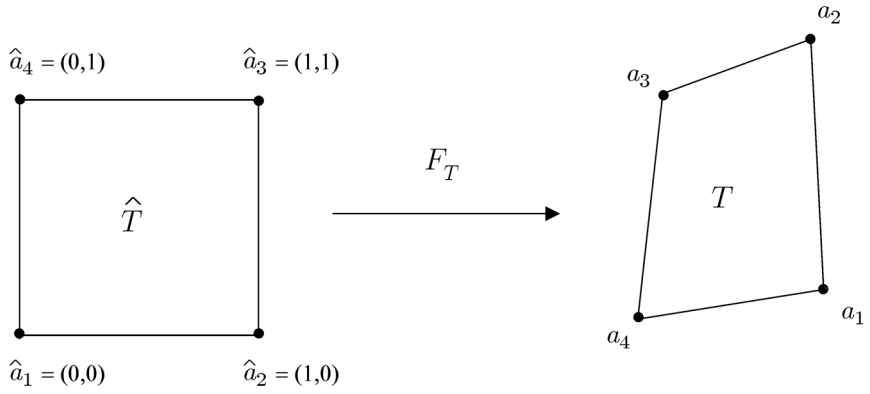

Figure 2.2: Quadrilateral element T and the corresponding map F_T

or, alternatively,

$$p_i^T(x) = \widehat{p}_i \circ F_T^{-1}(x), \quad 1 \leq i \leq 4.$$

It can be shown that under these conditions

$$p \in P_T \quad \Rightarrow \quad p \circ F_T \in \widehat{Q}_1 \subset \widehat{P}_2 \ \wedge \ p \circ F_T|_{\partial \widehat{T}_l} \in \widehat{P}_1,$$

where $\widehat{P}_i$ stands for the space of polynomials of degree i in each variable defined on $\widehat{T} = [0,1]^2$, while $\partial \widehat{T}_l$ is the side l of the reference square $\widehat{T}$, with $1 \leq l \leq 4$.

2.2. Global formulation

Let $\mathcal{T}_h$ be a triangulation of $\overline{\Omega}$ of finite elements type, compatible with the partition $\Gamma = \Gamma_1 \cup \Gamma_2$, made of quadrilaterals, that is:

(i) $\overline{\Omega} = \bigcup_{T \in \mathcal{T}_h} T$, where T is a non-degenerated quadrilateral;

(ii) $\overset{\circ}{T}_1 \cap \overset{\circ}{T}_2 = \varnothing, \ \forall T_1, T_2 \in \mathcal{T}_h, \ T_1 \neq T_2$;

(iii) $T_1 \cap T_2 = \varnothing$, or $T_1 \cap T_2 =$ shared corner, or $T_1 \cap T_2 =$ shared edge, $\forall T_1, T_2 \in \mathcal{T}_h, \ T_1 \neq T_2$;

(iv) $T \cap \Gamma_i = \varnothing$, or $T \cap \Gamma_i =$ corner of T, or $T \cap \Gamma_i =$ edge of T, for $i = 1, 2, \ \forall T \in \mathcal{T}_h$;

and consider

$$h_T = diam(T) = \max_{x,y \in T} \{|x - y|\}, \quad T \in \mathcal{T}_h,$$

$$h = \max_{T \in \mathcal{T}_h} h_T,$$

where $|z| = \left(\sum_{i=1}^{n} z_i^2 \right)^{1/2}$ denotes the Euclidean norm in $\mathbb{R}^n$.

We now define the space of finite elements, X_h, as

$$X_h = X_{1h} \times X_{2h},$$

where

$$X_{1h} = X_{2h} = \left\{ v_h \in C^0\left(\overline{\Omega}\right) : v_h|_T \in P_T, \ \forall T \in \mathcal{T}_h \right\}. \tag{2.3}$$

The space of admissible displacements, $V_h \subset V$, is defined by

$$V_h = \{ v_h \in X_h : v_h = 0 \text{ on } \Gamma_1 \}.$$

Therefore, the approximate counterpart of the continuous variational problem (1.7) is

$$\begin{aligned} &\text{Find } u_h = (u_{1h}, u_{2h}) \in V_h \text{ such that:} \\ &a(u_h, v_h) = l(v_h),\ \forall v_h = (v_{1h}, v_{2h}) \in V_h, \end{aligned} \tag{2.4}$$

with (cf. (1.5) and (1.6))

$$\begin{aligned} a(u_h, v_h) &= \int_\Omega \lambda \operatorname{div} u_h \operatorname{div} v_h \, dx + \int_\Omega 2\mu \sum_{i,j=1}^{2} \varepsilon_{ij}(u_h)\, \varepsilon_{ij}(v_h)\, dx, \\ l(v_h) &= \int_\Omega \sum_{i=1}^{2} f_i v_{ih} \, dx + \int_{\Gamma_2} \sum_{i=1}^{2} g_i v_{ih} \, d\gamma. \end{aligned}$$

Let Σ_h be the set of nodes forming the triangulation (see Figure 2.3), that is,

$$\Sigma_h = \bigcup_{T \in \mathcal{T}_h} \Sigma_T = \{a_i : 1 \le i \le N\}.$$

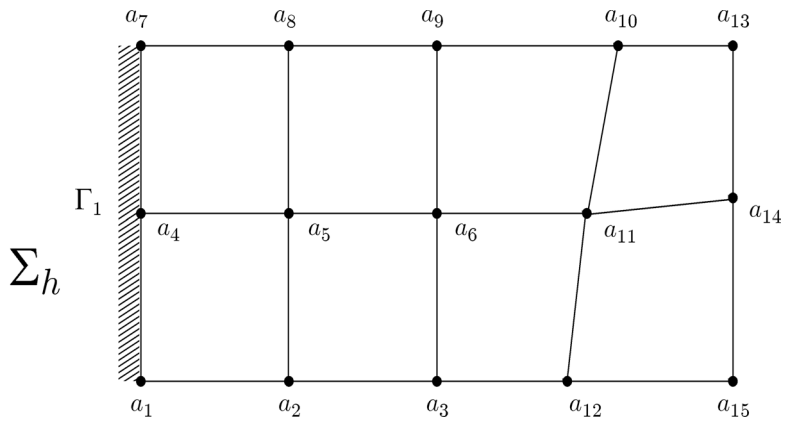

Figure 2.3: Triangulation nodes

Since every function v_{ih} of X_{ih} $(i = 1, 2)$ is univocally determined by the degrees of freedom $v_{ih}(a_1), v_{ih}(a_2), ..., v_{ih}(a_N)$, the dimension of X_{ih} is N. The (global) basis functions of X_{ih} are the N functions $\{w_k : 1 \le k \le N\}$ satisfying

$$w_k \in X_{ih}, \quad w_k(a_j) = \delta_{kj}, \quad i = 1, 2, \quad 1 \le k, j \le N. \tag{2.5}$$

Therefore, every function v_{ih} of X_{ih} has a unique representation

$$v_{ih} = \sum_{j=1}^{N} v_{ih}(a_j)\, w_j.$$

We now introduce the vector of the global degrees of freedom $\widetilde{v}$:

$$\widetilde{v} = \begin{pmatrix} v_{1h}(a_1) \\ v_{2h}(a_1) \\ \vdots \\ v_{1h}(a_N) \\ v_{2h}(a_N) \end{pmatrix}, \quad \widetilde{v} \in \mathbb{R}^{2N}, \quad v_{ih} \in X_{ih},\ i = 1, 2,$$

that is,

$$\begin{cases} \widetilde{v}_{2j-1} = v_{1h}(a_j) \\ \widetilde{v}_{2j} = v_{2h}(a_j) \end{cases}, \quad 1 \le j \le N.$$

Since $\{(w_j,0)\,,\ 1\le j\le N\}$ and $\{(0,w_j)\,,\ 1\le j\le N\}$ are bases of the spaces X_{1h} and X_{2h}, respectively, we write

$$v_h=(v_{1h},v_{2h})=\sum_{j=1}^{N}\widetilde{v}_{2j-1}\,(w_j,0)+\sum_{j=1}^{N}\widetilde{v}_{2j}\,(0,w_j)\,.$$

Then, the bilinear form a can be written as

$$\begin{aligned}a\,(u_h,v_h) &= a\left(\sum_{i=1}^{N}\widetilde{u}_{2i-1}\,(w_i,0)+\sum_{i=1}^{N}\widetilde{u}_{2i}\,(0,w_i)\,,\sum_{j=1}^{N}\widetilde{v}_{2j-1}\,(w_j,0)+\sum_{j=1}^{N}\widetilde{v}_{2j}\,(0,w_j)\right)\\ &= \sum_{i,j=1}^{N}\widetilde{v}_{2j-1}\ a\,((w_j,0)\,,(w_i,0))\ \ \widetilde{u}_{2i-1}+\sum_{i,j=1}^{N}\widetilde{v}_{2j}\ a\,((0,w_j)\,,(w_i,0))\ \ \widetilde{u}_{2i-1}+\\ &\quad+\sum_{i,j=1}^{N}\widetilde{v}_{2j-1}\ a\,((w_j,0)\,,(0,w_i))\ \ \widetilde{u}_{2i}+\sum_{i,j=1}^{N}\widetilde{v}_{2j}\ a\,((0,w_j)\,,(0,w_i))\ \ \widetilde{u}_{2i},\end{aligned}$$

leading to

$$a\,(u_h,v_h)=\widetilde{v}^{\,t}\ A\ \widetilde{u}, \tag{2.6}$$

where A is a matrix of order $2N$ with the following structure:

$$A=\begin{pmatrix} a\,((w_1,0)\,,(w_1,0)) & a\,((w_1,0)\,,(0,w_1)) & \cdots & a\,((w_1,0)\,,(0,w_N))\\ a\,((0,w_1)\,,(w_1,0)) & a\,((0,w_1)\,,(0,w_1)) & \cdots & a\,((0,w_1)\,,(0,w_N))\\ \vdots & \vdots & \vdots & \vdots\\ a\,((0,w_N)\,,(w_1,0)) & a\,((0,w_N)\,,(0,w_1)) & \cdots & a\,((0,w_N)\,,(0,w_N))\end{pmatrix}. \tag{2.7}$$

Since the bilinear form a is symmetric, we have

$$\begin{cases} A_{2i-1,2j-1}=a\,((w_i,0)\,,(w_j,0))\\ A_{2i-1,2j}=a\,((w_i,0)\,,(0,w_j))\\ A_{2i,2j-1}=a\,((0,w_i)\,,(w_j,0))\\ A_{2i,2j}=a\,((0,w_i)\,,(0,w_j))\end{cases},\quad 1\le i,j\le N. \tag{2.8}$$

In a similar way, we obtain for the linear functional l:

$$l\,(v_h)=\widetilde{v}^{\,t}\,b, \tag{2.9}$$

where $b\in\mathbb{R}^{2N}$ is given by

$$b=\begin{pmatrix} l\,((w_1,0))\\ l\,((0,w_1))\\ \vdots\\ l\,((w_N,0))\\ l\,((0,w_N))\end{pmatrix}, \tag{2.10}$$

that is

$$\begin{cases} b_{2i-1}=l\,((w_i,0))\\ b_{2i}=l\,((0,w_i))\end{cases},\quad 1\le i\le N.$$

Supposing that nodes a_{l_i}, $i=1,\ldots,S$, belong to Γ_1, then the members of V_h are such that

$$v_{1h}(a_{l_i})=v_{2h}(a_{l_i})=0,\quad i=1,\ldots,S,$$

or, equivalently,

$$\widetilde{v}_{2l_i-1}=\widetilde{v}_{2l_i}=0,\quad i=1,\ldots,S.$$

Hence, inserting (2.6) and (2.9) into (2.4), we conclude that the approximate problem corresponding to the continuous problem (1.7) is

$$\begin{aligned}&\text{Find } \widetilde{u} \in \mathbb{R}^{2N}, \text{ with } \widetilde{u}_{2l_i-1} = \widetilde{u}_{2l_i} = 0,\ i = 1, \ldots, S, \text{ satisfying:}\\ &\widetilde{v}^{\,t}\, A\, \widetilde{u} = \widetilde{v}^{\,t}\, b\\ &\forall \widetilde{v} \in \mathbb{R}^{2N}, \text{ such that } \widetilde{v}_{2l_i-1} = \widetilde{v}_{2l_i} = 0,\ i = 1, \ldots, S.\end{aligned} \tag{2.11}$$

2.3. Local formulation

Let $T \in \mathcal{T}_h$ be an arbitrary element of the triangulation. Since we are using Lagrange Q_1 elements and

$$Q_1 = \langle 1, x_1, x_2, x_1 x_2 \rangle \qquad \Rightarrow \qquad \dim Q_1 = 4,$$

each (quadrilateral) element T will have 4 nodes

$$\Sigma_T = \left\{ a_1^T, a_2^T, a_3^T, a_4^T \right\},$$

that coincide with the 4 vertices of the element. We also consider

$$p_i^T \in P_T, \quad 1 \le i \le 4,$$

the ith base polynomial of element T (T, P_T, Σ_T), and impose (cf. (2.5))

$$p_i^T \left(a_j^T \right) = \delta_{ij}, \quad 1 \le i, j \le 4. \tag{2.12}$$

Now, let v_{ih} be an arbitrary member of the finite element space X_{ih} $(i = 1, 2)$. We have $v_{ih}|_T \in P_T$ by definition (2.3), so that

$$v_{ih}|_T = \sum_{k=1}^{4} v_{ih}\left(a_k^T\right)\, p_k^T = \begin{pmatrix} p_1^T & p_2^T & p_3^T & p_4^T \end{pmatrix} \begin{pmatrix} v_{ih}\left(a_1^T\right) \\ v_{ih}\left(a_2^T\right) \\ v_{ih}\left(a_3^T\right) \\ v_{ih}\left(a_4^T\right) \end{pmatrix}$$

for $1 \le i \le 2$. We also have

$$\left.\frac{\partial v_{ih}}{\partial x_j}\right|_T = \left(\sum_{k=1}^{4} v_{ih}\left(a_k^T\right)\ \frac{\partial p_k^T}{\partial x_j} \right) = \begin{pmatrix} \frac{\partial p_1^T}{\partial x_j} & \frac{\partial p_2^T}{\partial x_j} & \frac{\partial p_3^T}{\partial x_j} & \frac{\partial p_4^T}{\partial x_j} \end{pmatrix} \begin{pmatrix} v_{ih}\left(a_1^T\right) \\ v_{ih}\left(a_2^T\right) \\ v_{ih}\left(a_3^T\right) \\ v_{ih}\left(a_4^T\right) \end{pmatrix}$$

for $1 \le i, j \le 2$. Therefore, defining the vector of local degrees of freedom, $v_T \in \mathbb{R}^8$,

$$v_T = \left[v_{1h}\left(a_1^T\right), v_{1h}\left(a_2^T\right), v_{1h}\left(a_3^T\right), v_{1h}\left(a_4^T\right), v_{2h}\left(a_1^T\right), v_{2h}\left(a_2^T\right), v_{2h}\left(a_3^T\right), v_{2h}\left(a_4^T\right) \right]^t,$$

we may write, on the one hand,

$$\left.\begin{pmatrix} v_{1h} \\ v_{2h} \end{pmatrix}\right|_T = \left[\mathcal{P}^T\right] v_T \tag{2.13}$$

where

$$\begin{aligned}\left[\mathcal{P}^T\right] &= \begin{pmatrix} p_1^T & p_2^T & p_3^T & p_4^T & 0 & 0 & 0 & 0 \\ 0 & 0 & 0 & 0 & p_1^T & p_2^T & p_3^T & p_4^T \end{pmatrix} \\ &= \begin{pmatrix} \left[P^T\right] & 0 \\ 0 & \left[P^T\right] \end{pmatrix} \in \mathcal{M}_{2\times 8},\end{aligned} \tag{2.14}$$

with

$$\left[P^T\right] = \begin{pmatrix} p_1^T & p_2^T & p_3^T & p_4^T \end{pmatrix} \in \mathcal{M}_{1\times 4},$$

and, on the other hand,

$$\left.\begin{pmatrix} \frac{\partial v_{1h}}{\partial x_1} \\ \frac{\partial v_{1h}}{\partial x_2} \\ \frac{\partial v_{2h}}{\partial x_1} \\ \frac{\partial v_{2h}}{\partial x_2} \end{pmatrix}\right|_T = \left[\mathcal{D}\mathcal{P}^T\right] v_T, \tag{2.15}$$

where

$$\begin{aligned} \left[\mathcal{D}\mathcal{P}^T\right] &= \begin{pmatrix} \frac{\partial p_1^T}{\partial x_1} & \frac{\partial p_2^T}{\partial x_1} & \frac{\partial p_3^T}{\partial x_1} & \frac{\partial p_4^T}{\partial x_1} & 0 & 0 & 0 & 0 \\ \frac{\partial p_1^T}{\partial x_2} & \frac{\partial p_2^T}{\partial x_2} & \frac{\partial p_3^T}{\partial x_2} & \frac{\partial p_4^T}{\partial x_2} & 0 & 0 & 0 & 0 \\ 0 & 0 & 0 & 0 & \frac{\partial p_1^T}{\partial x_1} & \frac{\partial p_2^T}{\partial x_1} & \frac{\partial p_3^T}{\partial x_1} & \frac{\partial p_4^T}{\partial x_1} \\ 0 & 0 & 0 & 0 & \frac{\partial p_1^T}{\partial x_2} & \frac{\partial p_2^T}{\partial x_2} & \frac{\partial p_3^T}{\partial x_2} & \frac{\partial p_4^T}{\partial x_2} \end{pmatrix} \\ &= \begin{pmatrix} \left[DP^T\right] & 0 \\ 0 & \left[DP^T\right] \end{pmatrix} \in \mathcal{M}_{4\times 8}, \end{aligned} \tag{2.16}$$

with

$$\left[DP^T\right] = \begin{pmatrix} \frac{\partial p_1^T}{\partial x_1} & \frac{\partial p_2^T}{\partial x_1} & \frac{\partial p_3^T}{\partial x_1} & \frac{\partial p_4^T}{\partial x_1} \\ \frac{\partial p_1^T}{\partial x_2} & \frac{\partial p_2^T}{\partial x_2} & \frac{\partial p_3^T}{\partial x_2} & \frac{\partial p_4^T}{\partial x_2} \end{pmatrix} \in \mathcal{M}_{2\times 4}.$$

At this stage, it is useful to consider the strain vector $\{\varepsilon\}$ and the stress vector $\{\sigma\}$, which are defined using the entries of the corresponding (symmetric) tensors. For the strain vector $\{\varepsilon\}$ we have (cf. (1.1))

$$\begin{aligned} \left\{\varepsilon\left(v_h\right)\right\}|_T &= \left.\begin{Bmatrix} \varepsilon_{11}\left(v_h\right) \\ \varepsilon_{22}\left(v_h\right) \\ 2\varepsilon_{12}\left(v_h\right) \end{Bmatrix}\right|_T = \begin{pmatrix} \frac{\partial v_{1h}}{\partial x_1} \\ \frac{\partial v_{2h}}{\partial x_2} \\ \frac{\partial v_{1h}}{\partial x_2} + \frac{\partial v_{2h}}{\partial x_1} \end{pmatrix} \\ &= \begin{pmatrix} 1 & 0 & 0 & 0 \\ 0 & 0 & 0 & 1 \\ 0 & 1 & 1 & 0 \end{pmatrix} \left.\begin{Bmatrix} \frac{\partial v_{1h}}{\partial x_1} \\ \frac{\partial v_{1h}}{\partial x_2} \\ \frac{\partial v_{2h}}{\partial x_1} \\ \frac{\partial v_{2h}}{\partial x_2} \end{Bmatrix}\right|_T \\ &= \left[\mathcal{D}\right]\left[\mathcal{D}\mathcal{P}^T\right] v_T, \end{aligned} \tag{2.17}$$

where (2.15) has been used, and

$$\left[\mathcal{D}\right] = \begin{pmatrix} 1 & 0 & 0 & 0 \\ 0 & 0 & 0 & 1 \\ 0 & 1 & 1 & 0 \end{pmatrix}.$$

The stress vector $\{\sigma\}$ is defined by (cf. (1.2))

$$\begin{aligned}
\{\sigma(v_h)\}|_T &= \left\{ \begin{array}{c} \sigma_{11}(v_h) \\ \sigma_{22}(v_h) \\ \sigma_{12}(v_h) \end{array} \right\}\Bigg|_T = \left(\begin{array}{c} \lambda(\varepsilon_{11}+\varepsilon_{22})+2\mu\varepsilon_{11} \\ \lambda(\varepsilon_{11}+\varepsilon_{22})+2\mu\varepsilon_{22} \\ 2\mu\varepsilon_{12} \end{array} \right)\Bigg|_T \\
&= \left(\begin{array}{ccc} \lambda+2\mu & \lambda & 0 \\ \lambda & \lambda+2\mu & 0 \\ 0 & 0 & \mu \end{array} \right)\Bigg|_T \left\{ \begin{array}{c} \varepsilon_{11} \\ \varepsilon_{22} \\ 2\varepsilon_{12} \end{array} \right\}\Bigg|_T \\
&= \left[E^T\right] \{\varepsilon(v_h)\}|_T \\
&= \left[E^T\right] [\mathcal{D}] \left[\mathcal{D}\mathcal{P}^T\right] v_T, \qquad (2.18)
\end{aligned}$$

with

$$\left[E^T\right] = \left(\begin{array}{ccc} \lambda+2\mu & \lambda & 0 \\ \lambda & \lambda+2\mu & 0 \\ 0 & 0 & \mu \end{array} \right)\Bigg|_T .$$

Thus, we can write the bilinear form (1.5) present in the approximate problem (2.4) as

$$a(u_h, v_h) = \int_\Omega \sum_{i,j=1}^{2} \sigma_{ij}(u_h)\, \varepsilon_{ij}(v_h)\, dx = \int_\Omega \{\varepsilon(v_h)\}^t \{\sigma(u_h)\}\, dx.$$

Taking into account that $\overline{\Omega} = \bigcup_{T\in\mathcal{T}_h} T$, we obtain using (2.17) and (2.18)

$$a(u_h, v_h) = \sum_{T\in\mathcal{T}_h} \int_T \{\varepsilon(v_h)\}^t\big|_T \ \{\sigma(u_h)\}|_T\, dx = \sum_{T\in\mathcal{T}_h} \int_T v_T^t \left[\mathcal{D}\mathcal{P}^T\right]^t [\mathcal{D}]^t \left[E^T\right] [\mathcal{D}] \left[\mathcal{D}\mathcal{P}^T\right] u_T\, dx.$$

Furthermore, defining

$$\left[\mathcal{E}^T\right] = [\mathcal{D}]^t \left[E^T\right] [\mathcal{D}] = \left(\begin{array}{cccc} \lambda+2\mu & 0 & 0 & \lambda \\ 0 & \mu & \mu & 0 \\ 0 & \mu & \mu & 0 \\ \lambda & 0 & 0 & \lambda+2\mu \end{array} \right)\Bigg|_T \in \mathcal{M}_{4\times 4},$$

we obtain

$$a(u_h, v_h) = \sum_{T\in\mathcal{T}_h} \int_T v_T^t \left[\mathcal{D}\mathcal{P}^T\right]^t \left[\mathcal{E}^T\right] \left[\mathcal{D}\mathcal{P}^T\right] u_T\, dx. \qquad (2.19)$$

Similarly, we have for the linear functional (1.6) present in the approximate problem (2.4)

$$l(v_h) = \int_\Omega \sum_{i=1}^{2} f_i v_{ih}\, dx + \int_{\Gamma_2} \sum_{i=1}^{2} g_i v_{ih}\, d\gamma = \sum_{T\in\mathcal{T}_h} \left(\int_T \sum_{i=1}^{2} f_i|_T\, v_{ih}|_T\, dx + \int_{T\cap\Gamma_2} \sum_{i=1}^{2} g_i|_{\partial T}\, v_{ih}|_T\, d\gamma \right),$$

resulting

$$l(v_h) = \sum_{T\in\mathcal{T}_h} \left(\int_T \left(\begin{array}{cc} v_{1h} & v_{2h} \end{array} \right)\big|_T \left[f^T\right] dx + \int_{T\cap\Gamma_2} \sum_{i=1}^{2} \left(\begin{array}{cc} v_{1h} & v_{2h} \end{array} \right)\big|_T \left[g^T\right] d\gamma \right),$$

where

$$\left[f^T\right] = \left(\begin{array}{c} f_1 \\ f_2 \end{array} \right)\Bigg|_T \quad \text{and} \quad \left[g^T\right] = \left(\begin{array}{c} g_1 \\ g_2 \end{array} \right)\Bigg|_{\partial T},$$

with $\left[f^T\right]$, $\left[g^T\right] \in \mathcal{M}_{2\times 1}$. Hence, using (2.13) we get

$$l(v_h) = \left(\sum_{T\in\mathcal{T}_h} \int_T v_T^t \left[\mathcal{P}^T\right]^t \left[f^T\right] dx + \int_{T\cap\Gamma_2} v_T^t \left[\mathcal{P}^T\right]^t \left[g^T\right] d\gamma \right). \qquad (2.20)$$

Expressions (2.19) and (2.20) allow us to write the approximate problem (2.4) as

Find $u_h \in X_h$ such that:

$$\sum_{T\in\mathcal{T}_h}\int_T v_T^t\left[\mathcal{D}\mathcal{P}^T\right]^t\left[\mathcal{E}^T\right]\left[\mathcal{D}\mathcal{P}^T\right]u_T\,dx=\sum_{T\in\mathcal{T}_h}\left(\int_T v_T^t\left[\mathcal{P}^T\right]^t\left[f^T\right]\,dx+\int_{T\cap\Gamma_2} v_T^t\left[\mathcal{P}^T\right]^t\left[g^T\right]\,d\gamma\right)$$

$\forall v_T \in V_h$.

2.4. Formulation using the global degrees of freedom

Let us consider once more the vectors of the global degrees of freedom

$$\widetilde{v}=\begin{pmatrix} v_{1h}(a_1)\\ v_{2h}(a_1)\\ \vdots\\ v_{1h}(a_N)\\ v_{2h}(a_N)\end{pmatrix},\quad \widetilde{u}=\begin{pmatrix} u_{1h}(a_1)\\ u_{2h}(a_1)\\ \vdots\\ u_{1h}(a_N)\\ u_{2h}(a_N)\end{pmatrix},\quad \widetilde{u},\widetilde{v}\in\mathbb{R}^{2N},\quad u_{ih},v_{ih}\in X_{ih},\ i=1,2.$$

Given the fact that for an element T, having nodes $a_1^T, a_2^T, a_3^T, a_4^T$, we have

$$a_\alpha^T = a_{n_\alpha^T},\quad 1\le\alpha\le 4,\quad 1\le n_\alpha^T\le N,$$

then there exists a matrix $B^T\in\mathcal{M}_{8\times 2N}$, depending on T, such that

$$v_T=\left[B^T\right]\ \widetilde{v}, \tag{2.21}$$

that is

$$\begin{pmatrix} v_{1h}(a_1^T)\\ v_{1h}(a_2^T)\\ v_{1h}(a_3^T)\\ v_{1h}(a_4^T)\\ v_{2h}(a_1^T)\\ v_{2h}(a_2^T)\\ v_{2h}(a_3^T)\\ v_{2h}(a_4^T)\end{pmatrix}=\begin{pmatrix} v_{1h}(a_{n_1^T})\\ v_{1h}(a_{n_2^T})\\ v_{1h}(a_{n_3^T})\\ v_{1h}(a_{n_4^T})\\ v_{2h}(a_{n_1^T})\\ v_{2h}(a_{n_2^T})\\ v_{2h}(a_{n_3^T})\\ v_{2h}(a_{n_4^T})\end{pmatrix}=\left[B^T\right]\begin{pmatrix} v_{1h}(a_1)\\ v_{2h}(a_1)\\ v_{1h}(a_2)\\ v_{2h}(a_2)\\ \vdots\\ v_{1h}(a_N)\\ v_{2h}(a_N)\end{pmatrix}.$$

It can be easily shown that

$$\left[B^T\right]_{i,j}=\delta_{j,2n_i^T-1}\quad\text{and}\quad\left[B^T\right]_{i+4,j}=\delta_{j,2n_i^T},$$

with $1\le i\le 4$ and $1\le j\le 2N$. We may also write

$$\left[B^T\right]_{ij}=\begin{cases}\delta_{j,2n_i^T-1} & if\quad 1\le i\le 4,\\ \delta_{j,2n_{i-4}^T} & if\quad 5\le i\le 8,\end{cases}=\delta_{j,\zeta_i^T}, \tag{2.22}$$

where

$$\zeta_i^T=\begin{cases}2n_i^T-1 & if\quad 1\le i\le 4,\\ 2n_{i-4}^T & if\quad 5\le i\le 8.\end{cases} \tag{2.23}$$

For example, for the triangulation shown in Figure 2.4,

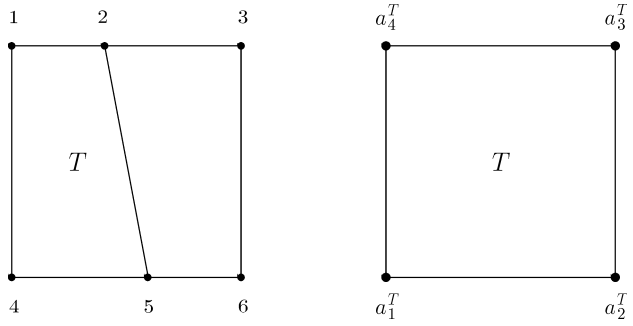

Figure 2.4: Node numbers: Global (left) and local (right)

we would have for element T ($N = 6$):

$$n_1^T = 4, \quad n_2^T = 5, \quad n_3^T = 2, \quad n_4^T = 1,$$

leading to

$$\zeta^T = \{7,\ 9,\ 3,\ 1,\ 8,\ 10,\ 4,\ 2\}$$

In this case $B^T \in \mathcal{M}_{8\times 12}$ would be given by (cf. (2.22))

$$\left[B^T\right] = \begin{pmatrix} 0 & \cdots & \cdots & \cdots & \cdots & 0 & 1 & 0 & \cdots & \cdots & \cdots & 0 \\ 0 & \cdots & \cdots & \cdots & \cdots & \cdots & \cdots & 0 & 1 & 0 & \cdots & 0 \\ 0 & 0 & 1 & 0 & \cdots & \cdots & \cdots & \cdots & \cdots & \cdots & \cdots & 0 \\ 1 & 0 & \cdots & \cdots & \cdots & \cdots & \cdots & \cdots & \cdots & \cdots & \cdots & 0 \\ 0 & \cdots & \cdots & \cdots & \cdots & \cdots & 0 & 1 & 0 & \cdots & \cdots & 0 \\ 0 & \cdots & \cdots & \cdots & \cdots & \cdots & \cdots & \cdots & 0 & 1 & 0 & 0 \\ 0 & \cdots & 0 & 1 & 0 & \cdots & \cdots & \cdots & \cdots & \cdots & \cdots & 0 \\ 0 & 1 & 0 & \cdots & \cdots & \cdots & \cdots & \cdots & \cdots & \cdots & \cdots & 0 \end{pmatrix}.$$

We are now able to write the approximate problem using the global degrees of freedom. For that we suppose that nodes a_{l_i}, $i = 1, \ldots, S$, belong to Γ_1, that is,

$$u_{1h}(a_{l_i}) = u_{2h}(a_{l_i}) = 0, \quad i = 1, \ldots, S,$$

or, equivalently,

$$\widetilde{u}_{2l_i-1} = \widetilde{u}_{2l_i} = 0, \quad i = 1, \ldots, S.$$

Hence, the approximate problem (2.4) can be written in the form

Find $\widetilde{u} \in \mathbb{R}^{2N}$, with $\widetilde{u}_{2l_i-1} = \widetilde{u}_{2l_i} = 0,\ i = 1, \ldots, S$, satisfying:

$$\sum_{T\in\mathcal{T}_h} \int_T \widetilde{v}^t \ \left[B^T\right]^t \ \left[\mathcal{D}\mathcal{P}^T\right]^t \ \left[\mathcal{E}^T\right] \ \left[\mathcal{D}\mathcal{P}^T\right] \ \left[B^T\right] \ \widetilde{u}\, dx =$$

$$= \sum_{T\in\mathcal{T}_h} \left(\int_T \widetilde{v}^t \ \left[B^T\right]^t \ \left[\mathcal{P}^T\right]^t \ \left[f^T\right] \, dx + \int_{T\cap\Gamma_2} \widetilde{v}^t \ \left[B^T\right]^t \ \left[\mathcal{P}^T\right]^t \ \left[g^T\right] \, d\gamma \right),$$

$\forall v_h \in V_h$, where $\widetilde{v} = \left[v_{1h}\left(a_1\right), v_{2h}\left(a_1\right), \ldots, v_{1h}\left(a_N\right), v_{2h}\left(a_N\right)\right]^t \in \mathbb{R}^{2N}$.

Since the mapping from $v_h \in V_h$ to $\widetilde{v} \in \mathbb{R}^{2N}$, such that

$$\widetilde{v}_{2l_i-1} = \widetilde{v}_{2l_i} = 0, \quad i = 1, \ldots, S,$$

is an isomorphism, the approximate problem (2.4) is equivalent to

$$\begin{aligned}
&\text{Find } \widetilde{u} \in \mathbb{R}^{2N}, \text{ with } \widetilde{u}_{2l_i-1} = \widetilde{u}_{2l_i} = 0,\ i = 1, \ldots, S, \text{ satisfying:} \\
&\widetilde{v}^t \left\{ \sum_{T \in \mathcal{T}_h} \left[B^T\right]^t \left(\int_T \left[\mathcal{D}\mathcal{P}^T\right]^t \left[\mathcal{E}^T\right] \left[\mathcal{D}\mathcal{P}^T\right] dx \right) \left[B^T\right] \right\} \widetilde{u} = \\
&\qquad = \widetilde{v}^t \left\{ \sum_{T \in \mathcal{T}_h} \left[B^T\right]^t \left(\int_T \left[\mathcal{P}^T\right]^t \left[f^T\right] dx + \int_{T \cap \Gamma_2} \left[\mathcal{P}^T\right]^t \left[g^T\right] d\gamma \right) \right\}, \\
&\forall \widetilde{v} \in \mathbb{R}^{2N}, \text{ such that } \widetilde{v}_{2l_i-1} = \widetilde{v}_{2l_i} = 0,\ i = 1, \ldots, S.
\end{aligned}$$

Defining the elementary rigidity matrix

$$\left[R^T\right] = \int_T \left[\mathcal{D}\mathcal{P}^T\right]^t \left[\mathcal{E}^T\right] \left[\mathcal{D}\mathcal{P}^T\right] dx, \quad R^T \in \mathcal{M}_{8\times 8}, \tag{2.24}$$

and the elementary second member vector

$$b^T = \int_T \left[\mathcal{P}^T\right]^t \left[f^T\right] dx + \int_{T \cap \Gamma_2} \left[\mathcal{P}^T\right]^t \left[g^T\right] d\gamma, \quad b^T \in \mathbb{R}^8, \tag{2.25}$$

the approximate problem is written

$$\begin{aligned}
&\text{Find } \widetilde{u} \in \mathbb{R}^{2N}, \text{ such that } \widetilde{u}_{2l_i-1} = \widetilde{u}_{2l_i} = 0,\ i = 1, \ldots, S, \text{ satisfying:} \\
&\widetilde{v}^t \left\{ \sum_{T \in \mathcal{T}_h} \left[B^T\right]^t \left[R^T\right] \left[B^T\right] \right\} \widetilde{u} = \widetilde{v}^t \left\{ \sum_{T \in \mathcal{T}_h} \left[B^T\right]^t b^T \right\}, \\
&\forall \widetilde{v} \in \mathbb{R}^{2N}, \text{ with } \widetilde{v}_{2l_i-1} = \widetilde{v}_{2l_i} = 0,\ i = 1, \ldots, S.
\end{aligned}$$

It is useful to define the global rigidity matrix

$$A = \sum_{T \in \mathcal{T}_h} \left[B^T\right]^t \left[R^T\right] \left[B^T\right], \quad A \in \mathcal{M}_{2N\times 2N}, \tag{2.26}$$

as well as the global second member vector

$$b = \sum_{T \in \mathcal{T}_h} \left[B^T\right]^t b^T, \quad b \in \mathbb{R}^{2N}. \tag{2.27}$$

The approximate problem is now

$$\begin{aligned}
&\text{Find } \widetilde{u} \in \mathbb{R}^{2N}, \text{ such that } \widetilde{u}_{2l_i-1} = \widetilde{u}_{2l_i} = 0,\ i = 1, \ldots, S, \text{ satisfying:} \\
&\widetilde{v}^t A \widetilde{u} = \widetilde{v}^t b, \\
&\forall \widetilde{v} \in \mathbb{R}^{2N}, \text{ with } \widetilde{v}_{2l_i-1} = \widetilde{v}_{2l_i} = 0,\ i = 1, \ldots, S.
\end{aligned} \tag{2.28}$$

Since the approximate problems (2.11) and (2.28) are the same, we conclude that there are two equivalent ways of defining the rigidity matrix A - (2.7) and (2.26) - and the second member vector b - (2.10) and (2.27).

Let us suppose that, for practical reasons, the numbers of the S nodes belonging to Γ_1 are the $N - S$ last ones, that is,

$$l_1 = M + 1,\ l_2 = M + 2,\ \ldots,\ l_S = M + S = N.$$

Then

$$v_h \in V_h \quad \Leftrightarrow \quad \widetilde{v} = \begin{pmatrix} \widetilde{v}_{\mathrm{I}} \\ \widetilde{v}_{\mathrm{II}} \end{pmatrix} = \begin{pmatrix} \widetilde{v}_{\mathrm{I}} \\ 0 \end{pmatrix},\ \widetilde{v}_{\mathrm{I}} \in \mathbb{R}^{2M}.$$

Using the following decomposition of A and b:

$$A = \begin{pmatrix} A_{\mathrm{II}} & A_{\mathrm{III}} \\ A_{\mathrm{III}} & A_{\mathrm{IIII}} \end{pmatrix}, \quad A_{\mathrm{II}} \in \mathcal{M}_{2M\times 2M},$$
$$b = \begin{pmatrix} b_{\mathrm{I}} \\ b_{\mathrm{II}} \end{pmatrix}, \quad b_{\mathrm{I}} \in \mathbb{R}^{2M},$$

the approximate problem (2.28) becomes

$$\begin{array}{l} \text{Find } \widetilde{u}_{\mathrm{I}} \in \mathbb{R}^{2M} \text{ such that:} \\ \begin{pmatrix} \widetilde{v}_{\mathrm{I}} \\ 0 \end{pmatrix}^t \begin{pmatrix} A_{\mathrm{II}} & A_{\mathrm{III}} \\ A_{\mathrm{III}} & A_{\mathrm{IIII}} \end{pmatrix} \begin{pmatrix} \widetilde{u}_{\mathrm{I}} \\ 0 \end{pmatrix} = \begin{pmatrix} \widetilde{v}_{\mathrm{I}} \\ 0 \end{pmatrix}^t \begin{pmatrix} b_{\mathrm{I}} \\ b_{\mathrm{II}} \end{pmatrix}, \\ \forall \widetilde{v}_I \in \mathbb{R}^{2M}, \end{array} \tag{2.29}$$

that is, the linear system of order $2M$

$$\begin{array}{l} \text{Find } \widetilde{u}_{\mathrm{I}} \in \mathbb{R}^{2M} \text{ such that:} \\ A_{\mathrm{II}}\, \widetilde{u}_{\mathrm{I}} = b_{\mathrm{I}}. \end{array}$$

There are several ways of solving this problem, in particular concerning the scheme used to impose the conditions to the nodes belonging to Γ_1. However, from the computational point of view, the best way is to solve a problem that is "computationally equivalent" to (2.29), namely,

$$\begin{array}{l} \text{Find } \widetilde{u} = (\widetilde{u}_{\mathrm{I}}, \widetilde{u}_{\mathrm{II}})^t \in \mathbb{R}^{2N}, \text{ with } \widetilde{u}_{\mathrm{I}} \in \mathbb{R}^{2M} \text{ and } \widetilde{u}_{\mathrm{II}} \in \mathbb{R}^{2S}, \text{ such that:} \\ \begin{pmatrix} A_{\mathrm{II}} & A_{\mathrm{III}} \\ A_{\mathrm{III}} & \theta\, \mathbb{I} \end{pmatrix} \begin{pmatrix} \widetilde{u}_{\mathrm{I}} \\ \widetilde{u}_{\mathrm{II}} \end{pmatrix} = \begin{pmatrix} b_{\mathrm{I}} \\ 0 \end{pmatrix}, \end{array} \tag{2.30}$$

where $\mathbb{I}$ is the identity matrix of order $2S$ and θ is a high value constant (for example, 10^{30}).

If, for sake of flexibility, we do not impose any particular scheme for the numbering of the nodes belonging to Γ_1, a simple algebraic manipulation of the system of equations (2.30) leads to the equivalent problem:

$$\begin{array}{l} \text{Find } \widetilde{u} \in \mathbb{R}^{2N} \text{ such that:} \\ \widetilde{A}\, \widetilde{u} \ = \widetilde{b}, \end{array}$$

where $\widetilde{A}$ and $\widetilde{b}$ are built using A and b as a base, respectively, taking into account the conditions imposed to the nodes lying on Γ_1. In this case, the entries of A and b coincide with those of $\widetilde{A}$ and $\widetilde{b}$, except the following ones:

$$\begin{cases} \widetilde{A}_{2l_i-1,2l_i-1} = \widetilde{A}_{2l_i,2l_i} = \theta \\ \widetilde{b}_{2l_i-1} = \widetilde{b}_{2l_i} = 0 \end{cases}, \quad i = 1, \ldots, S,$$

In this way, the matrix A and the vector b depend only on the triangulation and the finite element chosen, being not affected by the essential boundary conditions present in the problem. We also note that this procedure can be used to "block" any degrees of freedom that do not belong to Γ_1 if that is required by the nature of the problem being addressed.

Since $\widetilde{A}$ is a positive-definite symmetric band matrix, $\widetilde{A}\, \widetilde{u} \ = \widetilde{b}$ is solved using the Choleski direct solution method, the entries of $\widetilde{A}$ being stored as described at the end of § 2.5.

2.5. Some implementation considerations and algorithms

2.5.1. Main steps

1. Representation of the geometrical data concerning the triangulation (mesh generation).

2. Finite elements data (nodes, reference element, base polynomials, ...).

3. For each element: computation of the elementary rigidity matrix R^T and the elementary second member vector b^T (involves problem data, numerical integration quadrature formulae, ...).

4. Assembly of the rigidity matrix: $A = \sum_{T \in \mathcal{T}_h} \left[B^T\right]^t \left[R^T\right] \left[B^T\right]$.

5. Assembly of the second member vector: $b = \sum_{T \in \mathcal{T}_h} \left[B^T\right]^t \; b^T$.

6. Handling of essential boundary conditions: $A \to \widetilde{A}$, $b \to \widetilde{b}$.

7. Solution of the linear system $\widetilde{A}\widetilde{u} = \widetilde{b}$.

8. Complementary calculations (stresses, error estimates, ...).

9. Postprocessing: graphics, interface with other problems.

2.5.2. Representation of geometrical data for the triangulation

We suppose that the mesh is generated *a priori*, being therefore considered as input data for the problem. Anyway, to describe a triangulation appropriately we need the following data (see Figure 2.5):

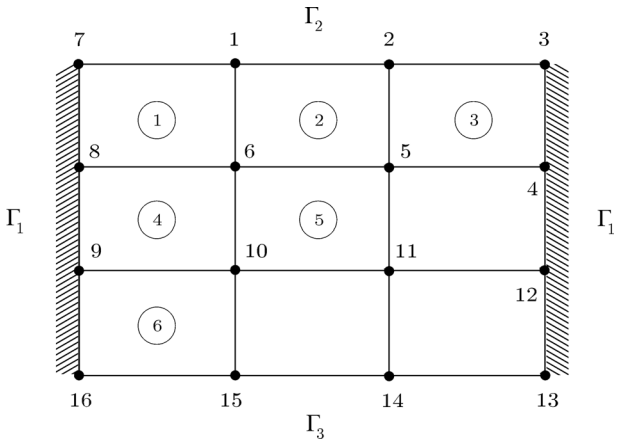

Figure 2.5: Triangulation data

a) *Coordinates of the N nodes*, $a_1, a_2, \ldots, a_N$. This information can be stored in a matrix $z\,(N, 2)$ of reals where z_{ij} is the jth coordinate of node number i. The origin of the (global) coordinate system is arbitrary.

b) *List of nodes in each of the N_e elements (connectivities):* lists the nodes $a_{n_1^T}, a_{n_2^T}, a_{n_3^T}, a_{n_4^T}$, of each element $T \in \mathcal{T}_h$. The description is made using a matrix of integers, $M\,(N_e, 4)$, where m_{ij} is the number the jth node of the ith element. In the (local) numbering of the nodes of each element these should be considered is counter-clockwise direction (see Figure 2.6).

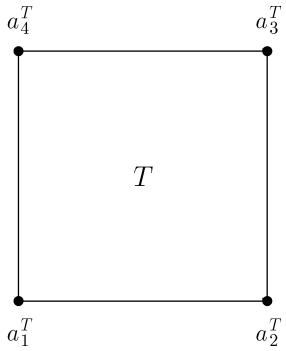

Figure 2.6: Local numbering of nodes

For the mesh in Figure 2.5 we would have:

$$M = \begin{pmatrix} 1 & 7 & 8 & 6 \\ 6 & 5 & 2 & 1 \\ 5 & 4 & 3 & 2 \\ 9 & 10 & 6 & 8 \\ 10 & 11 & 5 & 6 \\ \vdots & \vdots & \vdots & \vdots \end{pmatrix}.$$

c) *Reference numbers for nodes and edges:* Indicate if a given node/edge belongs to a given part of the boundary. These numbers are used to impose the boundary conditions. We have

$$l(i) = \begin{cases} 0 & \text{if} \quad a_i \text{ is an interior node} \\ j & \text{if} \quad \text{node } i \text{ belongs to } \Gamma_j \end{cases}, \quad 1 \leq i \leq N.$$

For the mesh in the previous example we would get:

$$l\,(1) = 2, \quad l\,(3) = 1, \quad l\,(8) = 1, \quad l\,(11) = 0, \quad l\,(14) = 3.$$

For the faces we consider a matrix of integers, $K\,(N_e, 4)$, where k_{ij} indicates the "position" of the jth face of the ith element. Therefore, for element number i we have

$$K(i,j) = \begin{cases} 0 \\ m \end{cases} \text{ if the face starting in the jth node } \begin{cases} \text{is interior,} \\ \text{belongs to } \Gamma_m. \end{cases}$$

We suppose that, for a given element T, the 4 faces are taken in the direct sense. Therefore, for the mesh in Figure 2.5 we obtain

$$K = \begin{pmatrix} 2 & 1 & 0 & 0 \\ 0 & 0 & 2 & 0 \\ 0 & 1 & 2 & 0 \\ 0 & 0 & 0 & 1 \\ 0 & 0 & 0 & 0 \\ \vdots & \vdots & \vdots & \vdots \end{pmatrix}.$$

2.5.3. Assembly of the rigidity matrix

As we have seen previously (cf. (2.26)), the rigidity matrix is given by

$$A = \sum_{T \in \mathcal{T}_h} \left[B^T\right]^t \left[R^T\right] \left[B^T\right],$$

where R^T is the elementary rigidity matrix. On the other hand, if T is a triangulation element with vertices

$$a_i^T = a_{n_i^T}, \quad 1 \le i \le 4,$$

then (cf. (2.22)),

$$\left[B^T\right]_{ij} = \delta_{j,\zeta_i^T}, \quad 1 \le i \le 8, \quad 1 \le j \le 2N,$$

with ζ_i^T given by (2.23). Therefore, the contribution of element T to the global matrix A is, taking $1 \le i, j \le 2N$

$$\begin{aligned}\left(\left[B^T\right]^t \left[R^T\right] \left[B^T\right]\right)_{ij} &= \sum_{m=1}^{8} \left(\left[B^T\right]^t \left[R^T\right]\right)_{im} \left[B^T\right]_{mj} = \sum_{l,m=1}^{8} \left[B^T\right]_{il}^t \left[R^T\right]_{lm} \left[B^T\right]_{mj} \\ &= \sum_{l,m=1}^{8} \left[R^T\right]_{lm} \left[B^T\right]_{li} \left[B^T\right]_{mj} \\ &= \sum_{l,m=1}^{8} \left[R^T\right]_{lm} \delta_{i,\zeta_l^T}\, \delta_{j,\zeta_m^T},\end{aligned}$$

that is,

$$\left(\left[B^T\right]^t \left[R^T\right] \left[B^T\right]\right)_{ij} = \begin{cases} \left[R^T\right]_{\alpha\beta} & \text{if} \quad i = \zeta_\alpha^T,\ j = \zeta_\beta^T, \text{ for some } \alpha, \beta \in \{1, 2, \ldots, 8\}, \\ 0 & \text{otherwise.} \end{cases}$$

Hence, the only entries of A to which T contributes to are $A_{\zeta_\alpha^T, \zeta_\beta^T}$, $1 \le \alpha, \beta \le 8$, which are modified by adding $\left[R^T\right]_{\alpha\beta}$. The algorithm to build the rigidity matrix is then

```
Initialize to zero the matrix A of order 2N
For all the elements T of the triangulation, 1, 2, ..., N_e, do
    For α = 1, ..., 8 do
        For β = 1, ..., 8 do
            A_{ζ_α^T, ζ_β^T} = A_{ζ_α^T, ζ_β^T} + R^T_{αβ}
        End of loop on β
    End of loop on α
End of loop on the triangulation elements
```

2.5.4. Assembly of the second member vector

As we have seen previously (cf. (2.27))

$$b = \sum_{T \in \mathcal{T}_h} \left[B^T\right]^t \ b^T$$

where $b^T \in \mathbb{R}^8$ and $b \in \mathbb{R}^{2N}$. The contribution of element T to the global vector b is, taking $1 \le j \le 2N$,

$$\left(\left[B^T\right]^t b^T\right)_j = \sum_{k=1}^{8} \left[B^T\right]_{jk}^t b_k^T = \sum_{k=1}^{8} \left[B^T\right]_{kj} b_k^T = \sum_{k=1}^{8} \delta_{j,\zeta_k^T}\ b_k^T,$$

that is,

$$\left(\left[B^T\right]^t b^T\right)_j = \begin{cases} b_\alpha^T & \text{if} \quad j = \zeta_\alpha^T, \text{ for some } \alpha \in \{1, 2, \ldots, 8\}, \\ 0 & \text{otherwise.} \end{cases}$$

Therefore, the only entries of b to which T contributes to are $b_{\zeta_\alpha^T}$, $1 \le \alpha \le 8$, that are modified by adding b_α^T. The algorithm to build the global second member vector is then

```
Initialize to zero the vector b ∈ ℝ^{2N}
For all the elements T of the triangulation, 1, 2, ..., N_e, do
    For α = 1, ..., 8 do
        b_{ζ_α^T} = b_{ζ_α^T} + b_α^T.
    End of loop on α
End of loop on the triangulation elements
```

2.5.5. Rigidity matrix bandwidth and profile

In order to establish the bandwidth and profile of the rigidity matrix A we consider (2.8) again:

$$\begin{cases} A_{2i-1,2j-1} = a\left((w_i,0),(w_j,0)\right) \\ A_{2i-1,2j} = a\left((w_i,0),(0,w_j)\right) \\ A_{2i,2j-1} = a\left((0,w_i),(w_j,0)\right) \\ A_{2i,2j} = a\left((0,w_i),(0,w_j)\right) \end{cases}, \quad 1 \le i,j \le N.$$

Due to the form of a (cf. (1.5)), the entries listed above, involving the 2 degrees of freedom of nodes i and j, are not zero only if the supports of the base functions w_i and w_j have non-empty intersection. Therefore, entries $2j-1$ and $2j$ of lines $2i-1$ and $2i$ of matrix A are not zero only if nodes i and j belong to the same element. So, A is a sparse matrix, as expected. Moreover, A is a symmetric matrix, having a (symmetric) profile as illustrated in Figure 2.7, where

$$\lambda(i) = \min\left\{j : 1 \le j \le i,\ A_{ij} \neq 0\right\}, \quad 1 \le i \le 2N,$$

that is,

$$A_{i1} = A_{i2} = \ldots = A_{i\,\lambda(i)-1} = 0, \quad 1 \le i \le 2N.$$

Therefore, the bandwidth of the rigidity matrix is given by

$$\text{bandwidth of } A = \max_{1\le j\le i\le 2N}\left\{i-j+1 : A_{ij}\neq 0\right\} = \max_{1\le i\le 2N}\left\{i-\lambda(i)+1\right\}.$$

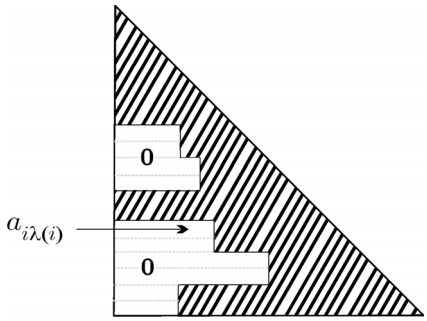

Figure 2.7: Rigidity matrix profile

For a given triangulation, the entries of λ are given by

$$\lambda(2i-1) = \lambda(2i) = \min\left\{2n_j^T - 1, \forall T \in \mathcal{T}_h : a_i \in T,\ 1 \le j \le 4\right\}, \quad 1 \le i \le N.$$

For computational reasons, it is advisable to store only the non-zero elements of each row of A

$$A_{i\,\lambda(i)}, A_{i\,\lambda(i)+1}, \ldots, A_{ii}, \quad 1 \le i \le 2N,$$

in a vector α. Since the matrix is symmetric, we need only to store the diagonal and lower triangle. In this way, to locate an element of A in vector α we just need to know the indexes vector μ:

$$\mu(1) = 0, \quad \mu(i+1) = \text{position in } \alpha \text{ of entry } A_{ii},\ 1 \leq i \leq 2N.$$

As a result

$$A_{ij} = \alpha(\mu(i) + j - \lambda(i) + 1), \quad j = \lambda(i), \lambda(i)+1, \ldots, i.$$

The pointer μ is obtained from vector λ:

$$\mu(i+1) = \mu(i) + i - \lambda(i) + 1, \quad 1 \leq i \leq 2N.$$

To minimize the bandwidth (and consequently the length of vector α and the memory needed to store A), it is essential that the non-zero elements stay as close as possible to the diagonal. For this reason, we should number the nodes so that for a given element the corresponding node numbers are as close as possible to each other. This is a problem without optimal solution. There are, however, some good numbering algorithms that can be used to minimize the bandwidth based on the theory of graphs (Gibbs, Grooms, Akha, Cuthill-Mckee, etc.).

2.6. Computation of elementary rigidity matrices and second member vectors

The computation of the elementary rigidity matrix (2.24) and of the second member vector (2.25) involves the evaluation of integrals. These integrals, involving the elementary matrices $[\mathcal{P}^T]$ and $[\mathcal{D}\mathcal{P}^T]$ - see (2.14) and (2.16), respectively - are calculated using a change of variable to the reference element as described below.

2.6.1. Change of variable to the reference square $\widehat{T}$

Let us consider again the reference finite element $\widehat{T}$. As we have seen previously (cf. § 2.1), for a given finite element T we consider the invertible map $F_T : \mathbb{R}^2 \to \mathbb{R}^2$, such that

$$T = F_T(\widehat{T}) \qquad \text{and} \qquad F_T(\widehat{x}) = \sum_{i=1}^{4} \left(a_i^T\right) \widehat{p}_i(\widehat{x}) \in \left(\widehat{Q}_1\right)^2,$$

where $\{a_i^T,\ i = 1, ..., 4\}$ stands for the set of nodes of T (recall Figures 2.1 and 2.2). In this way,

$$\begin{aligned} F_T(\widehat{x}) &= \begin{pmatrix} (F_T)_1(\widehat{x}) \\ (F_T)_2(\widehat{x}) \end{pmatrix} \\ &= \begin{pmatrix} c_{11}^T + c_{12}^T\widehat{x}_1 + c_{13}^T\widehat{x}_2 + c_{14}^T\widehat{x}_1\widehat{x}_2 \\ c_{21}^T + c_{22}^T\widehat{x}_1 + c_{23}^T\widehat{x}_2 + c_{24}^T\widehat{x}_1\widehat{x}_2 \end{pmatrix}, \end{aligned} \tag{2.31}$$

where $\widehat{x} = [\widehat{x}_1, \widehat{x}_2]^t \in [0,1]^2$. Denoting the coordinates of the vertices of T by

$$x_{ij} = x_i\left(a_j^T\right), \quad 1 \leq i \leq 2, \quad 1 \leq j \leq 4,$$

it can be easily shown that

$$c_{i1}^T = x_{i1}, \quad c_{i2}^T = x_{i2} - x_{i1}, \quad c_{i3}^T = x_{i4} - x_{i1}, \quad c_{i4}^T = x_{i3} + x_{i1} - x_{i2} - x_{i4},$$

with $i = 1, 2$. On the other hand, we have shown that (cf. (2.2))

$$\widehat{p}_i(\widehat{x}) = p_i^T(x), \quad 1 \leq i \leq 4. \tag{2.32}$$

This result, together with condition (cf. (2.12))

$$p_i^T \in P_T, \quad p_i^T(a_j^T) = \delta_{ij}, \quad 1 \leq i, j \leq 4,$$

leads to

$$\widehat{p}_i \in \widehat{Q}_1, \quad \widehat{p}_i\left(\widehat{a}_j\right) = \delta_{ij}, \quad 1 \leq i, j \leq 4.$$

Therefore,

$$\widehat{p}_1 = \left(1-\widehat{x}_1\right)\left(1-\widehat{x}_2\right), \quad \widehat{p}_2 = \left(1-\widehat{x}_2\right)\widehat{x}_1, \quad \widehat{p}_3 = \widehat{x}_1\widehat{x}_2, \quad \widehat{p}_4 = \left(1-\widehat{x}_1\right)\widehat{x}_2.$$

From (2.14) and (2.32) we obtain

$$\left[\mathcal{P}^T\right](x) = \left[\mathcal{P}^T\right] \circ F_T\left(\widehat{x}\right) = \left[\widehat{\mathcal{P}}\right]\left(\widehat{x}\right), \tag{2.33}$$

where

$$[\widehat{\mathcal{P}}] = \begin{pmatrix} \widehat{p}_1 & \widehat{p}_2 & \widehat{p}_3 & \widehat{p}_4 & 0 & 0 & 0 & 0 \\ 0 & 0 & 0 & 0 & \widehat{p}_1 & \widehat{p}_2 & \widehat{p}_3 & \widehat{p}_4 \end{pmatrix} = \begin{pmatrix} [\widehat{P}] & 0 \\ 0 & [\widehat{P}] \end{pmatrix} \in \mathcal{M}_{2\times 8},$$

with $[\widehat{P}] \in \mathcal{M}_{1\times 4}$ given by

$$[\widehat{P}] = \begin{pmatrix} \widehat{p}_1 & \widehat{p}_2 & \widehat{p}_3 & \widehat{p}_4 \end{pmatrix} = \begin{pmatrix} \left(1-\widehat{x}_1\right)\left(1-\widehat{x}_2\right) & \left(1-\widehat{x}_2\right)\widehat{x}_1 & \widehat{x}_1\widehat{x}_2 & \left(1-\widehat{x}_1\right)\widehat{x}_2 \end{pmatrix}$$

Furthermore, defining

$$\widehat{\nabla}\widehat{p}_i = \begin{pmatrix} \frac{\partial \widehat{p}_i}{\partial \widehat{x}_1} \\ \frac{\partial \widehat{p}_i}{\partial \widehat{x}_2} \end{pmatrix} \in \mathbb{R}^2, \quad \nabla p_i^T = \begin{pmatrix} \frac{\partial p_i^T}{\partial x_1} \\ \frac{\partial p_i^T}{\partial x_2} \end{pmatrix} \in \mathbb{R}^2, \qquad i = 1, 2,$$

and taking into account that

$$\frac{\partial \widehat{p}_i(\widehat{x})}{\partial \widehat{x}_j} = \frac{\partial p_i^T(x)}{\partial \widehat{x}_j} = \sum_{k=1}^{2} \frac{\partial x_k}{\partial \widehat{x}_j}\frac{\partial p_i^T}{\partial x_k} = \sum_{k=1}^{2} \frac{\partial \left(F_T\right)_k\left(\widehat{x}\right)}{\partial \widehat{x}_j}\frac{\partial p_i^T}{\partial x_k},$$

we get

$$\left(\widehat{\nabla}\widehat{p}_1 \mid \widehat{\nabla}\widehat{p}_2 \mid \widehat{\nabla}\widehat{p}_3 \mid \widehat{\nabla}\widehat{p}_4\right)\left(\widehat{x}\right) = \left[F_T'\left(\widehat{x}\right)\right] \ \left(\nabla p_1^T \mid \nabla p_2^T \mid \nabla p_3^T \mid \nabla p_4^T\right)(x),$$

where $F_T'\left(\widehat{x}\right) \in \mathcal{M}_{2\times 2}$ is given by (cf. (2.31))

$$F_T'\left(\widehat{x}\right) = \begin{pmatrix} \frac{\partial (F_T)_1}{\partial \widehat{x}_1} & \frac{\partial (F_T)_2}{\partial \widehat{x}_1} \\ \frac{\partial (F_T)_1}{\partial \widehat{x}_2} & \frac{\partial (F_T)_2}{\partial \widehat{x}_2} \end{pmatrix} = \begin{pmatrix} c_{12}^T + c_{14}^T\widehat{x}_2 & c_{22}^T + c_{24}^T\widehat{x}_2 \\ c_{13}^T + c_{14}^T\widehat{x}_1 & c_{23}^T + c_{24}^T\widehat{x}_1 \end{pmatrix}.$$

So, we can write

$$\left(\nabla p_1^T \mid \nabla p_2^T \mid \nabla p_3^T \mid \nabla p_4^T\right)(x) = \left[F_T'\left(\widehat{x}\right)\right]^{-1} \ \left(\widehat{\nabla}\widehat{p}_1 \mid \widehat{\nabla}\widehat{p}_2 \mid \widehat{\nabla}\widehat{p}_3 \mid \widehat{\nabla}\widehat{p}_4\right)\left(\widehat{x}\right).$$

Taking

$$G_T(\widehat{x}) = \left[F_T'\left(\widehat{x}\right)\right]^{-1} = \frac{1}{\det\left[F_T'\left(\widehat{x}\right)\right]} \begin{pmatrix} c_{23}^T + c_{24}^T\widehat{x}_1 & -c_{22}^T - c_{24}^T\widehat{x}_2 \\ -c_{13}^T - c_{14}^T\widehat{x}_1 & c_{12}^T + c_{14}^T\widehat{x}_2 \end{pmatrix} \in \mathcal{M}_{2\times 2} \tag{2.34}$$

and defining

$$\mathcal{G}_T(\widehat{x}) = \begin{pmatrix} G_T(\widehat{x}) & 0 \\ 0 & G_T(\widehat{x}) \end{pmatrix} \in \mathcal{M}_{4\times 4}, \tag{2.35}$$

leads to (cf. (2.16))

$$\left[\mathcal{D}\mathcal{P}^T\right](x) = \mathcal{G}_T(\widehat{x}) \ [\widehat{\mathcal{D}}\widehat{\mathcal{P}}](\widehat{x}), \tag{2.36}$$

where

$$\left[\widehat{\mathcal{D}}\widehat{\mathcal{P}}\right] = \begin{pmatrix} \frac{\partial \widehat{p}_1}{\partial \widehat{x}_1} & \frac{\partial \widehat{p}_2}{\partial \widehat{x}_1} & \frac{\partial \widehat{p}_3}{\partial \widehat{x}_1} & \frac{\partial \widehat{p}_4}{\partial \widehat{x}_1} & 0 & 0 & 0 & 0 \\ \frac{\partial \widehat{p}_1}{\partial \widehat{x}_2} & \frac{\partial \widehat{p}_2}{\partial \widehat{x}_2} & \frac{\partial \widehat{p}_3}{\partial \widehat{x}_2} & \frac{\partial \widehat{p}_4}{\partial \widehat{x}_2} & 0 & 0 & 0 & 0 \\ 0 & 0 & 0 & 0 & \frac{\partial \widehat{p}_1}{\partial \widehat{x}_1} & \frac{\partial \widehat{p}_2}{\partial \widehat{x}_1} & \frac{\partial \widehat{p}_3}{\partial \widehat{x}_1} & \frac{\partial \widehat{p}_4}{\partial \widehat{x}_1} \\ 0 & 0 & 0 & 0 & \frac{\partial \widehat{p}_1}{\partial \widehat{x}_2} & \frac{\partial \widehat{p}_2}{\partial \widehat{x}_2} & \frac{\partial \widehat{p}_3}{\partial \widehat{x}_2} & \frac{\partial \widehat{p}_4}{\partial \widehat{x}_2} \end{pmatrix} = \begin{pmatrix} [\widehat{D}\widehat{P}] & 0 \\ 0 & [\widehat{D}\widehat{P}] \end{pmatrix} \in \mathcal{M}_{4\times 8}, \tag{2.37}$$

with $[\widehat{D}\widehat{P}] \in \mathcal{M}_{2\times 4}$ given by

$$[\widehat{D}\widehat{P}] = \begin{pmatrix} \frac{\partial \widehat{p}_1}{\partial \widehat{x}_1} & \frac{\partial \widehat{p}_2}{\partial \widehat{x}_1} & \frac{\partial \widehat{p}_3}{\partial \widehat{x}_1} & \frac{\partial \widehat{p}_4}{\partial \widehat{x}_1} \\ \frac{\partial \widehat{p}_1}{\partial \widehat{x}_2} & \frac{\partial \widehat{p}_2}{\partial \widehat{x}_2} & \frac{\partial \widehat{p}_3}{\partial \widehat{x}_2} & \frac{\partial \widehat{p}_4}{\partial \widehat{x}_2} \end{pmatrix} = \begin{pmatrix} -(1-\widehat{x}_2) & (1-\widehat{x}_2) & \widehat{x}_2 & -\widehat{x}_2 \\ -(1-\widehat{x}_1) & -\widehat{x}_1 & \widehat{x}_1 & (1-\widehat{x}_1) \end{pmatrix}. \tag{2.38}$$

We can now express the integrals over T present in the elementary rigidity matrices and second member vectors in the following manner,

$$\int_T \psi(x)\, dx = \int_{\widehat{T}} \left(\psi \circ F_T\right)(\widehat{x})\, \det\left[F_T'(\widehat{x})\right]\, d\widehat{x}, \tag{2.39}$$

where

$$\det\left[F_T'(\widehat{x})\right] = \left(c_{12}^T c_{23}^T - c_{13}^T c_{22}^T\right) + \left(c_{12}^T c_{24}^T - c_{14}^T c_{22}^T\right)\widehat{x}_1 + \left(c_{14}^T c_{23}^T - c_{13}^T c_{24}^T\right)\widehat{x}_2.$$

The adoption of the "positive" direction for the local numbering of nodes (cf. § 2.5 and Figure 2.6) ensures that $\det\left[F_T'(\widehat{x})\right] > 0$.

Using the change of variable $x = F_T(\widehat{x})$, we get for the rigidity matrix (cf. (2.24) and (2.36))

$$\begin{aligned} \left[R^T\right] &= \int_T \left[\mathcal{D}\mathcal{P}^T\right]^t \left[\mathcal{E}^T\right] \left[\mathcal{D}\mathcal{P}^T\right] dx \\ &= \int_{\widehat{T}} \left[\mathcal{D}\mathcal{P}^T\right]^t \circ F_T \left[\mathcal{E}^T \circ F_T\right] \left[\mathcal{D}\mathcal{P}^T\right] \circ F_T \left(\det F_T'\right) d\widehat{x} \\ &= \int_{\widehat{T}} [\widehat{\mathcal{D}}\widehat{\mathcal{P}}]^t \mathcal{G}_T^t \left[\mathcal{E}^T \circ F_T\right] \mathcal{G}_T [\widehat{\mathcal{D}}\widehat{\mathcal{P}}] \left(\det F_T'\right) d\widehat{x}. \end{aligned} \tag{2.40}$$

Similarly, the "f-term" of the second member vector becomes (cf. (2.25) and (2.33))

$$\begin{aligned} b_f^T &= \int_T \left[\mathcal{P}^T\right]^t \left[f^T\right] dx \\ &= \int_{\widehat{T}} \left[\mathcal{P}^T\right]^t \circ F_T \left(\left[f^T\right] \circ F_T\right) \left(\det F_T'\right) d\widehat{x} \\ &= \int_{\widehat{T}} [\widehat{\mathcal{P}}]^t \left[f^T \circ F_T\right] \left(\det F_T'\right) d\widehat{x}. \end{aligned} \tag{2.41}$$

The nature of the integral present in the "g-term" of b^T (cf. (2.25)) is different from the previous ones, since it is defined over ∂T,

$$b_g^T = \int_{T\cap\partial\Gamma_2} \left[\mathcal{P}^T\right]^t \left[g^T\right] d\gamma. \tag{2.42}$$

Let us consider the integral

$$\int_{T\cap\partial\Gamma_2} \varphi(x)\, d\gamma$$

and define

$$\chi_l^T = \begin{cases} 1 & \text{if the side } l \text{ of } T \subset \Gamma_2, \\ 0 & \text{otherwise,} \end{cases}$$

where $1 \le l \le 4$. Therefore,

$$\int_{T\cap\partial\Gamma_2} \varphi(x)\, d\gamma = \sum_{l=1}^4 \chi_l^T \int_{\partial T_l} \varphi(x)\, d\gamma. \tag{2.43}$$

Since each side of element T is a linear segment, the change of variable $x = F_T(\widehat{x})$ leads to

$$\int_{\partial T_l} \varphi(x)\, d\gamma = \delta_l^T \int_{\partial \widehat{T}_l} (\varphi \circ F_T)(\widehat{x})\; d\widehat{\gamma},$$

where δ_l^T is the size of segment l of element T. From (2.42) and (2.43) we get

$$\begin{aligned} b_g^T &= \sum_{l=1}^{4} \chi_l^T \int_{\partial T_l} \left[\mathcal{P}^T\right]^t \left[g^T\right]\, d\gamma \\ &= \sum_{l=1}^{4} \chi_l^T\, \delta_l^T \int_{\partial \widehat{T}_l} \left[\mathcal{P}^T\right]^t \circ F_T \left(\left[g^T\right] \circ F_T\right)\, d\widehat{\gamma} \\ &= \sum_{l=1}^{4} \chi_l^T\, \delta_l^T \int_{\partial \widehat{T}_l} \left[\widehat{\mathcal{P}}\right]^t \left[g^T \circ F_T\right]\, d\widehat{\gamma}, \end{aligned} \tag{2.44}$$

where (2.33) has been used.

2.6.2. Elementary calculations

In order to compute the integrals present in the expression giving the elementary rigidity matrix, as well as those for the "f-term" and "g-term" of the elementary second member vector, we use the Gauss-Legendre quadrature formulae with k nodes for the interval $[0, 1]$:

$$\int_0^1 \widehat{\phi}(\widehat{x})\; d\widehat{x} \sim \sum_{i=1}^{k} \widehat{\omega}_i \widehat{\phi}\left(\widehat{b}_i\right),$$

where $\widehat{\omega}_i$ $(i = 1, 2)$ are the quadrature weights, while $\widehat{b}_i$ $(i = 1, 2)$ are the quadrature nodes which are obtained through an affine transformation of the k roots in $[-1, 1]$ of the Legendre polynomial of degree k. These formulae are exact for polynomials of degree $2k - 1$ defined on $[0, 1]$. Table 2.1 summarizes some relevant data for the Gauss-Legendre quadrature formulae.

k	$2k-1$	$\widehat{b}_i$	$\widehat{\omega}_i$	order
1	1	$\frac{1}{2}$	1	2
2	3	$\pm\frac{\sqrt{3}}{6} + \frac{1}{2}$	$\frac{1}{2}, \frac{1}{2}$	4
3	5	$\pm\frac{\sqrt{15}}{10} + \frac{1}{2}, \frac{1}{2}$	$\frac{5}{18}, \frac{5}{18}, \frac{8}{18}$	6

Table 2.1: Data for Gauss-Legendre quadrature formulae with 1, 2 and 3 nodes

Computation of the elementary rigidity matrix

We have for the elementary rigidity matrix (cf. (2.40))

$$\left[R^T\right] = \int_{\widehat{T}} [\widehat{\mathcal{D}}\widehat{\mathcal{P}}]^t \mathcal{G}_T^t \left[\mathcal{E}^T \circ F_T\right] \mathcal{G}_T [\widehat{\mathcal{D}}\widehat{\mathcal{P}}] \left(\det F_T'\right)\, d\widehat{x}. \tag{2.45}$$

If $\mathcal{E}^T$ and F_T' are both constant (homogeneous isotropic material and parallelogram quadrilaterals), the integrand above involves at most polynomials of degree 2 in each variable, since in that case $\mathcal{G}_T$

and $\det F'_T$ are also constant. Therefore, under this hypothesis, to integrate

$$\int_{\widehat{T}} [\widehat{\mathcal{D}}\widehat{\mathcal{P}}]^t \mathcal{G}_T^t \left[\mathcal{E}^T \circ F_T\right] \mathcal{G}_T [\widehat{\mathcal{D}}\widehat{\mathcal{P}}] \left(\det F'_T\right) d\widehat{x}$$

exactly we need to use a quadrature formula that must be exact for polynomials that are P_2 in each variable. That can be ensured using the Gauss-Legendre quadrature formula with 2 nodes (exact for polynomials of degree 3 in each variable)

$$\int_{\widehat{T}} \widehat{\psi}\left(\widehat{x}\right) d\widehat{x} \sim \sum_{l=1}^{2} \widehat{\omega}_l \, \widehat{\psi}\left(\widehat{b}_l\right), \quad \widehat{b}_l \in \widehat{T},$$

in combination with the Frobenius theorem:

$$\begin{aligned}
\int_{\widehat{T}} \widehat{\psi}\left(\widehat{x}\right) d\widehat{x} &= \int_0^1 \left[\int_0^1 \widehat{\psi}\left(\widehat{x}_1, \widehat{x}_2\right) d\widehat{x}_2\right] d\widehat{x}_1 \\
&\sim \omega_1 \int_0^1 \widehat{\psi}\left(\widehat{b}_1, \widehat{x}_2\right) d\widehat{x}_2 + \omega_2 \int_0^1 \widehat{\psi}\left(\widehat{b}_2, \widehat{x}_2\right) d\widehat{x}_2 \\
&\sim \omega_1^2 \, \widehat{\psi}\left(\widehat{b}_1, \widehat{b}_1\right) + \omega_1 \, \omega_2 \left[\widehat{\psi}\left(\widehat{b}_1, \widehat{b}_2\right) + \widehat{\psi}\left(\widehat{b}_2, \widehat{b}_1\right)\right] + \omega_2^2 \, \widehat{\psi}\left(\widehat{b}_2, \widehat{b}_2\right),
\end{aligned}$$

where

$$\omega_1 = \omega_2 = \frac{1}{2}$$

and

$$\widehat{b}_1 = \frac{1}{2} + \frac{\sqrt{3}}{6}, \quad \widehat{b}_2 = \frac{1}{2} - \frac{\sqrt{3}}{6}.$$

Schematically,

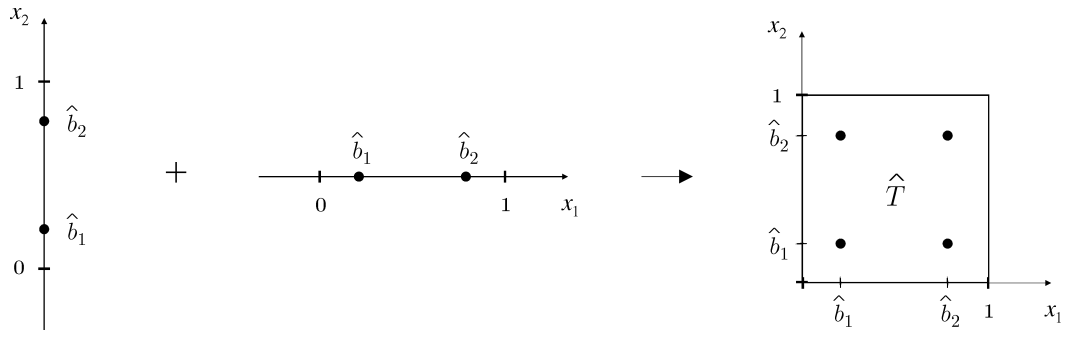

In this way,

$$\int_{\widehat{T}} \widehat{\psi}\left(\widehat{x}\right) d\widehat{x} \sim \frac{1}{4} \left[\widehat{\psi}\left(\widehat{b}_1, \widehat{b}_1\right) + \widehat{\psi}\left(\widehat{b}_1, \widehat{b}_2\right) + \widehat{\psi}\left(\widehat{b}_2, \widehat{b}_1\right) + \widehat{\psi}\left(\widehat{b}_2, \widehat{b}_2\right)\right],$$

leading to

$$\left[R^T\right] \sim \frac{1}{4} \left[\widehat{\psi}\left(\widehat{b}_1, \widehat{b}_1\right) + \widehat{\psi}\left(\widehat{b}_1, \widehat{b}_2\right) + \widehat{\psi}\left(\widehat{b}_2, \widehat{b}_1\right) + \widehat{\psi}\left(\widehat{b}_2, \widehat{b}_2\right)\right],$$

where

$$\widehat{\psi} = [\widehat{\mathcal{D}}\widehat{\mathcal{P}}]^t \, \mathcal{G}_T^t \left[\mathcal{E}^T \circ F_T\right] \mathcal{G}_T \left[\widehat{\mathcal{D}}\widehat{\mathcal{P}}\right] \left(\det F'_T\right) \in \mathcal{M}_{8\times 8}.$$

It should be stressed that the hypothesis used to obtain this result, namely the assumption that we are dealing with a homogeneous isotropic material and parallelogram quadrilaterals, in combination with the order of the quadrature scheme used, does retain the order of convergence of the finite element method - see e.g. Ciarlet (1993) and references therein.

Defining

$$\begin{aligned}[\mathcal{H}_T] &= \left(\det F_T'\right)\, \mathcal{G}_T[\widehat{\mathcal{D}}\widehat{\mathcal{P}}] = \left(\det F_T'\right) \begin{pmatrix} G_T & 0 \\ 0 & G_T \end{pmatrix} \begin{pmatrix} \widehat{D}\widehat{P} & 0 \\ 0 & \widehat{D}\widehat{P} \end{pmatrix} \\ &= \begin{pmatrix} H_T & 0 \\ 0 & H_T \end{pmatrix} \in \mathcal{M}_{4\times 8},\end{aligned}$$

with

$$[H_T] = \left(\det F_T'\right)\, [G_T] \left[\widehat{D}\widehat{P}\right] \in \mathcal{M}_{2\times 4},$$

and since

$$\left[\mathcal{E}^T\right] = \left.\begin{pmatrix} \lambda+2\mu & 0 & 0 & \lambda \\ 0 & \mu & \mu & 0 \\ 0 & \mu & \mu & 0 \\ \lambda & 0 & 0 & \lambda+2\mu \end{pmatrix}\right|_T,$$

we finally get

$$\widehat{\psi}_T = \frac{1}{\det F_T'}[\mathcal{H}_T]^t\, \left[\mathcal{E}^T \circ F_T\right]\, [\mathcal{H}_T]\,,$$

or

$$\left[\widehat{\psi}_T\right]_{ij} = \frac{1}{\det F_T'} \sum_{1\le k,l\le 4} [\mathcal{H}_T]_{ki}\, \left[\mathcal{E}^T\right]_{kl} \circ F_T\, [\mathcal{H}_T]_{lj}\,, \quad 1 \le i,j \le 8.$$

Computation of the "f-term" of the elementary second member vector

As for the rigidity matrix, the "f-term" of the elementary second member vector (cf. (2.41))

$$b_f^T = \int_{\widehat{T}} \left(\det F_T'\right)\, [\widehat{\mathcal{P}}]^t\, \left(\left[f^T \circ F_T\right]\right)\, d\widehat{x}, \tag{2.46}$$

involves at most polynomials of degree 2 in each variable if f^T and $F_T'(\widehat{x})$ are assumed constant. Therefore, it can be integrated exactly using the Gauss-Legendre quadrature formula with 2 nodes. Hence,

$$b_f^T \sim \frac{1}{4}\left[\widehat{\varphi}\left(\widehat{b}_1,\widehat{b}_1\right) + \widehat{\varphi}\left(\widehat{b}_1,\widehat{b}_2\right) + \widehat{\varphi}\left(\widehat{b}_2,\widehat{b}_1\right) + \widehat{\varphi}\left(\widehat{b}_2,\widehat{b}_2\right)\right],$$

where

$$[\widehat{\varphi}] = \left(\det F_T'\right)\, [\widehat{\mathcal{P}}]^t\, \left[f^T \circ F_T\right] \in \mathbb{R}^8.$$

Thus,

$$[\widehat{\varphi}]_i = \left(\det F_T'\right) \sum_{1\le k\le 2} [\widehat{\mathcal{P}}]_{ki}\, f_k^T \circ F_T \quad 1 \le i \le 8.$$

Again, it can be shown that assuming f^T and F_T' constant, together with the quadrature scheme used, retains the order of convergence of the finite element method.

Computation of the "g-term" of the elementary second member vector

To evaluate the integrals present in the "g-term" of the elementary second member vector (cf. (2.44))

$$b_g^T = \sum_{l=1}^{4} \chi_l^T \, \delta_l^T \int\limits_{\partial \widehat{T}_l} \left[\widehat{\mathcal{P}}\right]^t \, \left[g^T \circ F_T\right] \, d\widehat{\gamma}, \tag{2.47}$$

we define the following change of variable for face $\partial \widehat{T}_l = \left[\widehat{a}_l, \widehat{a}_{\overline{l+1}}\right]$

$$\widehat{\sigma} \in [0,1] \rightarrow \widehat{\varphi}_l\left(\widehat{\sigma}\right) = \left(\widehat{a}_{\overline{l+1}} - \widehat{a}_l\right) \widehat{\sigma} + \widehat{a}_l, \quad 1 \leq l \leq 4,$$

where $\overline{i} = i \bmod 5$. Then

$$\int\limits_{\partial \widehat{T}_l} \widehat{\psi} \, d\widehat{\gamma} = \int_0^1 \widehat{\psi}\left(\widehat{\varphi}_l\left(\widehat{\sigma}\right)\right) \, d\widehat{\sigma},$$

yielding

$$\int\limits_{\partial \widehat{T}_l} \left[\widehat{\mathcal{P}}\right]^t \, \left[g^T \circ F_T\right] \, d\widehat{\gamma} = \int_0^1 \left[\widehat{\mathcal{P}}\left(\widehat{\varphi}_l\left(\widehat{\sigma}\right)\right)\right]^t \left[g^T\left(F_T\left(\widehat{\varphi}_l\left(\widehat{\sigma}\right)\right)\right)\right] \, d\widehat{\sigma}. \tag{2.48}$$

If we assume that g^T is constant, the integrand above involves at most polynomials of degree 1 in $\widehat{\sigma}$. Therefore, under this hypothesis, to integrate

$$\int_0^1 \left[\widehat{\mathcal{P}}\left(\widehat{\varphi}_l\left(\widehat{\sigma}\right)\right)\right]^t \left[g^T\left(F_T\left(\widehat{\varphi}_l\left(\widehat{\sigma}\right)\right)\right)\right] \, d\widehat{\sigma}$$

exactly we need to use a quadrature formula that must be exact for P_1 polynomials. That can be ensured using the Gauss-Legendre quadrature formula with one node (exact for polynomials of first degree):

$$\int_0^1 \widehat{\psi} \, d\widehat{\sigma} \sim \widehat{\psi}\left(\frac{1}{2}\right), \tag{2.49}$$

Defining

$$\widehat{c}_l = \widehat{\varphi}_l\left(\frac{1}{2}\right),$$

the center of face $\partial \widehat{T}_l$ of the reference element, (2.48) and (2.49) lead to

$$\begin{aligned} \int\limits_{\partial \widehat{T}_l} \left[\widehat{\mathcal{P}}\right]^t \, \left[g^T \circ F_T\right] \, d\widehat{\gamma} &\sim \left[\widehat{\mathcal{P}}\left(\widehat{\varphi}_l\left(\frac{1}{2}\right)\right)\right]^t g^T\left(F_T\left(\widehat{\varphi}_l\left(\frac{1}{2}\right)\right)\right) \\ &= \left[\widehat{\mathcal{P}}\left(\widehat{c}_l\right)\right]^t \left[g^T\left(F_T\left(\widehat{c}_l\right)\right)\right]. \end{aligned}$$

Therefore, taking into account that $c_l = F_T\left(\widehat{c}_l\right)$, we obtain (cf. (2.42))

$$\begin{aligned} b_g^T &\sim \sum_{l=1}^{4} \chi_l^T \, \delta_l^T \left[\widehat{\mathcal{P}}\left(\widehat{c}_l\right)\right]^t \left[g^T\left(c_l\right)\right] \\ &= \frac{1}{2} \begin{pmatrix} \chi_1^T \, \delta_1^T \, g_1\left(c_1\right) + \chi_4^T \, \delta_4^T \, g_1\left(c_4\right) \\ \chi_1^T \, \delta_1^T \, g_1\left(c_1\right) + \chi_2^T \, \delta_2^T \, g_1\left(c_2\right) \\ \chi_2^T \, \delta_2^T \, g_1\left(c_2\right) + \chi_3^T \, \delta_3^T \, g_1\left(c_3\right) \\ \chi_3^T \, \delta_3^T \, g_1\left(c_3\right) + \chi_4^T \, \delta_4^T \, g_1\left(c_4\right) \\ \chi_1^T \, \delta_1^T \, g_2\left(c_1\right) + \chi_4^T \, \delta_4^T \, g_2\left(c_4\right) \\ \chi_1^T \, \delta_1^T \, g_2\left(c_1\right) + \chi_2^T \, \delta_2^T \, g_2\left(c_2\right) \\ \chi_2^T \, \delta_2^T \, g_2\left(c_2\right) + \chi_3^T \, \delta_3^T \, g_2\left(c_3\right) \\ \chi_3^T \, \delta_3^T \, g_2\left(c_3\right) + \chi_4^T \, \delta_4^T \, g_2\left(c_4\right) \end{pmatrix}. \end{aligned}$$

Alternatively, if we define

$$b_g^{l,T} = \delta_l^T \left[\widehat{\mathcal{P}}\left(\widehat{c}_l\right)\right]^t \left[g^T\left(c_l\right)\right] \in \mathbb{R}^8, \quad 1 \leq l \leq 4,$$

then only four entries of $b_g^{l,T}$ are non zero, namely,

$$\left[b_g^{l,T}\right]_l = \left[b_g^{l,T}\right]_{\overline{l+1}} = \frac{\delta_l^T}{2} g_1\left(c_l\right), \quad \left[b_g^{l,T}\right]_{l+4} = \left[b_g^{l,T}\right]_{\overline{l+1}+4} = \frac{\delta_l^T}{2} g_2\left(c_l\right),$$

leading to

$$b_g^T \sim \sum_{l=1}^{4} \chi_l^T \, b_g^{l,T}.$$

2.7. Postprocessing calculations

After the numerical solution of the linear elasticity problem has been obtained, it is useful to compute some quantities that are often used in the analysis of results, namely the main stresses and the von Mises stress. On the other hand, when the problem being solved has a known analytic solution, it is possible to compute the error $\|u - u_h\|_{0,\Omega}$, allowing to derive the order of approximation of the solution. In the following paragraphs we give some hints on the computation of these quantities when the approximated displacement field is known.

2.7.1. Computation of main stresses and von Mises stress

Here we will focus on the computation of the stress tensor for a given point $x \in T$:

$$\sigma\left(x\right) = \sigma\left(u_h\right)|_T = \left.\begin{pmatrix} \sigma_{11}\left(u_h\right) & \sigma_{12}\left(u_h\right) \\ \sigma_{21}\left(u_h\right) & \sigma_{22}\left(u_h\right) \end{pmatrix}\right|_T$$

In order no to burden the notation we will use $\sigma = \sigma\left(u_h\right)$.

The main stresses, σ_1 and σ_2, can be obtained from the eigenvalues $\{\lambda_1, \lambda_2\}$ and eigenvectors $\{v_1, v_2\}$ of matrix σ. These are given by:

$$\begin{aligned} \lambda_1 &= \frac{1}{2}\left(\sigma_{11} + \sigma_{22} - \sqrt{\left(\sigma_{11} - \sigma_{22}\right)^2 + 4\sigma_{12}^2}\right), \\ v_1 &= \left(2\sigma_{12}, \quad \sigma_{11} - \sigma_{22} - \sqrt{\left(\sigma_{11} - \sigma_{22}\right)^2 + 4\sigma_{12}^2}\right) \end{aligned}$$

and

$$\begin{aligned} \lambda_2 &= \frac{1}{2}\left(\sigma_{11} + \sigma_{22} + \sqrt{\left(\sigma_{11} - \sigma_{22}\right)^2 + 4\sigma_{12}^2}\right), \\ v_2 &= \left(2\sigma_{12}, \quad \sigma_{11} - \sigma_{22} + \sqrt{\left(\sigma_{11} - \sigma_{22}\right)^2 + 4\sigma_{12}^2}\right), \end{aligned}$$

where we used the fact that $\sigma_{12} = \sigma_{21}$.

On the other hand, the von Mises stress is the invariant given by

$$\|\sigma\|_{VM} = \sqrt{I_1^2 - 3I_2},$$

where I_1 and I_2 are, respectively, the first and second invariants of the stress tensor σ:

$$\begin{aligned} I_1 &= tr\left(\sigma\right) = \lambda_1 + \lambda_2, \\ I_2 &= \frac{1}{2}\left\{\left[tr\left(\sigma\right)\right]^2 - tr(\sigma^2)\right\} = \lambda_1\lambda_2. \end{aligned}$$

Thus,

$$\begin{aligned} \|\sigma\|_{VM} &= \sqrt{(\lambda_1+\lambda_2)^2 - 3\lambda_1\lambda_2} \\ &= \sqrt{\sigma_{11}^2+\sigma_{22}^2-\sigma_{11}\sigma_{22}+3\sigma_{12}^2}. \end{aligned}$$

Hence, to compute the approximate main stresses and von Mises stress at a given point of $T \in \mathcal{T}_h$ we only need to calculate an approximation of σ at that point. As we have seen previously (cf. (2.18)), the stress vector $\{\sigma\}$ is given by

$$\{\sigma\}|_T = \left.\left\{ \begin{array}{c} \sigma_{11} \\ \sigma_{22} \\ \sigma_{12} \end{array} \right\}\right|_T = \left[E^T\right] [\mathcal{D}] \left[\mathcal{D}\mathcal{P}^T\right](x)\, u_T,$$

where

$$\left[E^T\right] [\mathcal{D}] = \left.\left(\begin{array}{cccc} \lambda+2\mu & 0 & 0 & \lambda \\ \lambda & 0 & 0 & \lambda+2\mu \\ 0 & \mu & \mu & 0 \end{array} \right)\right|_T,$$

while

$$u_T = \left[u_{1h}\left(a_1^T\right), u_{1h}\left(a_2^T\right), u_{1h}\left(a_3^T\right), u_{1h}\left(a_4^T\right), u_{2h}\left(a_1^T\right), u_{2h}\left(a_2^T\right), u_{2h}\left(a_3^T\right), u_{2h}\left(a_4^T\right)\right]^t$$

is the vector of local degrees of freedom. We recall that (cf. (2.21))

$$u_T = \left[B^T\right]\ \widetilde{u},$$

where $\widetilde{u}$ is the vector of global degrees of freedom. Using (2.36) and taking into account that $\widehat{x} = F_T^{-1}(x)$, we obtain

$$\left.\left\{ \begin{array}{c} \sigma_{11} \\ \sigma_{22} \\ \sigma_{12} \end{array} \right\}\right|_T = \left[E^T\right] [\mathcal{D}]\ \mathcal{G}_T(\widehat{x})\, [\widehat{\mathcal{D}}\widehat{\mathcal{P}}](\widehat{x})\, u_T,$$

with $\mathcal{G}_T(\widehat{x})$ and $[\widehat{\mathcal{D}}\widehat{\mathcal{P}}](\widehat{x})$ given by (2.35) and (2.37), respectively. If we consider $u_T = [u_{1T}, u_{2T}]^t$, we can derive

$$\left.\left\{ \begin{array}{c} \sigma_{11} \\ \sigma_{22} \\ \sigma_{12} \end{array} \right\}\right|_T = \left[E^T\right] [\mathcal{D}] \left\{ \begin{array}{c} G_T(\widehat{x})\, [\widehat{D}\widehat{P}](\widehat{x})\, u_{1T} \\ G_T(\widehat{x})\, [\widehat{D}\widehat{P}](\widehat{x})\, u_{2T} \end{array} \right\},$$

where $G_T(\widehat{x})$ and $[\widehat{D}\widehat{P}](\widehat{x})$ are given by (2.34) and (2.38), respectively.

For postprocessing purposes the main stresses and the von Mises stress are first evaluated at the barycentre a_T of each element T using

$$\left.\left\{ \begin{array}{c} \sigma_{11} \\ \sigma_{22} \\ \sigma_{12} \end{array} \right\}\right|_{a_T} = \left[E^T\right] [\mathcal{D}] \left\{ \begin{array}{c} G_T\left(\widehat{a}\right)\ \left[\widehat{D}\widehat{P}\right]\left(\widehat{a}\right)\ u_{1T} \\ G_T\left(\widehat{a}\right)\ \left[\widehat{D}\widehat{P}\right]\left(\widehat{a}\right)\ u_{2T} \end{array} \right\},$$

where $a_T = F_T\left(\widehat{a}\right)$ and $\widehat{a} = (1/2, 1/2)$. The value of these quantities at each node of the triangulation is obtained taking the average over the barycentre values of the elements to which the node belongs to. The weights used in this average can be either constant - that is, $1/m$, where m is the number of elements that contribute to a given node - or proporcional to the area of each element involved, the latter being the "default" setting.

2.7.2. Computation of $\|u - u_h\|_{0,\Omega}$

When the analytic solution of the problem u is known it is useful to compute the error

$$\|u - u_h\|_{0,\Omega}^2 = \sum_{T \in \mathcal{T}_h} \|u - u_h\|_{0,T}^2 = \sum_{T \in \mathcal{T}_h} \sum_{i=1}^{2} \int_T (u_i - u_{ih}|_T)^2 \, dx, \tag{2.50}$$

since the estimate

$$\|u - u_h\|_{0,\Omega} \leq Ch^2 \, |u|_{1,\Omega}, \tag{2.51}$$

where

$$|u|_{1,\Omega} = \left(\sum_{i,j=1}^{2} \left\| \frac{\partial u_i}{\partial x_j} \right\|_{0,\Omega}^2 \right)^{1/2},$$

holds for the problem conditions imposed previously - namely, the fact that $f \in \left[L^2(\Omega)\right]^2$ implying that $u \in \left[H^2(\Omega)\right]^2$ - [cf. Ciarlet (1993)], allows to test the order of approximation of the solution. The constant C does not depend on h, satisfying

$$\frac{\|u - u_h\|_{0,\Omega}}{|u|_{1,\Omega}} = Ch^2 \tag{2.52}$$

whenever $h \to 0$.

In view of (2.50) - (2.52), we will devote our attention to the computation of

$$\int_T (u_i(x) - u_{ih}(x)|_T)^2 \, dx, \quad i = 1, 2.$$

Using (2.13) and (2.14) one has

$$u_{ih}(x)|_T = \left[P^T\right](x) \, u_{iT}, \quad i = 1, 2.$$

The change of variable $x = F_T(\widehat{x})$ in combination with (2.32) and (2.39) leads to

$$\int_T \left(u_i(x) - \left[P^T\right](x) \, u_{iT}\right)^2 dx = \int_{\widehat{T}} \left\{ (u_i \circ F_T)(\widehat{x}) - [\widehat{P}](\widehat{x}) \, u_{iT} \right\}^2 \det\left[F_T'(\widehat{x})\right] \, d\widehat{x}, \quad i = 1, 2.$$

Hence,

$$\|u - u_h\|_{0,\Omega}^2 = \sum_{T \in \mathcal{T}_h} \sum_{i=1}^{2} \int_{\widehat{T}} \left\{ (u_i \circ F_T)(\widehat{x}) - [\widehat{P}](\widehat{x}) \, u_{iT} \right\}^2 \det\left[F_T'(\widehat{x})\right] \, d\widehat{x},$$

the integral on the right-hand side being evaluated numerically using a quadrature scheme similar to the one used for the computation of the elementary rigidity matrices.

3. Tests and results

The principles presented in the previous sections were implemented in a C++ numerical code, allowing to solve the linear elasticity problem for a 2D elastic body. Both preprocessing (mesh, displacement constrains, loads) and postprocessing (displacements, main stresses, von Mises stress, error estimates) are handled using the software GiD (version 7.2). The relevant files needed for the interface between the numerical code and GiD are presented in Appendix A.

Here we present some tests by solving a certain number of 2D linear elasticity problems for which an analytic solution can be obtained. Both structured and unstructured meshes are used, as well as homogeneous and non-homogeneous bodies. At the end of this chapter we present some results for a problem (deformation of a 2D wrench) for which an analytic solution cannot be derived, and compare them with those obtained using MODULEF.

In the following discussion the values of all physical quantities are given in S.I. unit system unless stated otherwise.

3.1. Test problem 1 - Homogeneous square plate; solution $\in (Q_1)^2$

3.1.1. Problem description

We consider the homogeneous square plate presented in Figure 3.1, having Young modulus E and Poisson ratio ν with values

$$\begin{aligned} E &= 5 \times 10^9 \ (Pa), \\ \nu &= 0.3, \end{aligned}$$

that are typical of rock material. The corresponding values of the Lamé's constants λ and μ are obtained from the following relations:

$$\lambda = \frac{E\nu}{(1+\nu)(1-2\nu)} \tag{3.1a}$$

$$\mu = \frac{E}{2(1+\nu)}, \tag{3.1b}$$

yielding

$$\begin{aligned} \lambda &= 2.8846 \times 10^9 \ (Pa), \\ \mu &= 1.9231 \times 10^9 \ (Pa). \end{aligned}$$

The linear elasticity problem for this plate is

$$\begin{aligned} &\text{Find } u = (u_1, u_2) \text{ such that:} \\ &-\sum_{j=1}^{2} \frac{\partial}{\partial x_j} \sigma_{ij}(u) = f_i \quad \text{in} \quad \Omega, \quad 1 \le i \le 2, \\ &u_i = 0 \quad \text{on} \quad \Gamma_1, \quad 1 \le i \le 2, \\ &\sum_{j=1}^{2} \sigma_{ij}(u)\, \nu_j = g_i \quad \text{on} \quad \Gamma_2, \quad 1 \le i \le 2, \end{aligned} \tag{3.2}$$

with $\overline{\Omega} = [0,1]^2$, $\Gamma_2 = \gamma_1 \cup \gamma_2$, while the loads imposed are:

$$f_1 = 2(\mu+\lambda) \times 10^{-2} = 9.6154 \times 10^7 \quad \left(N\,m^{-3}\right),$$
$$f_2 = -(\mu+\lambda) \times 10^{-2} = -4.8077 \times 10^7 \quad \left(N\,m^{-3}\right),$$

over Ω,

$$g_1|_{\gamma_1} = [(2\mu+\lambda)\,x_2 - 2\lambda] \times 10^{-2} = (6.7308x_2 - 5.7692) \times 10^7 \quad \left(N\,m^{-2}\right),$$
$$g_2|_{\gamma_1} = \mu\,(1-2x_2) \times 10^{-2} = (1.9231 - 3.8462x_2) \times 10^7 \quad \left(N\,m^{-2}\right),$$

on boundary γ_1, and

$$g_1|_{\gamma_2} = \mu\,(x_1-2) \times 10^{-2} = (1.9231x_1 - 3.8462) \times 10^7 \quad \left(N\,m^{-2}\right),$$
$$g_2|_{\gamma_2} = [-2\,(2\mu+\lambda)\,x_1 + \lambda] \times 10^{-2} = (-13.462x_1 + 2.8846) \times 10^7 \quad \left(N\,m^{-2}\right),$$

on boundary γ_2.

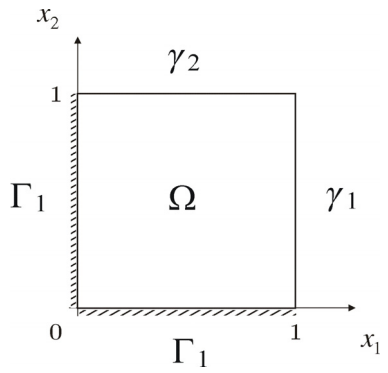

Figure 3.1: Schematic representation of the homogenous square plate of Problem 1

As we have seen in § 1.2, considering the space of admissible displacements

$$V = \left\{ v = (v_1, v_2) \in \left[H^1(\Omega)\right]^2 : (v_1, v_2) = (0,0) \text{ on } \Gamma_1 \right\} \tag{3.3}$$

and the linearized strain tensor

$$\varepsilon_{ij}(v) = \frac{1}{2}\left(\frac{\partial v_i}{\partial x_j} + \frac{\partial v_j}{\partial x_i}\right), \qquad 1 \le i,j \le 2,$$

the corresponding variational problem is

Find $u \in V$ such that:

$$\int_\Omega \sum_{i,j=1}^{2} \left\{ \lambda \left(\sum_{k=1}^{2} \varepsilon_{kk}(u) \right) \delta_{ij} + 2\mu\varepsilon_{ij}(u) \right\} \varepsilon_{ij}(v)\, dx = \int_\Omega \sum_{i=1}^{2} f_i v_i\, dx + \int_{\Gamma_2} \sum_{i=1}^{2} g_i v_i\, d\gamma, \tag{3.4}$$

$\forall v = (v_1, v_2) \in V.$

The analytic solution of this problem is known:

$$u_1(x_1,x_2) = x_1x_2 \times 10^{-2} \quad (m),$$
$$u_2(x_1,x_2) = -2\,x_1x_2 \times 10^{-2} \quad (m).$$

Since $u \in [Q_1(\Omega)]^2$, we expect the numerical solution to coincide with the analytic solution if the quadrature formulae used allow to integrate the elementary rigidity matrices and the elementary second member vectors exactly. Taking into account that

$$f \in [P_0(\Omega)]^2, \quad g \in [P_1(\Gamma_2)]^2,$$

and the fact that the mesh used is made of parallelogram quadrilaterals, it is easy to show that one can compute exactly:

(i) the elementary rigidity matrices (2.45) using the Gauss-Legendre quadrature formula with 2 nodes;

(ii) the "f-term" of the elementary second member vectors (2.46) using the Gauss-Legendre quadrature formula with 2 nodes;

(iii) the "g-term" of the elementary second member vectors (2.47) using the Gauss-Legendre quadrature formula with 2 nodes.

As we have seen in § 2.6, conditions (i) and (ii) should be used to retain the order of convergence of the finite element method. As to condition (iii), a 2 node quadrature formula is now prescribed instead of the 1 node formula mentioned in § 2.6. Since the code allows the user to choose the number of nodes to use in each of these integrations, we will also present the "exact solution" obtained.

3.1.2. Results

We computed the solution for 5 different uniform meshes of square finite elements, having different values for h, in order to check the convergence rate of the method. The relevant data is presented in Table 3.1, where $|u|_{1,\Omega} = 1.8257 \times 10^{-2}$. Plotting the values of $\|u - u_h\|_{0,\Omega} / |u|_{1,\Omega}$ against those of h (see Figure 3.2) we see that the numerical results obtained agree well with the error estimate (2.52), leading to $C = 0.102$.

The results for the 30×30 mesh (cf. Figure 3.3) concerning the displacements ($|u_h|$, u_{1h} and u_{2h}), the von Mises stress ($\|\sigma_h\|_{VM}$), and the error estimate for each element ($\|u - u_h\|_{0,T}$) and for each node ($|u - u_h|$), are presented in Figures 3.4 to 3.7.[1] Taking into account that

$$\|u - u_h\|_{0,\Omega} \sim 4 \times 10^{-6}, \quad \max_{T \in \mathcal{T}_h} \|u - u_h\|_{0,T} \sim 10^{-6}, \quad \max_{\Sigma_h} |u - u_h| \sim 5 \times 10^{-5},$$

we conclude that the numerical results are very close to the analytic predictions. Furthermore, the value of the von Mises stress obtained at the point $(x_1, x_2) = (1, 0)$, $1.2156 \times 10^8\, Pa$, agrees well with value prescribed by the analytic solution, $1.2163 \times 10^8\, Pa$.

A further calculation has been performed for the 30×30 mesh using the Gauss-Legendre quadrature formula with 2 nodes for all the numerical integrations (see discussion above), yielding

$$\|u - u_h\|_{0,\Omega} \sim 5 \times 10^{-16}, \quad \max_{T \in \mathcal{T}_h} \|u - u_h\|_{0,T} \sim 4 \times 10^{-17}, \quad \max_{\Sigma_h} |u - u_h| \sim 10^{-15}.$$

These results show that the "exact solution" is obtained under these conditions, as expected. In this case, the value of the von Mises stress obtained at the point $(1, 0)$ coincides with the one predicted by the analytic solution.

[1] Throughout the text, results concerning displacements, stresses and error estimates will be always presented in the deformed configuration.

elements	h	$\max_{\Sigma_h} \lvert u - u_h \rvert$	$\lVert u - u_h \rVert_{0,\Omega}$	$\lVert u - u_h \rVert_{0,\Omega} \ / \ \lvert u \rvert_{1,\Omega}$
10×10	1.4142×10^{-1}	3.0220×10^{-4}	3.7074×10^{-5}	2.0307×10^{-1}
16×16	8.8388×10^{-2}	1.3598×10^{-4}	1.4555×10^{-5}	7.9723×10^{-4}
20×20	7.0711×10^{-2}	9.2482×10^{-5}	9.3272×10^{-6}	5.1088×10^{-4}
25×25	5.6569×10^{-2}	6.2680×10^{-5}	5.9743×10^{-6}	3.2723×10^{-4}
30×30	4.7141×10^{-2}	4.5509×10^{-5}	4.1507×10^{-6}	2.2735×10^{-4}

Table 3.1: Error estimates for different meshes for Problem 1

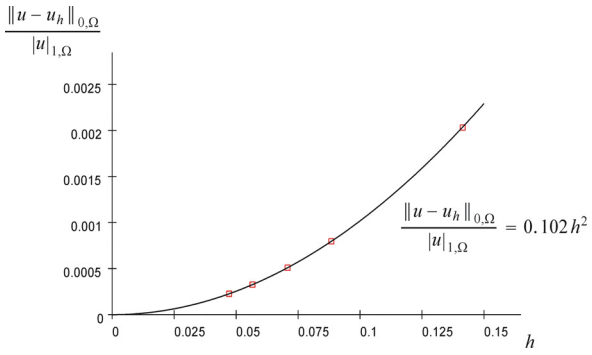

Figure 3.2: Order of convergence of the numerical solution for Problem 1 from data presented in Table 3.1

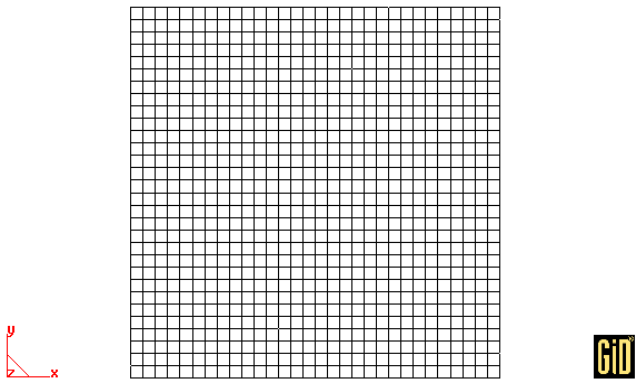

Figure 3.3: Problem 1 : the 30×30 finite elements mesh

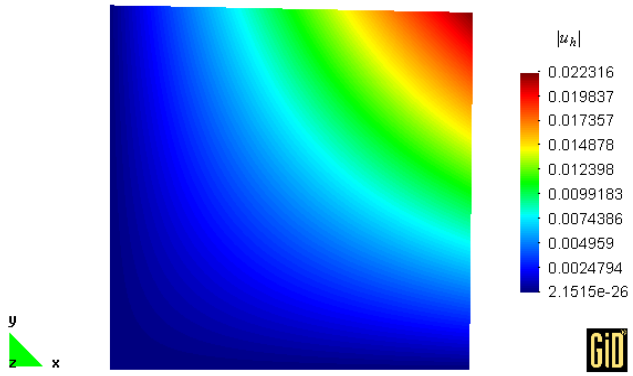

Figure 3.4: Problem 1 : the displacement field $|u_h|$ for the mesh presented in Figure 3.3

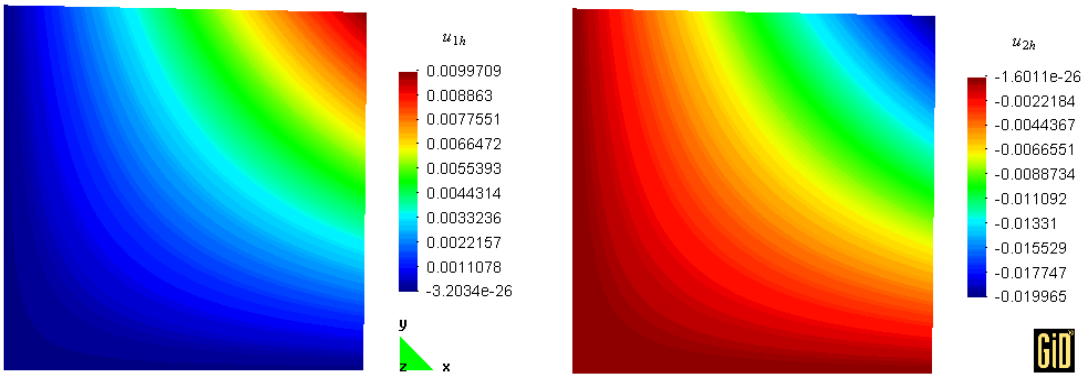

Figure 3.5: Problem 1 : the displacement fields u_{1h} (left) and u_{2h} (right) for the mesh presented in Figure 3.3

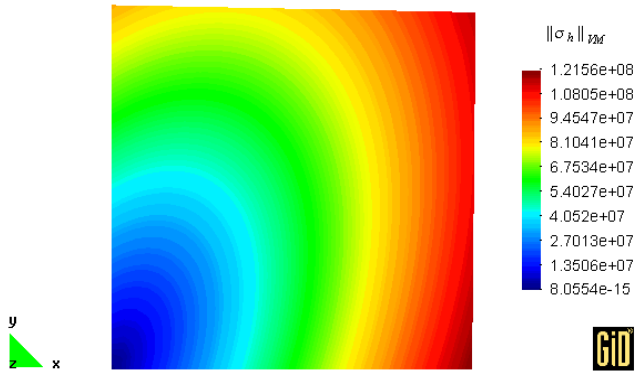

Figure 3.6: Problem 1 : the von Mises stress field for the mesh presented in Figure 3.3

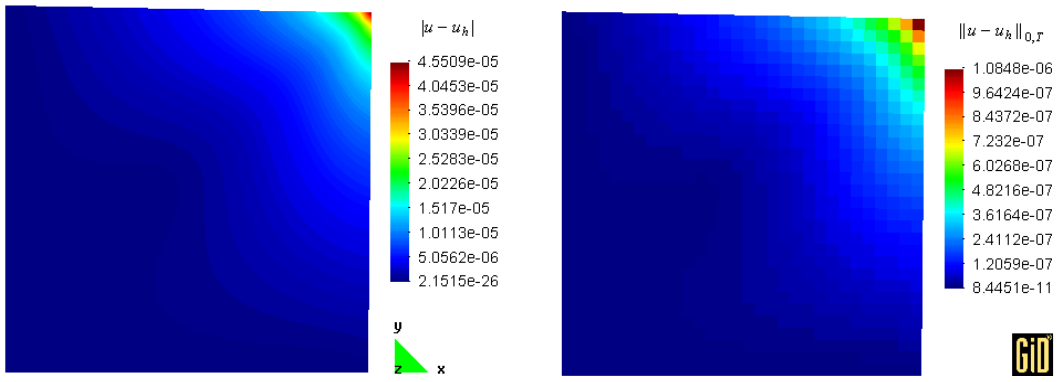

Figure 3.7: Problem 1 : the distribution of $|u - u_h|$ (left) and $\|u - u_h\|_{0,T}$ (right) for the mesh presented in Figure 3.3

3.2. Test problem 2 - Homogeneous square plate; solution $\notin (Q_1)^2$

3.2.1. Problem description

The plate (geometry and material), as well as the displacement constrains imposed, are the ones considered in Problem 1 (cf. Figure 3.1). However, the loads imposed are different, namely,

$$f_1 = [e^{x_2}(\lambda+\mu) - 2x_2 e^{x_1}(\lambda+2\mu)] \times 10^{-2} = (4.8077e^{x_2} - 13.462x_2 e^{x_1}) \times 10^7 \quad \left(N\,m^{-3}\right),$$
$$f_2 = [-2e^{x_1}(\lambda+\mu) + x_1 e^{x_2}(\lambda+2\mu)] \times 10^{-2} = (-9.6154e^{x_1} + 6.7308x_1 e^{x_2}) \times 10^7 \quad \left(N\,m^{-3}\right),$$

over Ω,

$$g_1|_{\gamma_1} = [2(\lambda+2\mu)\,e\,x_2 - \lambda e^{x_2}] \times 10^{-2} = (13.462e\,x_2 - 2.8846) \times 10^7 \quad \left(N\,m^{-2}\right),$$
$$g_2|_{\gamma_1} = \mu(2e - e^{x_2} - 1) \times 10^{-2} = (3.8462e - 1.9231e^{x_2} - 1.9231) \times 10^7 \quad \left(N\,m^{-2}\right),$$

on boundary γ_1, and

$$g_1|_{\gamma_2} = \mu(2e^{x_1} - e - 1) \times 10^{-2} = \left(3.8462e^{x_1} - 1.9231 \times 10^7 e - 1.9231\right) \times 10^7 \quad \left(N\,m^{-2}\right),$$
$$g_2|_{\gamma_2} = [2\lambda e^{x_1} - (\lambda+2\mu)\,e\,x_1] \times 10^{-2} = (5.7692e^{x_1} - 6.7308e\,x_1) \times 10^7 \quad \left(N\,m^{-2}\right),$$

on boundary γ_2. The space of admissible displacements is again defined by (3.3) and the solution of (3.4) is now

$$\begin{aligned} u_1(x_1,x_2) &= 2(e^{x_1}-1)x_2 \times 10^{-2} \quad (m), \\ u_2(x_1,x_2) &= -(e^{x_2}-1)x_1 \times 10^{-2} \quad (m). \end{aligned}$$

In this case $u \notin [Q_1(\Omega)]^2$ and therefore u_h does not coincide with u.

3.2.2. Results

As in the previous problem, we computed the solution for 5 different uniform meshes of square finite elements, having different values for h, in order to check the convergence rate of the method. The relevant data is presented in Table 3.2, where $|u|_{1,\Omega} = 3.0189 \times 10^{-2}$. Plotting the values of $\|u-u_h\|_{0,\Omega} / |u|_{1,\Omega}$ against those of h (see Figure 3.8) we see that the numerical results obtained agree well with the error estimate (2.52), leading to $C = 0.108$.

The results for the 30×30 mesh, already used in Problem 1, concerning the displacements ($|u_h|$, u_{1h}, and u_{2h}), the von Mises stress ($\|\sigma_h\|_{VM}$), and the error estimate for each element ($\|u-u_h\|_{0,T}$) and for each node ($|u-u_h|$), are presented in Figures 3.9 to 3.12. Since

$$\|u-u_h\|_{0,\Omega} \sim 7 \times 10^{-6}, \quad \max_{T\in\mathcal{T}_h} \|u-u_h\|_{0,T} \sim 2 \times 10^{-6}, \quad \max_{\Sigma_h} |u-u_h| \sim 10^{-4},$$

we conclude that the numerical results agree well with the analytic predictions. The value of the von Mises stress obtained at the point $(x_1,x_2) = (1,1)$, $2.9812 \times 10^8\,Pa$, agrees well with the value prescribed by the analytic solution, $3.0682 \times 10^8\,Pa$.

The error $\|u-u_h\|_{0,T}$ (and $|u-u_h|$) can be reduced if the number of elements around the top right corner of the plate is increased (see Figure 3.13). Figure 3.14 presents the error distribution obtained for the refined mesh. In this case,

$$\|u-u_h\|_{0,\Omega} \sim 2 \times 10^{-6}, \quad \max_{T\in\mathcal{T}_h} \|u-u_h\|_{0,T} \sim 10^{-7}, \quad \max_{\Sigma_h} |u-u_h| \sim 10^{-5}.$$

We conclude that the error has been improved with respect to result obtained with the uniform mesh although the number of elements remains unchanged. For this mesh, the value of the von Mises stress obtained at the point $(x_1,x_2) = (1,1)$ is $3.0417 \times 10^8\,Pa$, a value closer to the analytic prediction when compared to the one obtained with the original mesh.

elements	h	$\max_{\Sigma_h} \lvert u - u_h \rvert$	$\lVert u - u_h \rVert_{0,\Omega}$	$\lVert u - u_h \rVert_{0,\Omega} \ / \ \lvert u \rvert_{1,\Omega}$
10×10	1.4142×10^{-1}	7.1389×10^{-4}	6.4587×10^{-5}	2.1394×10^{-3}
16×16	8.8388×10^{-2}	3.2632×10^{-4}	2.5460×10^{-5}	8.4335×10^{-4}
20×20	7.0711×10^{-2}	2.2339×10^{-4}	1.6332×10^{-5}	5.4099×10^{-4}
25×25	5.6569×10^{-2}	1.5232×10^{-4}	1.0469×10^{-5}	3.4678×10^{-4}
30×30	4.7141×10^{-2}	1.1110×10^{-4}	7.2764×10^{-6}	2.4103×10^{-4}

Table 3.2: Error estimates for different meshes for Problem 2

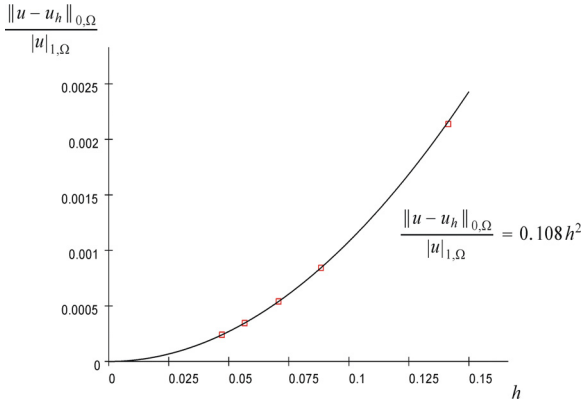

Figure 3.8: Order of convergence of the numerical solution for Problem 2 from data presented in Table 3.2

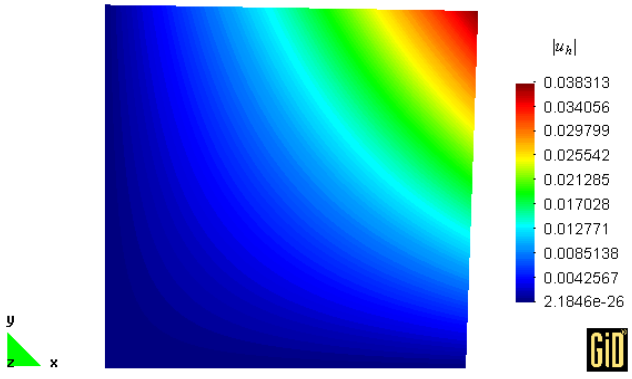

Figure 3.9: Problem 2 : the displacement field $|u_h|$ for the mesh presented in Figure 3.3

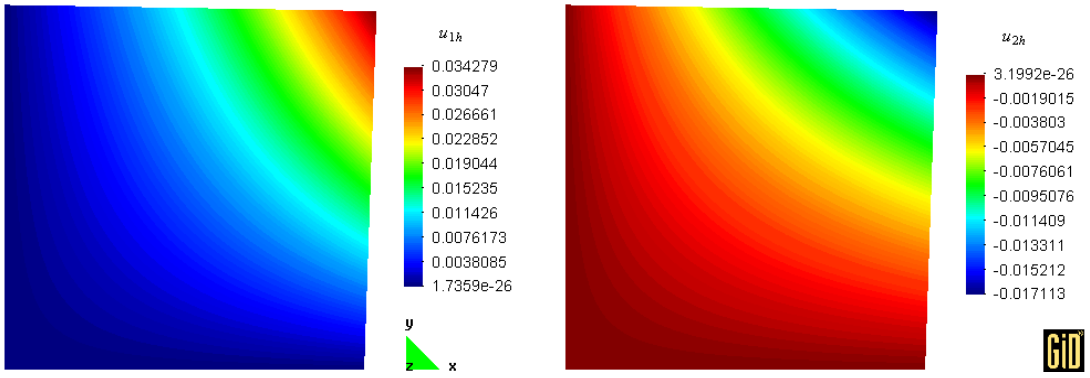

Figure 3.10: Problem 2 : the displacement fields u_{1h} (left) and u_{2h} (right) for the mesh presented in Figure 3.3

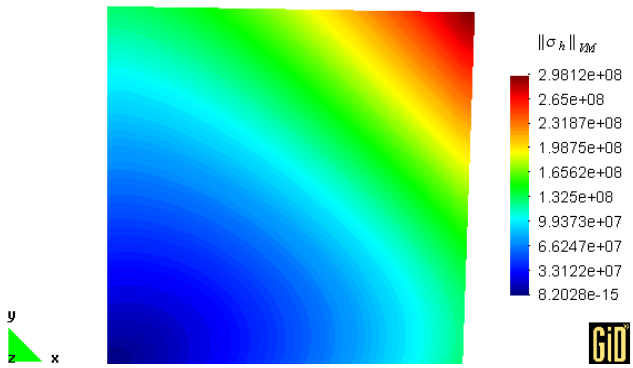

Figure 3.11: Problem 2 : the von Mises stress field for the mesh presented in Figure 3.3

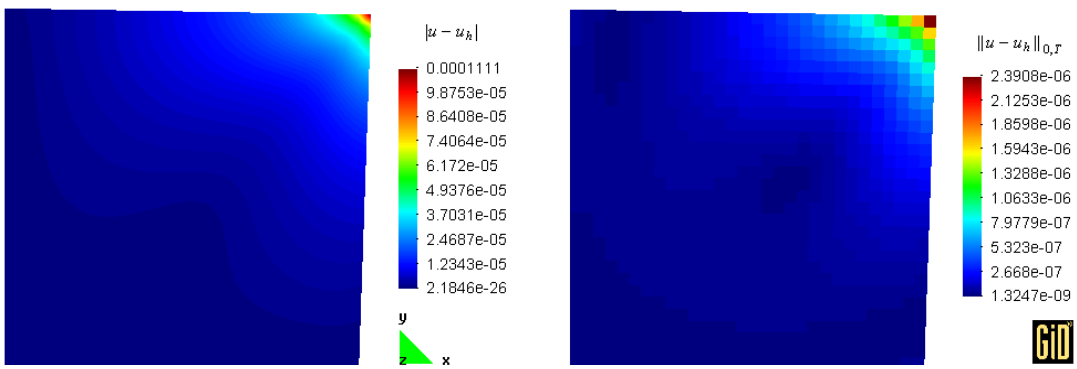

Figure 3.12: Problem 2 : the distribution of $|u-u_h|$ (left) and $\|u-u_h\|_{0,T}$ (right) for the mesh presented in Figure 3.3

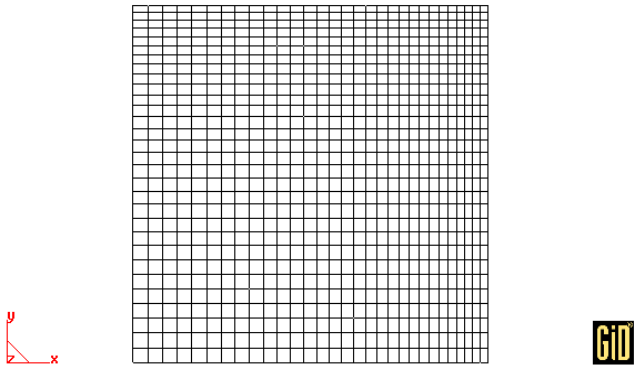

Figure 3.13: Problem 2 : the 30×30 finite elements refined mesh

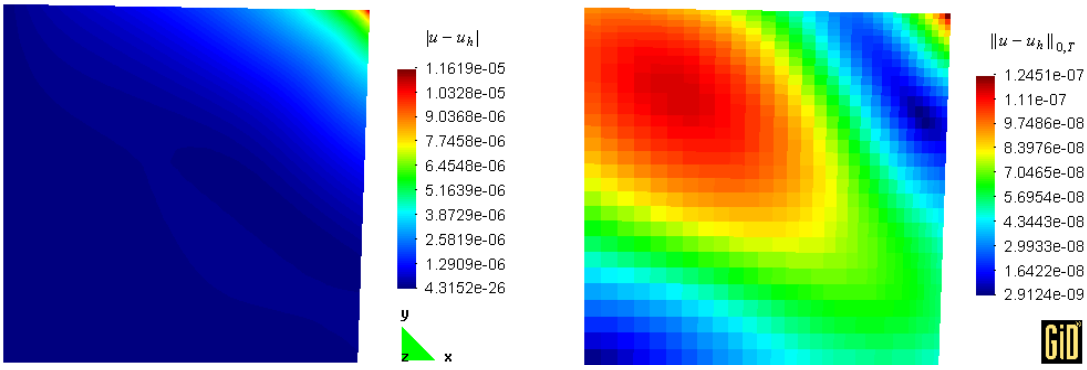

Figure 3.14: Problem 2 : the distribution of $|u-u_h|$ (left) and $\|u-u_h\|_{0,T}$ (right) for the refined mesh presented in Figure 3.13

3.3. Test problem 3 - Homogeneous triangular plate; solution $\in (Q_1)^2$

3.3.1. Problem description

We consider the homogeneous triangular plate presented in Figure 3.15, having Young modulus E and Poisson ratio ν with values $E = 5 \times 10^9$ (Pa) and $\nu = 0.3$ as in Problem 1 and Problem 2. The linear elasticity problem for this plate is

$$\begin{aligned} &\text{Find } u = (u_1, u_2) \text{ such that:} \\ &-\sum_{j=1}^{2} \frac{\partial}{\partial x_j} \sigma_{ij}(u) = f_i \quad \text{in} \quad \Omega, \quad 1 \le i \le 2, \\ &u_1 = 0.1, \; u_2 = -0.05 \quad \text{on} \quad \Gamma_1, \\ &\sum_{j=1}^{2} \sigma_{ij}(u)\, \nu_j = g_i \quad \text{on} \quad \Gamma_2, \quad 1 \le i \le 2, \end{aligned} \tag{3.5}$$

with $\Gamma_2 = \gamma_1 \cup \gamma_2$, while the loads imposed are:

$$f_1 = 2(\mu + \lambda) \times 10^{-2} = 9.6154 \times 10^7 \quad \left(N\, m^{-3}\right),$$
$$f_2 = -(\mu + \lambda) \times 10^{-2} = -4.8077 \times 10^7 \quad \left(N\, m^{-3}\right),$$

over Ω,

$$g_1|_{\gamma_1} = -\mu(x_1 + 2) \times 10^{-2} = -(1.9231 x_1 + 3.8462) \times 10^7 \quad \left(N\, m^{-2}\right),$$
$$g_2|_{\gamma_1} = -[\lambda - 2x_1(\lambda + 2\mu)] \times 10^{-2} = -(2.8846 - 13.462 x_1) \times 10^7 \quad \left(N\, m^{-2}\right),$$

on boundary γ_1, and

$$\begin{aligned} g_1|_{\gamma_2} &= \frac{1}{\sqrt{41}}\left[5\mu\left(x_1-2x_2+2\right)+4\left(\left(\lambda+2\mu\right)\left(x_2+1\right)-2\lambda x_1\right)\right]\times 10^{-2} \\ &= \left(1.2013x_2-2.1023x_1+7.2081\right)\times 10^{7} \quad \left(N\,m^{-2}\right), \\ g_2|_{\gamma_2} &= \frac{1}{\sqrt{41}}\left[4\mu\left(x_1-2x_2+2\right)+5\left(\lambda\left(x_2+1\right)-2x_1\left(\lambda+2\mu\right)\right)\right]\times 10^{-2} \\ &= \left(4.6552-0.15021x_2-9.3104x_1\right)\times 10^{7} \quad \left(N\,m^{-2}\right). \end{aligned}$$

on boundary γ_2.

Considering the space of admissible displacements

$$V=\left\{v=(v_1,v_2)\in\left[H^1\left(\Omega\right)\right]^2:(v_1,v_2)=(0.1,-0.05)\text{ on }\Gamma_1\right\}, \tag{3.6}$$

the variational problem corresponding to (3.5) has analytic solution:

$$\begin{aligned} u_1\left(x_1,x_2\right) &= \left[10+x_1\left(x_2+1\right)\right]\times 10^{-2} \quad (m), \\ u_2\left(x_1,x_2\right) &= \left[-5-2x_1(x_2-1)\right]\times 10^{-2} \quad (m). \end{aligned}$$

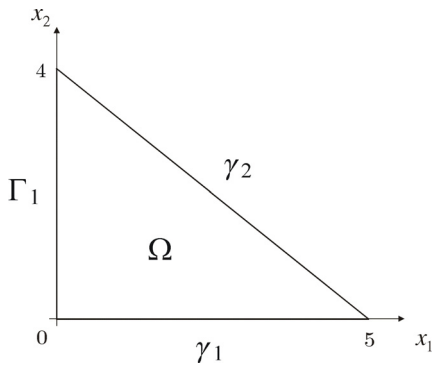

Figure 3.15: Schematic representation of the homogenous triangular plate of Problem 3

Since $u\in\left[Q_1\left(\Omega\right)\right]^2$, we would expect the numerical solution to coincide with the analytic solution if the elementary rigidity matrices and the elementary second member vectors were integrated exactly. However, that is not possible since the finite elements involved are not parallelograms as was the case in Problem 1. Still, we expect to obtain a numerical solution that is very close to the analytic one, even when relatively coarse meshes are used, if the Gauss-Legendre quadrature formula with 2 nodes is employed as we did in Problem 1.

3.3.2. Results

As in the previous problems, we computed the solution for 5 different meshes, having different values for h. The relevant data is presented in Table 3.3, where $|u|_{1,\Omega}=0.17654$. Plotting the values of $\|u-u_h\|_{0,\Omega}/|u|_{1,\Omega}$ against those of h (see Figure 3.16) we see that the numerical results obtained agree well with the error estimate (2.52), leading to $C=0.0186$.

The results obtained with the 7257 elements mesh (cf. Figure 3.17) for the displacements ($|u_h|$, u_{1h}, and u_{2h}), the von Mises stress ($\|\sigma_h\|_{VM}$), and the error estimate for each element ($\|u-u_h\|_{0,T}$) and for each node ($|u-u_h|$), are presented in Figures 3.18 to 3.21. Since

$$\|u-u_h\|_{0,\Omega}\sim 4\times 10^{-5},\quad \max_{T\in\mathcal{T}_h}\|u-u_h\|_{0,T}\sim 4\times 10^{-6},\quad \max_{\Sigma_h}|u-u_h|\sim 2\times 10^{-4},$$

we conclude that the numerical results agree well with the analytic predictions. The value of the von Mises stress obtained at the point $(x_1, x_2) = (5, 0)$, $6.0904 \times 10^8\, Pa$, is close to the value prescribed by the analytic solution, $6.1306 \times 10^8\, Pa$.

The error $\|u - u_h\|_{0,T}$ (and $|u - u_h|$) can be reduced if the number of elements around the right corner of the triangular plate is increased (see Figure 3.22). Figure 3.23 presents the error distribution obtained for the refined mesh. Comparing the maximum values of $\|u - u_h\|_{0,T}$ and $|u - u_h|$ present in Figures 3.21 and 3.23, and taking into account that $\|u - u_h\|_{0,\Omega} = 2.3287 \times 10^{-5}$ for the refined mesh, we conclude that the error improves although the number of elements remains unchanged. Furthermore, for the refined mesh, the value of the von Mises stress obtained at the point $(x_1, x_2) = (5, 0)$, $6.1186 \times 10^8\, Pa$, is now closer to the analytic prediction.

A further calculation has been performed for the refined mesh using the Gauss-Legendre quadrature formula with 2 nodes for all the numerical integrations, leading to

$$\|u - u_h\|_{0,\Omega} \sim 2 \times 10^{-5}, \quad \max_{T \in \mathcal{T}_h} \|u - u_h\|_{0,T} \sim 8 \times 10^{-7}, \quad \max_{\Sigma_h} |u - u_h| \sim 10^{-5}.$$

The error improves with respect to the one obtained with the "default" integration schemes, but only moderately. This is due to the fact that some integrations are still not performed exactly due to the geometry of the finite elements in the mesh. The value of the von Mises stress obtained at the point $(x_1, x_2) = (5, 0)$, $6.1204 \times 10^8\, Pa$, is now even closer to the analytic prediction.

elements	h	$\max_{\Sigma_h} \lvert u - u_h \rvert$	$\|u - u_h\|_{0,\Omega}$	$\|u - u_h\|_{0,\Omega} \,/\, \lvert u \rvert_{1,\Omega}$
1149	2.4460×10^{-1}	7.1900×10^{-4}	1.9717×10^{-4}	1.1169×10^{-3}
1587	2.3150×10^{-1}	6.1101×10^{-4}	1.7496×10^{-4}	9.9105×10^{-4}
2063	1.8467×10^{-1}	4.0970×10^{-4}	1.1277×10^{-4}	6.3878×10^{-4}
3241	1.5311×10^{-1}	3.1685×10^{-4}	7.7949×10^{-5}	4.4154×10^{-4}
7257	1.0413×10^{-1}	1.5598×10^{-4}	3.5735×10^{-5}	2.0242×10^{-4}

Table 3.3: Error estimates for different meshes for Problem 3

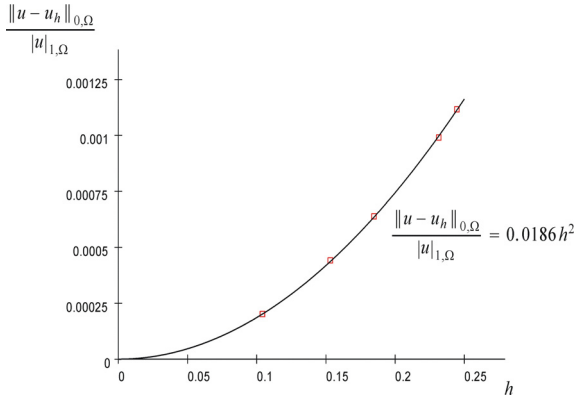

Figure 3.16: Order of convergence of the numerical solution for Problem 3 from data presented in Table 3.3

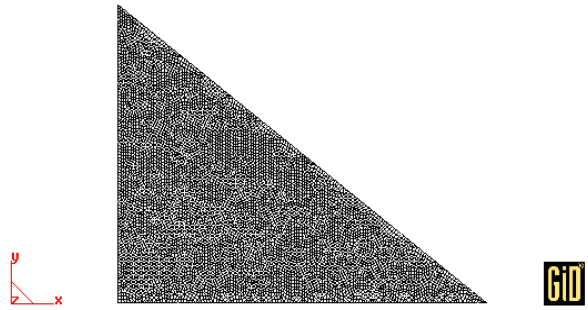

Figure 3.17: Problem 3 : the 7257 finite elements mesh

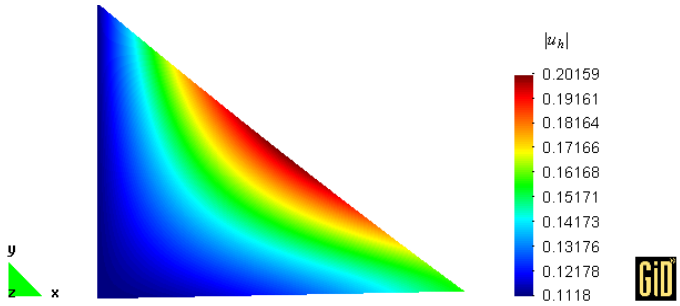

Figure 3.18: Problem 3 : the displacement field $|u_h|$ for the mesh presented in Figure 3.17

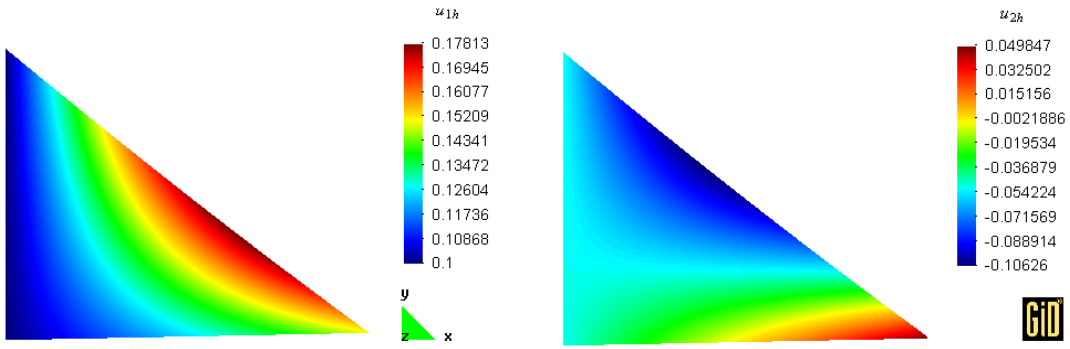

Figure 3.19: Problem 3 : the displacement fields u_{1h} (left) and u_{2h} (right) for the mesh presented in Figure 3.17

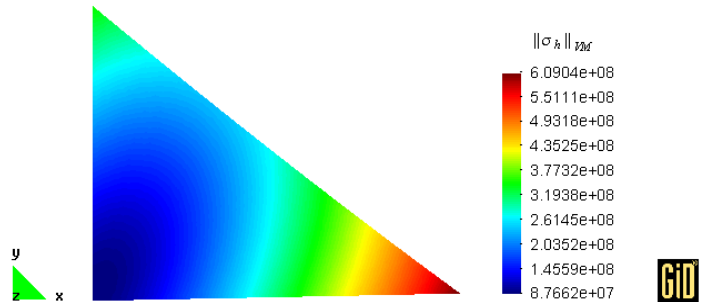

Figure 3.20: Problem 3 : the von Mises stress field for the mesh presented in Figure 3.17

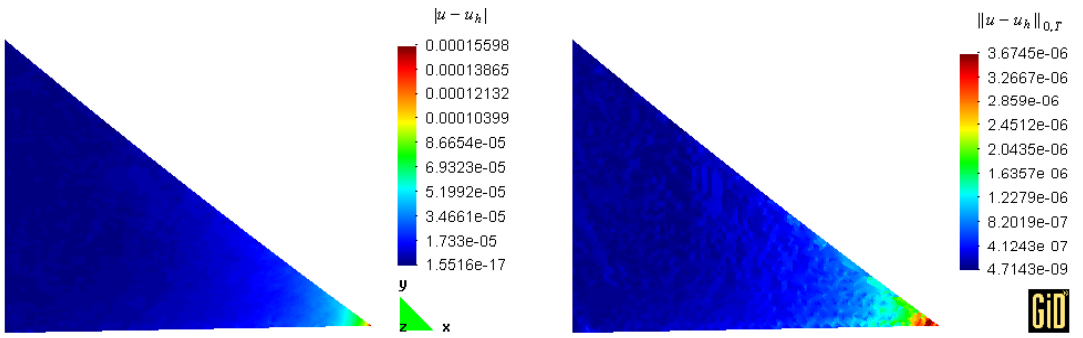

Figure 3.21: Problem 3 : the distribution of $|u-u_h|$ (left) and $\|u-u_h\|_{0,T}$ (right) for the mesh presented in Figure 3.17

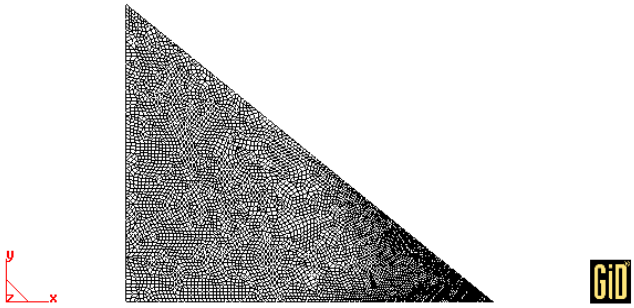

Figure 3.22: Problem 3 : the 7257 finite elements refined mesh

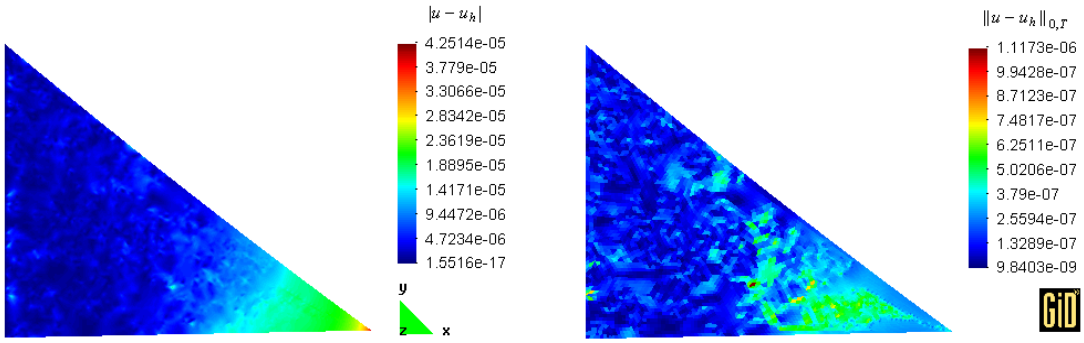

Figure 3.23: Problem 3 : the distribution of $|u-u_h|$ (left) and $\|u-u_h\|_{0,T}$ (right) for the mesh presented in Figure 3.22

3.4. Test problem 4 - Homogeneous triangular plate; solution $\notin (Q_1)^2$

3.4.1. Problem description

We consider again the homogeneous triangular plate of Problem 3 (cf. Figure 3.15), subject to the same displacement constrains, but with different loads imposed:

$$f_1 = [4(\mu+\lambda)x_2 - 2(\lambda+2\mu)(x_2+1)] \times 10^{-2} = (5.7692x_2 - 13.462) \times 10^7 \quad \left(N\,m^{-3}\right),$$
$$f_2 = 2(\lambda+3\mu)x_1 \times 10^{-2} = 17.308x_1 \times 10^7 \quad \left(N\,m^{-3}\right),$$

over Ω,

$$g_1|_{\gamma_1} = -\mu\left(x_1^2 - 2x_2^2 + 2\right) \times 10^{-2} = \left(3.8462x_2^2 - 1.9231x_1^2 - 3.8462\right) \times 10^7 \quad \left(N\,m^{-2}\right),$$
$$g_2|_{\gamma_1} = \left[4x_1x_2\left(\lambda + 2\mu\right) - 2\lambda\left(1 + x_2\right)x_1\right] \times 10^{-2} = \left(21.154x_2 - 5.7692\right)x_1 \times 10^7 \quad \left(N\,m^{-2}\right),$$

on boundary γ_1, and

$$\begin{aligned} g_1|_{\gamma_2} &= \frac{1}{\sqrt{41}}\left[8\left(\left(\lambda + 2\mu\right)\left(1 + x_2\right) - 2\lambda x_2\right)x_1 + 5\mu\left(x_1^2 - 2x_2^2 + 2\right)\right] \times 10^{-2} \\ &= \left(8.4094x_1 + 1.2014x_1x_2 + 1.5017x_1^2 - 3.0034x_2^2 + 3.0034\right) \times 10^7 \quad \left(N\,m^{-2}\right), \\ g_2|_{\gamma_2} &= \frac{1}{\sqrt{41}}\left[10\left(\lambda\left(1 + x_2\right) - 2x_2\left(\lambda + 2\mu\right)\right)x_1 + 4\mu\left(x_1^2 - 2x_2^2 + 2\right)\right] \times 10^{-2} \\ &= \left(4.5050x_1 - 16.518x_1x_2 + 1.2014x_1^2 - 2.4027x_2^2 + 2.4027\right) \times 10^7 \quad \left(N\,m^{-2}\right). \end{aligned}$$

on boundary γ_2.

The space of admissible displacements is again defined by (3.6) and the solution of (3.4) is now

$$\begin{aligned} u_1 &= \left[10 + x_1^2\left(x_2 + 1\right)\right] \times 10^{-2} \quad (m), \\ u_2 &= \left[-5 - 2x_1(x_2^2 - 1)\right] \times 10^{-2} \quad (m). \end{aligned}$$

In this case $u \notin \left[Q_1\left(\Omega\right)\right]^2$ and therefore u_h does not coincide with u even if all the numerical integrations were performed exactly.

3.4.2. Results

We computed the solution for 5 different meshes, having different values for h as in the previous problems. The relevant data is presented in Table 3.4., where $|u|_{1,\Omega} = 0.47415$. Plotting the values of $\|u - u_h\|_{0,\Omega} \,/\, |u|_{1,\Omega}$ against those of h (see Figure 3.24) we see that the numerical results obtained agree well with the error estimate (2.52), leading to $C = 0.0633$.

The results obtained with the 29241 elements mesh (cf. Figure 3.25) for the displacements ($|u_h|$, u_{1h}, and u_{2h}), the von Mises stress ($\|\sigma_h\|_{VM}$), and the error estimate for each element ($\|u - u_h\|_{0,T}$) and for each node ($|u - u_h|$), are presented in Figures 3.26 to 3.29. Since

$$\|u - u_h\|_{0,\Omega} \sim 8 \times 10^{-5}, \quad \max_{T \in \mathcal{T}_h} \|u - u_h\|_{0,T} \sim 4 \times 10^{-6}, \quad \max_{\Sigma_h} |u - u_h| \sim 3 \times 10^{-4},$$

we conclude that the numerical results agree well with the analytic predictions, even if a relatively large number of elements is needed to achieve this level of approximation. The value of the von Mises stress obtained at the point $(x_1, x_2) = (2.7277, 1.8178)$, $1.1886 \times 10^9\, Pa$, is close to the value prescribed by the analytic solution, $1.1959 \times 10^9\, Pa$.

elements	h	$\max_{\Sigma_h} \lvert u - u_h \rvert$	$\|u - u_h\|_{0,\Omega}$	$\|u - u_h\|_{0,\Omega} \,/\, \lvert u \rvert_{1,\Omega}$
2063	1.8467×10^{-1}	3.7498×10^{-3}	1.1029×10^{-3}	2.3260×10^{-3}
3241	1.5311×10^{-1}	2.2261×10^{-3}	6.8995×10^{-4}	1.4551×10^{-3}
7257	1.0413×10^{-1}	1.0804×10^{-3}	3.0656×10^{-4}	6.4654×10^{-4}
18732	7.0576×10^{-2}	4.4039×10^{-4}	1.1895×10^{-4}	2.5087×10^{-4}
29241	5.5962×10^{-2}	3.2086×10^{-4}	7.6205×10^{-5}	1.6072×10^{-4}

Table 3.4: Error estimates for different meshes for Problem 4

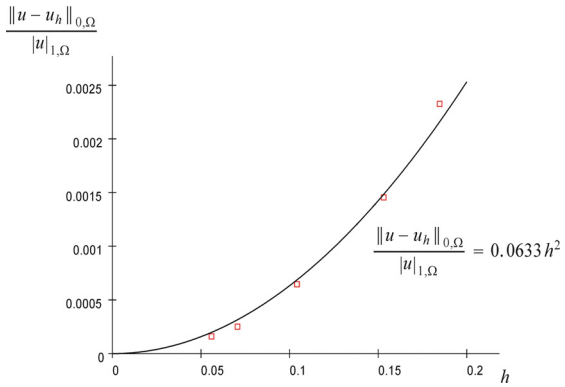

Figure 3.24: Order of convergence of the numerical solution for Problem 4 from data of Table 3.4

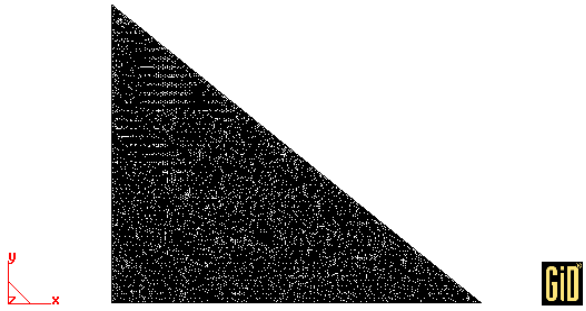

Figure 3.25: Problem 4 : the 29241 finite elements mesh

Figure 3.26: Problem 4 : the displacement field $|u_h|$ for the mesh presented in Figure 3.25

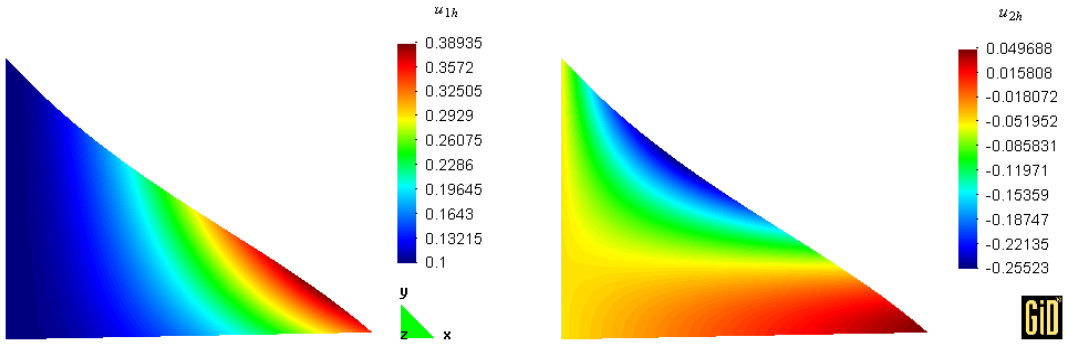

Figure 3.27: Problem 4 : the displacement fields u_{1h} (left) and u_{2h} (right) for the mesh presented in Figure 3.25

Figure 3.28: Problem 4 : the von Mises stress field for the mesh presented in Figure 3.25

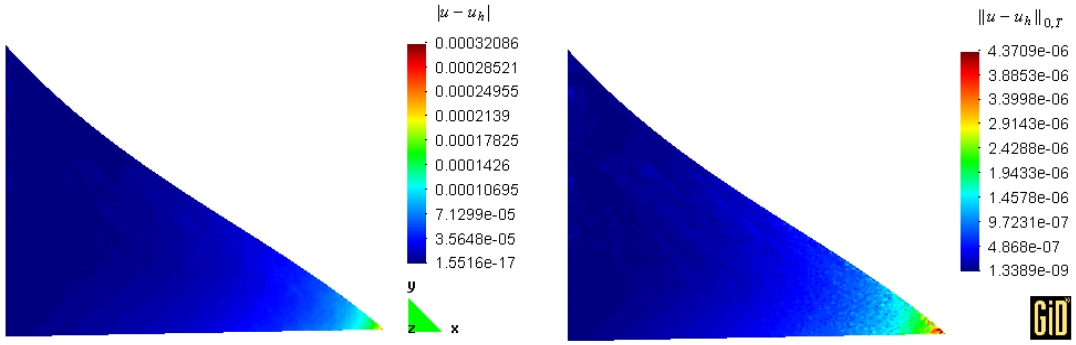

Figure 3.29: Problem 4 : the distribution of $|u-u_h|$ (left) and $\|u-u_h\|_{0,T}$ (right) for the mesh presented in Figure 3.25

3.5. Test problem 5 - Non homogeneous plate; solution $\notin (Q_1)^2$

3.5.1. Problem description

We consider the plate presented in Figure 3.30. The composition of the plate is not homogeneous: the material in region Ω_R (rock) has Young modulus $E_R = 5 \times 10^9\ (Pa)$ and Poisson ratio $\nu_R = 0.3$, while the material in region Ω_C (concrete) is such that $E_C = 4 \times 10^9\ (Pa)$ and $\nu_C = 0.2$. The corresponding values of the Lamé's constants λ and μ are obtained from (3.1), leading to

$$\begin{aligned} \lambda_R &= 2.8846 \times 10^9\ (Pa)\,, \quad \mu_R = 1.9231 \times 10^9\ (Pa)\,, \\ \lambda_C &= 1.1111 \times 10^9\ (Pa)\,, \quad \mu_C = 1.6667 \times 10^9\ (Pa)\,. \end{aligned}$$

The linear elasticity problem for this plate is

$$\begin{aligned} &\text{Find } u = (u_1, u_2) \text{ such that:} \\ &-\sum_{j=1}^{2} \frac{\partial}{\partial x_j} \sigma_{ij}(u) = f_i \quad \text{in} \quad \Omega, \quad 1 \le i \le 2, \\ &u_1 = 0,\ u_2 = 0 \quad \text{on} \quad \Gamma_1 \cup I_1, \\ &\sum_{j=1}^{2} \sigma_{ij}(u)\, \nu_j = g_i \quad \text{on} \quad \Gamma_2, \quad 1 \le i \le 2, \end{aligned} \tag{3.7}$$

with $\Omega = \Omega_R \cup \Omega_C \cup I_1$ and $\Gamma_2 = \cup_{i=1,4}\gamma_i$. The loads imposed are:

$$\begin{aligned} f_1 &= \left[\lambda_R\left(\pi x_2 - 1\right) + \mu_R\left(2\pi x_2 - 1\right)\right] \pi \sin\left(\pi x_1\right) \times 10^{-2} \\ &= \left(66.430 x_2 - 15.104\right) \sin\left(\pi x_1\right) \times 10^7 \quad \left(N\, m^{-3}\right), \\ f_2 &= -\left[\lambda_R + \mu_R\left(1 + \pi x_2\right)\right] \pi \cos\left(\pi x_1\right) \times 10^{-2} \\ &= -\left(18.980 x_2 + 15.104\right) \cos\left(\pi x_1\right) \times 10^7 \quad \left(N\, m^{-3}\right), \end{aligned}$$

over Ω_R,

$$\begin{aligned} f_1 &= \left[\lambda_C\left(\pi x_2 - 1\right) + \mu_C\left(2\pi x_2 - 1\right)\right] \pi \sin\left(\pi x_1\right) \times 10^{-2} \\ &= \left(43.865 x_2 - 8.7267\right) \left(\sin \pi x_1\right) \times 10^7 \quad \left(N\, m^{-3}\right), \\ f_2 &= -\left[\lambda_C + \mu_C\left(1 + \pi x_2\right)\right] \pi \cos\left(\pi x_1\right) \times 10^{-2} \\ &= -\left(16.450 x_2 + 8.7267\right) \cos\left(\pi x_1\right) \times 10^7 \quad \left(N\, m^{-3}\right), \end{aligned}$$

over Ω_C,

$$\begin{aligned} g_1|_{\gamma_1} &= \left(\lambda_C + 2\mu_C\right) \pi x_2 \times 10^{-2} = 13.963 x_2 \times 10^7 \quad \left(N\, m^{-2}\right), \\ g_2|_{\gamma_1} &= 0 \quad \left(N\, m^{-2}\right), \end{aligned}$$

on boundary γ_1,

$$\begin{aligned} g_1|_{\gamma_2} &= \mu_C\left(1 + \pi\right) \sin \pi x_1 \times 10^{-2} = 6.9028 \sin \pi x_1 \times 10^7 \quad \left(N\, m^{-2}\right), \\ g_2|_{\gamma_2} &= \pi \lambda_C \cos \pi x_1 + \left(\lambda_C + 2\mu_C\right)\left(1 - \cos \pi x_1\right) \times 10^{-2} \\ &= \left(4.4445 - 0.95388 \cos \pi x_1\right) \times 10^7 \quad \left(N\, m^{-2}\right), \end{aligned}$$

on boundary γ_2,

$$\begin{aligned} g_1|_{\gamma_3} &= \left(\lambda_R + 2\mu_R\right) \pi x_2 \times 10^{-2} = 21.145 x_2 \times 10^7 \quad \left(N\, m^{-2}\right), \\ g_2|_{\gamma_3} &= 0 \quad \left(N\, m^{-2}\right), \end{aligned}$$

on boundary γ_3,

$$\begin{aligned} g_1|_{\gamma_4} &= \mu_C\left(1 + 2\pi\right) \sin \pi x_1 \times 10^{-2} = 14.006 \sin \pi x_1 \times 10^7 \quad \left(N\, m^{-2}\right), \\ g_2|_{\gamma_4} &= \left[2\pi \lambda_C \cos \pi x_1 + \left(\lambda_C + 2\mu_C\right)\left(1 - \cos \pi x_1\right)\right] \times 10^{-2} \\ &= \left(2.5367 \cos \pi x_1 - 4.4445\right) \times 10^7 \quad \left(N\, m^{-2}\right), \end{aligned}$$

on boundary γ_4.

Considering the space of admissible displacements

$$V = \left\{ v = (v_1, v_2) \in \left[H^1(\Omega)\right]^2 : (v_1, v_2) = (0,0) \text{ on } \Gamma_1 \right\}, \tag{3.8}$$

the variational problem corresponding to (3.7) has analytic solution:

$$\begin{aligned} u_1(x_1, x_2) &= x_2 \sin \pi x_1 \times 10^{-2} \quad (m), \\ u_2(x_1, x_2) &= x_2\left(1 - \cos \pi x_1\right) \times 10^{-2} \quad (m). \end{aligned}$$

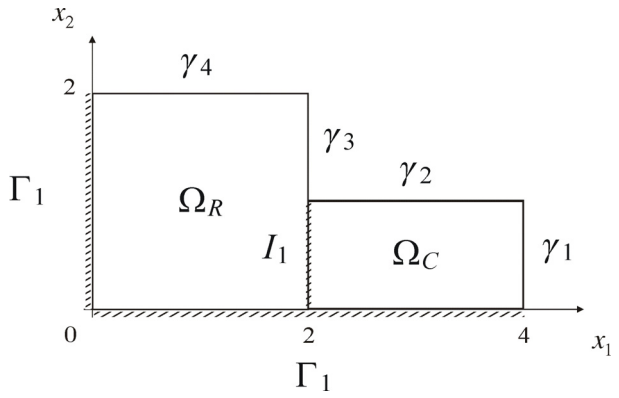

Figure 3.30: Schematic representation of the plate of Problem 5

In this case $u \notin [Q_1(\Omega)]^2$ and therefore u_h does not coincide with u even if all the numerical integrations were performed exactly.

3.5.2. Results

Following the methodology used in the previous test problems, we computed the solution for 5 different uniform meshes, having different values for h. The relevant data is presented in Table 3.5, where $|u|_{1,\Omega} = 8.4391 \times 10^{-2}$. Plotting the values of $\|u - u_h\|_{0,\Omega} / |u|_{1,\Omega}$ against those of h (see Figure 3.31) we see that the numerical results obtained agree well with the error estimate (2.52), leading to $C = 0.200$.

The results obtained with the 3675 elements mesh (cf. Figure 3.32) for the displacements ($|u_h|$, u_{1h}, and u_{2h}), the von Mises stress ($\|\sigma_h\|_{VM}$), and the error estimate for each element ($\|u - u_h\|_{0,T}$) and for each node ($|u - u_h|$), are presented in Figures 3.33 to 3.36. Since

$$\|u - u_h\|_{0,\Omega} \sim 7 \times 10^{-5}, \quad \max_{T \in \mathcal{T}_h} \|u - u_h\|_{0,T} \sim 5 \times 10^{-6}, \quad \max_{\Sigma_h} |u - u_h| \sim 10^{-4},$$

we conclude that the numerical results agree well with the analytic predictions. The value of the von Mises stress obtained at the point $(x_1, x_2) = (0, 2)$, $3.6591 \times 10^8\, Pa$, is close to the value prescribed by the analytic solution, $3.6750 \times 10^8\, Pa$.

elements	h	$\max_{\Sigma_h} \lvert u - u_h \rvert$	$\|u - u_h\|_{0,\Omega}$	$\|u - u_h\|_{0,\Omega} \ / \ \lvert u \rvert_{1,\Omega}$
675	1.4902×10^{-1}	5.6821×10^{-4}	3.7357×10^{-4}	4.4267×10^{-3}
1200	1.1180×10^{-1}	3.3276×10^{-4}	2.1080×10^{-4}	2.4979×10^{-3}
1875	8.9443×10^{-2}	2.1939×10^{-4}	1.3512×10^{-4}	1.6011×10^{-3}
2700	7.4536×10^{-2}	1.5597×10^{-4}	9.3908×10^{-5}	1.1128×10^{-3}
3675	6.3888×10^{-2}	1.1682×10^{-4}	6.9029×10^{-5}	8.1797×10^{-4}

Table 3.5: Error estimates for different meshes for Problem 3

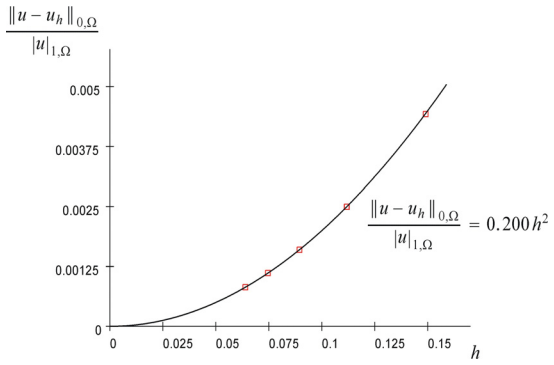

Figure 3.31: Order of convergence of the numerical solution for Problem 5 from data of Table 3.5

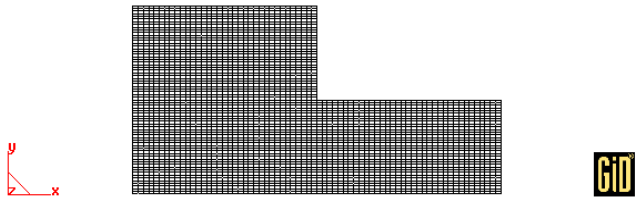

Figure 3.32: Problem 5 : the 3675 finite elements mesh

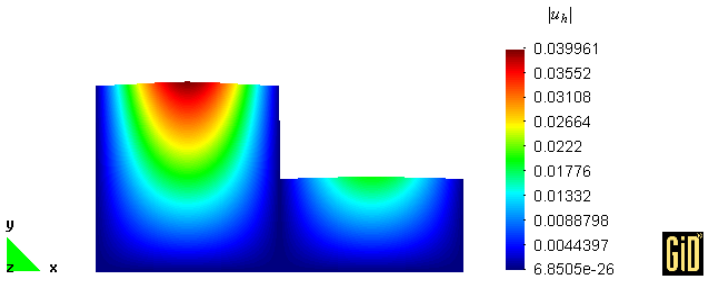

Figure 3.33: Problem 5 : the displacement field $|u_h|$ for the mesh presented in Figure 3.32

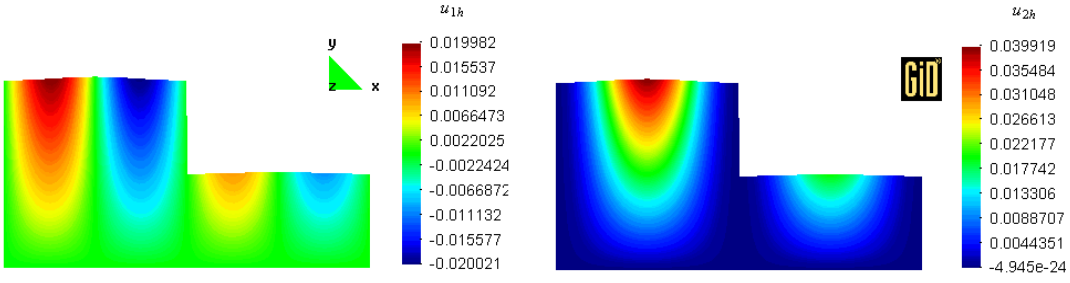

Figure 3.34: Problem 5 : the displacement fields u_{1h} (left) and u_{2h} (right) for the mesh presented in Figure 3.32

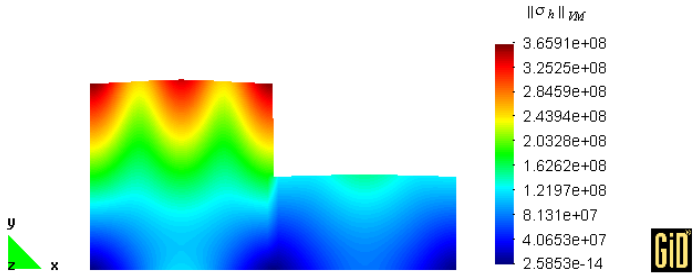

Figure 3.35: Problem 5 : the von Mises stress field for the mesh presented in Figure 3.32

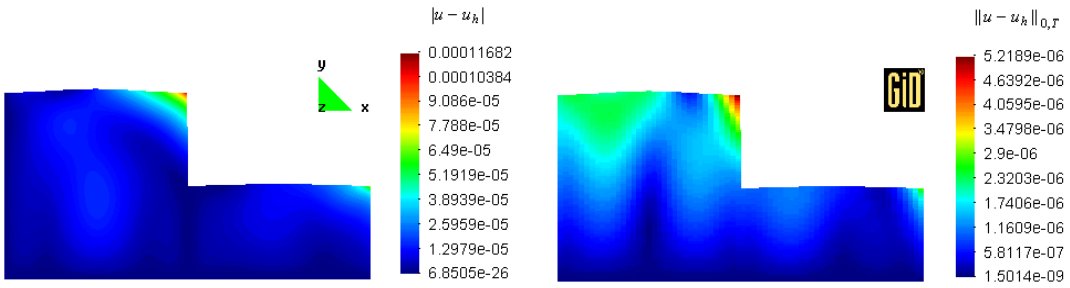

Figure 3.36: Problem 5 : the distribution of $|u-u_h|$ (left) and $\|u-u_h\|_{0,T}$ (right) for the mesh presented in Figure 3.32

3.6. Test problem 6 - 2D wrench

3.6.1. Problem description

Finally, we consider the homogeneous 2D wrench presented in Figure 3.37. The mechanical tool is made of steel, having Young modulus $E = 2 \times 10^8 \left(N\,cm^{-2}\right)$ and Poisson ratio $\nu = 0.3$. The corresponding values of the Lamé's constants λ and μ are (cf. (3.1))

$$\lambda = 2.8846 \times 10^5 \left(N\,cm^{-2}\right), \quad \mu = 1.9231 \times 10^5 \left(N\,cm^{-2}\right).$$

We assume the boundary Γ_2 is submitted to a force $(-100, -100)\ Nm^{-2}$ and that boundary Γ_1 does not move. Therefore, the linear elasticity problem for this tool is

$$\begin{aligned} &\text{Find } u = (u_1, u_2) \text{ such that:} \\ &-\sum_{j=1}^{2} \frac{\partial}{\partial x_j} \sigma_{ij}(u) = 0 \quad \text{in} \quad \Omega, \quad 1 \le i \le 2, \\ &u_1 = 0,\ u_2 = 0 \quad \text{on} \quad \Gamma_1, \\ &\sum_{j=1}^{2} \sigma_{ij}(u)\,\nu_j = g_i \quad \text{on} \quad \Gamma_2, \quad 1 \le i \le 2, \end{aligned} \tag{3.9}$$

where

$$\begin{aligned} g_1|_{\Gamma_2} &= -0.01 \quad \left(N\,cm^{-2}\right), \\ g_2|_{\Gamma_2} &= -0.01 \quad \left(N\,cm^{-2}\right). \end{aligned}$$

Since this problem has no analytic solution, we compare our numerical results with the ones obtained by Rodríguez and Campo (2004) using the MODULEF package.

To make the comparison possible we had to make small adjustments to some of the "default" settings of our code in order to match those of MODULEF, namely:

(H1) the constitutive law used is

$$\begin{aligned}\sigma_{ij} &= \frac{2\mu\lambda}{2\mu+\lambda}\left(\sum_{k=1}^{2}\varepsilon_{kk}\right)\delta_{ij}+2\mu\varepsilon_{ij}, \qquad 1\le i,j\le 2,\\ &= \widetilde{\lambda}\left(\sum_{k=1}^{2}\varepsilon_{kk}\right)\delta_{ij}+2\mu\varepsilon_{ij}, \qquad 1\le i,j\le 2,\end{aligned}$$

where $\widetilde{\lambda} = 2\mu\lambda\,(2\mu+\lambda)^{-1}$ is the "homogenized" Lamé coefficient, instead of Hooke's law (cf. (1.2))

$$\sigma_{ij} = \lambda\left(\sum_{k=1}^{2}\varepsilon_{kk}\right)\delta_{ij}+2\mu\varepsilon_{ij}, \qquad 1\le i,j\le 2.$$

In practice, this corresponds to use a plane stress model instead of a plane model for the displacements [see e.g. Ciarlet (1993)];

(H2) all numerical integrations are performed using 2 points in each direction, the quadrature points coinciding with the nodes defining the element (or surface), whereas the "default" quadrature schemes involve Gauss-Legendre quadrature points, 2 points in each direction in 2D integrations and only one point in 1D integrations; Since the surface loads are constant, all possible settings for 1D integrations lead to the same results;

(H3) nodal main stresses, and particularly von Mises stresses, are computed averaging over the values at the barycentre of the elements to which the node belongs to using equal weights, instead of weights proportional to the area of the elements involved (the "default" setting).

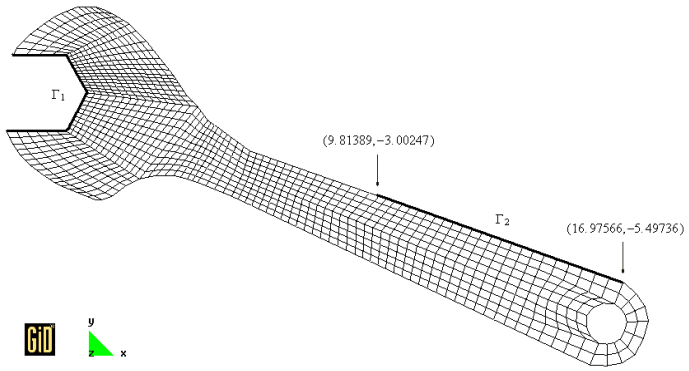

Figure 3.37: Schematic representation of the wrench of Problem 6; the coordinates are presented in *cm*

3.6.2. Results

The numerical results were obtained for the mesh presented in Figure 3.37, involving 1153 nodes and 1046 elements.

The results obtained under conditions (H1)-(H3) for the displacements and the von Mises stress coincide with those obtained using MODULEF. The results obtained for the displacements ($|u_h^o|$, u_{1h}^o, and u_{2h}^o) and the von Mises stress ($\|\sigma_h^o\|_{VM}$) are presented in Figures 3.38 to 3.40. The corresponding results obtained with the "default" settings - $|u_h|$, u_{1h}, u_{2h} and $\|\sigma_h\|_{VM}$ - are presented in Figures 3.41 to 3.44. These figures also present the differences with respect to the MODULEF results, that is, under conditions (H1)-(H3).

From the analysis of Figures 3.41 to 3.43 we conclude that the differences observed for the three displacement fields are proportional to the field values, that is, for each field the relative differences are essentially constant. In fact, one has

	mean value	standard deviation
$\frac{u_{1h}}{u^o_{1h}}$	1.037	0.047
$\frac{u_{2h}}{u^o_{2h}}$	1.045	0.084

The situation for the von Mises stress seems to be less evident, at least from the direct analysis of Figure 3.44. However, one finds that

	mean value	standard deviation
$\frac{\|\sigma_h\|_{VM}}{\|\sigma^o_h\|_{VM}}$	1.029	0.036

Therefore, the values obtained for the displacements and the von Mises stress with the "default" settings are, in general, a few percent higher than those obtained with MODULEF.

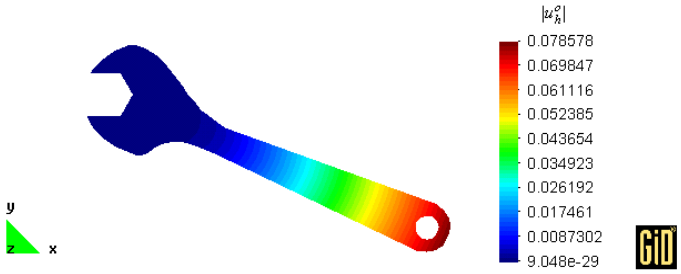

Figure 3.38: Problem 6 : the displacement field $|u_h|$ (in cm) for the mesh presented in Figure 3.37 using MODULEF settings

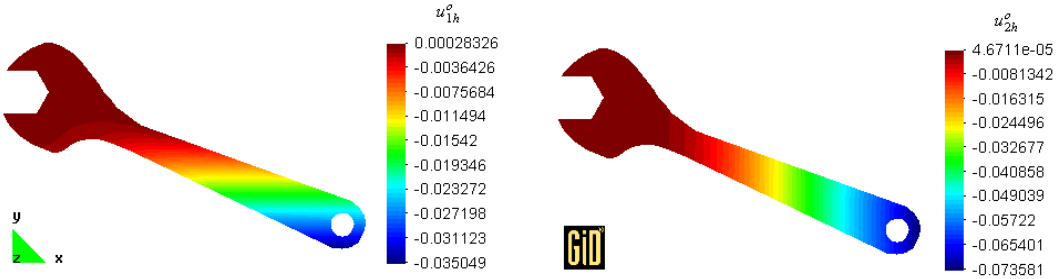

Figure 3.39: Problem 6 : the displacement fields u_{1h} (left) and u_{2h} (right) - both in cm- for the mesh presented in Figure 3.37 using MODULEF settings

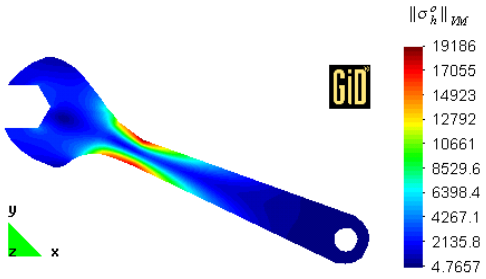

Figure 3.40: Problem 6 : the von Mises stress field (in $N\ cm^{-2}$) for the mesh presented in Figure 3.37 using MODULEF settings

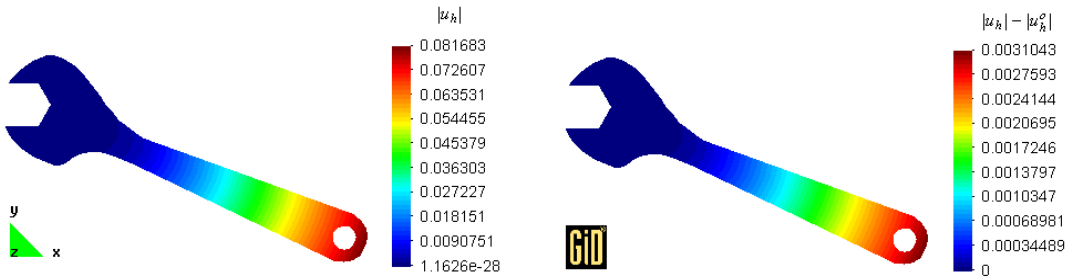

Figure 3.41: Problem 6 : the displacement field $|u_h|$ (left) and its difference with respect to the MODULEF result $|u_h^o|$ (right) for the mesh presented in Figure 3.37; all results are in cm

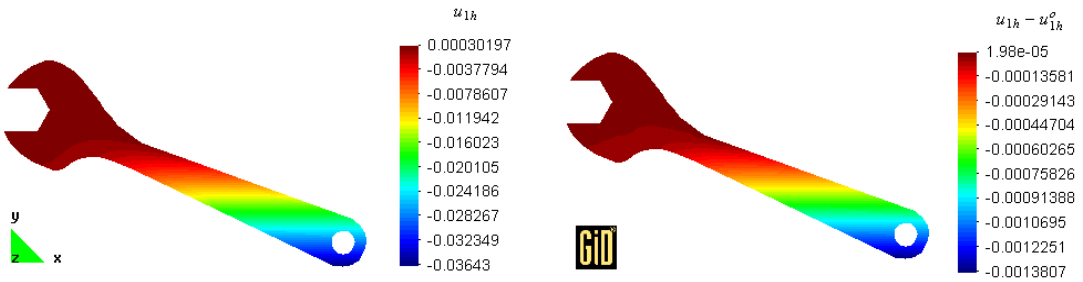

Figure 3.42: Problem 6 : the displacement field u_{1h} (left) and its difference with respect to the MODULEF result u_{1h}^o (right) for the mesh presented in Figure 3.37; all results are in cm

Figure 3.43: Problem 6 : the displacement field u_{2h} (left) and its difference with respect to the MODULEF result u_{2h}^o (right) for the mesh presented in Figure 3.37; all results are in cm

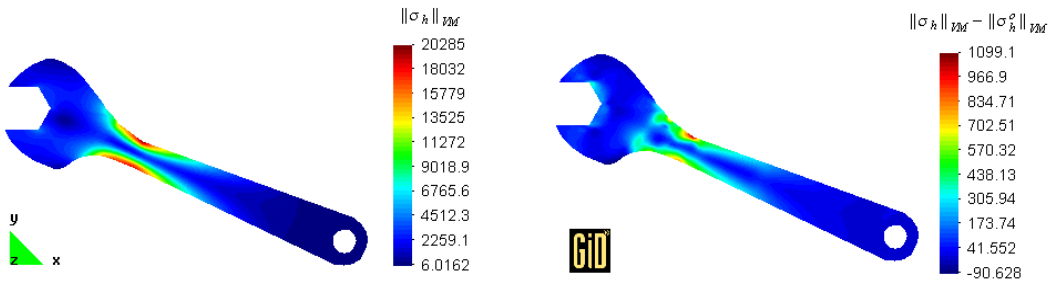

Figure 3.44: Problem 6 : the von Mises stress field $\|\sigma_h\|_{VM}$ (left) and its difference with respect to the MODULEF result $\|\sigma_h^o\|_{VM}$ (right) for the mesh presented in Figure 3.37; all results are in $N\,cm^{-2}$

References

Adams, R.A. (1975): Sobolev spaces. Academic Press, New-York

Ciarlet, P.G. (1993): Handbook of numerical analysis, Vol. II, Finite elements (Part I). P.G. Ciarlet, J.L. Lions (ed.). North-Holland, Amsterdam

Duvaut, G., Lions, J.L. (1972): Les inéquations en mechanique et en physique. Dunod, Paris

Raviart, P.-A., Thomas, J.-M. (1998): Introduction à l´analyse numérique des équations aux dérivées partielles. Dudod, Paris

Rodríguez, A., Campo, M. (2004): Private communication

A. Files used for GiD interfacing

Here we present the relevant files used for the interface between the numerical code and GiD (version 7.2) for both preprocessing and postprocessing.

A.1. Configuration files

These files generate the conditions and material properties, as well as the proper general problem data to be transferred to the mesh.

A.1.1. Conditions file (.cnd)

The file with extension's name *.cnd* contains all the information about the conditions that can be applied to different entities:

NUMBER: 1 CONDITION: Point-Constrains
CONDTYPE: over points
CONDMESHTYPE: over nodes
QUESTION: Displacement_along_X_axis_-_Flag
VALUE: 0
HELP: 0: locked; 1: given below; other: computed in code
QUESTION: Displacement_along_X_axis_-_Value
VALUE : 0.0
QUESTION: Displacement_along_Y_axis_-_Flag
VALUE: 0
HELP: 0: locked; 1: given below; other: computed in code
QUESTION: Displacement_along_Y_axis_-_Value
VALUE : 0.0
END CONDITION
NUMBER: 2 CONDITION: Line-Constrains
CONDTYPE: over lines
CONDMESHTYPE: over nodes
QUESTION: Displacement_along_X_axis_-_Flag
VALUE: 0
HELP: 0: locked; 1: given below; other: computed in code
QUESTION: Displacement_along_X_axis_-_Value
VALUE : 0.0
QUESTION: Displacement_along_Y_axis_-_Flag
VALUE: 0
HELP: 0: locked; 1: given below; other: computed in code
QUESTION: Displacement_along_Y_axis_-_Value
VALUE : 0.0
END CONDITION
NUMBER: 3 CONDITION: Surface-Constrains
CONDTYPE: over surfaces
CONDMESHTYPE: over nodes
QUESTION: Displacement_along_X_axis_-_Flag
VALUE: 0

HELP: 0: locked; 1: given below; other: computed in code
QUESTION: Displacement_along_X_axis_-_Value
VALUE : 0.0
QUESTION: Displacement_along_Y_axis_-_Flag
VALUE: 0
HELP: 0: locked; 1: given below; other: computed in code
QUESTION: Displacement_along_Y_axis_-_Value
VALUE : 0.0
END CONDITION
NUMBER: 4 CONDITION: Point-Loads
CONDTYPE: over points
CONDMESHTYPE: over nodes
QUESTION: P_flag
VALUE: 0
HELP: 0: no load; 1: load given below; other: load computed in code
QUESTION: Px
VALUE: 0.0
QUESTION: Py
VALUE: 0.0
END CONDITION
NUMBER: 5 CONDITION: Face-Loads
CONDTYPE: over lines
CONDMESHTYPE: over face elems
QUESTION: G_flag
VALUE: 0
HELP: 0: no load; 1: load given below; other: load computed in code
QUESTION: Gx
VALUE: 0.0
QUESTION: Gy
VALUE: 0.0
END CONDITION
NUMBER: 6 CONDITION: Element-Loads
CONDTYPE: over surfaces
CONDMESHTYPE: over elems
QUESTION: F_flag
VALUE: 0
HELP: 0: no load; 1: load given below; other: load computed in code
QUESTION: Fx
VALUE: 0.0
QUESTION: Fy
VALUE: 0.0
END CONDITION

A.1.2. Materials file (.mat)

The file with extension's name *.mat* includes the definition of different materials through their properties. These are base materials as they can be used as templates during the pre-processing step for the creation of newer ones:

NUMBER: 1 MATERIAL: rock
QUESTION: Young's_modulus_-_E:
VALUE: 5000000000
QUESTION: Poisson's_ratio_-_nu:
VALUE: 0.3

```
END MATERIAL
NUMBER: 2 MATERIAL: concrete
QUESTION: Young's_modulus_-_E:
VALUE: 4000000000
QUESTION: Poisson's_ratio_-_nu:
VALUE: 0.2
END MATERIAL
```

A.1.3. Problem and intervals data file (.prb)

The file with extension's name *.prb* contains all the information about the general problem and intervals data:

```
PROBLEM DATA
QUESTION: title
VALUE: elasticity
HELP: project name for header of data file
QUESTION: analytic_solution_known#CB#(1,0)
VALUE: 0
HELP: if this flag is set, an error estimate is computed using the analytic solution
QUESTION: gauss_points_for_elements
VALUE: 2
HELP: gauss points per direction in element integration (rigidity matrix and f-loads)
QUESTION: gauss_points_for_g-faces
VALUE: 1
HELP: gauss points per direction in boundary integration (g-loads)
QUESTION: gauss_points_for_error_estimation
VALUE: 2
HELP: gauss points per direction in element integration (error estimates)
VALUE: 2
END PROBLEM DATA
```

A.1.4. Template file (.bas)

Once the user has generated the mesh, assigned the conditions and the materials properties, as well as the general problem and intervals data for the solver, it is necessary to produce the data input files to be processed by that code. The template file, with extension's name *.bas*, describes the format and structure of the required data input file for the solver that is used in a particular case:

```
-------------------------------------------------------------
                ELASTICITY GENERAL DATA FILE
-------------------------------------------------------------

------------------- Problem Title --------------------
 *GenData(title)

------------------ Control Parameters ------------------
 Analytic Solution
*set var as = GenData(2,int)
*format "%10i"
*as

---------------- Gauss Points per Direction ----------------
 Elements    g-Faces    Error Estimation
*set var gel = GenData(3,int)
```

```
*set var ggf = GenData(4,int)
*set var gee = GenData(5,int)
*format "%6i%10i%14i"
*gel *ggf *gee

------------------ Problem Dimensions ------------------
 Nodes  Elements  Nodes/Element  Nodes/Face  Faces/Element  Dimension
*set var npf = 2
*set var fpe = 4
*format "%6i%9i%8i%13i%12i%12i"
*npoin *nelem *nnode *npf *fpe *ndime

 Materials    Parameters/Material
*set var npar = 2
*format "%10i%14i"
*nmats *npar

 Nodes Constrained    Point Loads    Face Loads    Element Loads
*set cond Surface-Constrains *nodes *or(1,int) *or(3,int)
*add cond Line-Constrains *nodes *or(1,int) *or(3,int)
*add cond Point-Constrains *nodes *or(1,int) *or(3,int)
*set var constr = CondNumEntities
*set cond Point-Loads *nodes
*set var point = CondNumEntities
*set cond Face-Loads *elems *CanRepeat
*set var face = CondNumEntities
*set cond Element-Loads *elems
*set var element = CondNumEntities
*format "%18i%14i%13i%16i"
*constr *point *face *element

------------------ Materials Properties ------------------
 Material   Young's Modulus   Poisson's ratio
*loop materials
*format "%9i%16.7e%17.7e"
*matnum() *MatProp(1) *MatProp(2)
*end

------------------ Nodes Coordinates ------------------
 Node          X             Y             Z
*set elems(all)
*loop nodes
*format "%5i%16.7e%16.7e%16.7e"
*NodesNum *NodesCoord
*end nodes

------------------ Connectivities ------------------
 Element    Node(1)   Node(2)   Node(3)   Node(4)   Material
*loop elems
*format "%8i%10i%10i%10i%10i%10i"
*ElemsNum *ElemsConec *ElemsMat
*end elems
*set cond Surface-Constrains *nodes *or(1,int) *or(3,int)
*add cond Line-Constrains *nodes *or(1,int) *or(3,int)
*add cond Point-Constrains *nodes *or(1,int) *or(3,int)
*if(condNumEntities(int)>0)

------------------ Nodes Constrained ------------------
```

```
 Node   Codes(x,y)   Displacement Values(x,y)
*loop nodes *OnlyIncond
*format "%5i%5i%3i%15.5e%14.5e"
*NodesNum *cond(1,int) *cond(3,int) *cond(2,real) *cond(4,real)
*end
*endif
*set cond Point-Loads *nodes
*if(condNumEntities(int)>0)
```

Point Loads

```
 Node   Code         Load Values(x,y)
*loop nodes *OnlyIncond
*format "%5i%5i%15.5e%14.5e"
*NodesNum *cond(1,int) *cond(2,real) *cond(3,real)
*end
*endif
*set cond Face-Loads *elems *CanRepeat
*if(condNumEntities(int)>0)
```

Face Loads

```
 Element   LNode(1)   LNode(2)   Code         Load Values(x,y)
*loop elems *OnlyIncond
*format "%8i%10i%11i%5i%15.5e%14.5e"
*elemsnum() *localnodes *cond(1,int) *cond(2,real) *cond(3,real)
*end
*endif
*set cond Element-Loads *elems
*if(condNumEntities(int)>0)
```

Element Loads

```
 Element   Code         Load Values(x,y)
*loop elems *OnlyIncond
*format "%8i%5i%15.5e%14.5e"
*elemsnum *cond(1,int) *cond(2,real) *cond(3,real)
*end
*endif
```

A.2. Input and output files

A.2.1. Calculation (input) file

The GiD command (Files→Export→Calculation file) writes the data file needed by the solver module. The data file, with extension *.dat*, has the following structure:

```
ELASTICITY GENERAL DATA FILE

Problem Title
elasticity – test problem 1 : square

Control Parameters
Analytic Solution
        1

Gauss Points per Direction
Elements    g-Faces    Error Estimation
    2           1              2
```

Problem Dimensions

Nodes	Elements	Nodes/Element	Nodes/Face	Faces/Element	Dimension
961	900	4	2	4	2

Materials	Parameters/Material
1	2

Nodes Constrained	Point Loads	Face Loads	Element Loads
61	0	60	900

Materials Properties

Material	Young Modulus	Poisson's ratio
1	5.0000000e+09	3.0000000e-01

Nodes Coordinates

Node	X	Y	Z
1	1.0000000e+00	0.0000000e+00	
2	1.0000000e+00	3.3333333e-02	
⋮			

Connectivities

Element	Node(1)	Node(2)	Node(3)	Node(4)	Material
1	959	956	960	961	1
2	958	953	956	959	1
⋮					

Nodes Constrained

Node	Codes(x,y)	Displacement Values(x,y)	
1	1 1	0.00000e+00	0.00000e+00
3	1 1	0.00000e+00	0.00000e+00
⋮			

Face Loads

Element	LNode(1)	LNode(2)	Code	Load Values(x,y)	
31	3	4	4	0.00000e+00	0.00000e+00
61	3	4	4	0.00000e+00	0.00000e+00
⋮					

Element Loads

Element	Code	Load Values(x,y)	
1	2	0.00000e+00	0.00000e+00
2	2	0.00000e+00	0.00000e+00
⋮			

A.2.2. Postprocess files

The results obtained from the code can be postprocessed using GiD. For that one has to supply two files: a file with extension *.post.res* for the results (displacements, stresses, error estimates, etc.), and another file with extension *.post.msh* containing the postprocess mesh. If the postprocess mesh is not provided, GiD uses the preprocess mesh.

The data file with extension *.post.res* has the following structure:

```
GiD Post Results File 1.0

Result "Displacements" "Load Analysis" 1 Vector OnNodes
    ComponentNames "X-displ", "Y-displ", "Z-displ"
Values
   1    1.239316e-24    -2.518696e-24    0.000000e+00
   2    3.333333e-04    -6.666667e-04    0.000000e+00
   ⋮

 961    1.720085e-24    -1.076389e-24    0.000000e+00
End Values

Result "Main Stresses" "Load Analysis" 1 MainMatrix OnNodes
Values
   1 -1.391552e+00 -5.315254e+07 0.000000e+00 9.732490e-01 -2.297529e-01 0.000000e+00
     2.297529e-01 9.732490e-01 0.000000e+00 0.000000e+00 0.000000e+00 0.000000e+00
   2 -1.375765e+08 -5.152609e+07 0.000000e+00 9.769415e-01 -2.135070e-01 0.000000e+00
     2.135070e-01 9.769415e-01 0.000000e+00 0.000000e+00 0.000000e+00 0.000000e+00
   ⋮
 961 5.075616e+06 9.107823e+07 0.000000e+00 -8.506508e-01 -5.257311e-01 0.000000e+00
     -5.257311e-01 8.506508e-01 0.000000e+00 0.000000e+00 0.000000e+00 0.000000e+00
End Values

Result"von Mises Stress" "Load Analysis" 1 Scalar OnNodes
Values
   1    1.216261e+08
   2    1.203887e+08
   ⋮
 961    8.864947e+07
End Values
```

```
GaussPoints "Barycentre" ElemType Quadrilateral
      Number of Gauss Points: 1
      Natural Coordinates: Internal
End GaussPoints

Result "Error Estimate L2" "Load Analysis" 1 Scalar OnGaussPoints "Barycentre"
Values
   1    1.474247e-18
   2    9.969235e-19
   ⋮
 900    1.693434e-18
End Values

Result "Error Estimate Euclidean" "Load Analysis" 1 Scalar OnNodes
Values
   1    2.807087e-24
   2    1.065382e-16
   ⋮
 961    2.029115e-24
End Values
```

The data file with extension *.post.msh* has the following structure:

```
Mesh Dimension 2 ElemType Quadrilateral Nnode 4
Coordinates
 # Node          X              Y              Z
      1     1.000000e+00   -2.518696e-24
      2     1.000333e+00    3.266667e-02
      ⋮
    961     1.720085e-24    1.000000e+00
End Coordinates

Elements
 # Element   Node(1)   Node(2)   Node(3)   Node(4)   Material
      1        959       956       960       961        1
      2        958       953       956       959        1
      ⋮
    900          3         1         2         4        1
End Elements
```